



TÉCNICO
LISBOA

Separation of Bacteriophage Tails to Develop Novel Recognition Elements

Inês Alexandra Rocha Morgado Simões

Thesis to obtain the Master of Science Degree in:

Biotechnology

Supervisors:

Professor Ana Margarida Nunes da Mata Pires de Azevedo
Doctor Verónica Martins Romão

Examination Committee:

Chairperson: Professor Luís Joaquim Pina da Fonseca
Supervisor: Professor Ana Margarida Nunes da Mata Pires de Azevedo
Member of the Committee: Professor Marília Clemente Velez Mateus

December 2020

Preface

The work presented in this thesis was performed at Institute for Bioengineering and Biosciences (iBB) of Instituto Superior Técnico, Universidade de Lisboa (Lisbon, Portugal) in the BioEngineering Research Group (BERG), during the period September 2019-October 2020, under the supervision of Prof. Ana Margarida Nunes da Mata Pires de Azevedo (BERG-iBB) and Dr. Verónica Martins Romão (INESC-MN).

I declare that this document is an original work of my own authorship and that it fulfills all the requirements of the Code of Conduct and Good Practices of the Universidade de Lisboa.

Acknowledgments

First of all, I would like to thank to my supervisors, Professor Ana Avezedo and Doctor Verónica Romão, for offering me the opportunity to work on such challenging and promising project. Most importantly, thank you for the helpful guidance, motivation and availability enabled on me throughout this part of my academic journey.

I would also like to thank to Professor Isabel Sá-Correia and Professor Arsénio Fialho for all the guidance and knowledge offered throughout my Master's Degree.

I am also grateful for my laboratory colleagues, namely Diogo Faria and Sara Rosa for all of the support and availability to discuss ideas and for the warm welcoming to the laboratory. A special thanks to João Lampreia for all of his incredible help, guidance, knowledge and friendship shared with me.

To all of my close friends and colleagues I made along my academic life, thank you for the often share of doubts, great moments, support and most of all, good times. Special thanks to Marta Patinha for being on my side everyday throughout the laboratory work and also for the sharing of laughs and her amazing friendship. To Hugo Ganchas and Sílvia Sustelo, an endless thank you for supporting and motivating me the whole way through.

A huge thank you to my family, particularly to my parents, Luis and Paula Simões, and to my brother, André Simões, for their constant encouragement, unconditional support, understanding and values transmitted to me along my growth. I couldn't make this far without them.

Thank you very much to all of you.

Abstract

As the world's population grows, the use of antibiotics became an indispensable medical treatment and prevention for bacterial infections. However, the constant, broad and sometimes inconsiderate use of antibiotics resulted in antibiotic resistance bacteria which represent a global health concern. The lack of early diagnosis and pathogen identification intensifies the cause of this resistance. Biosensors allow a fast, reliable and ease-to-use medical diagnosis with the support of recognition elements. In this context, bacteriophages represent promising recognition elements for identification of antibiotic resistant bacteria due to their exceptional characteristics. The current phage-based biosensors are not effective since bacteriophages infect and induce lysis of the host bacteria in their natural state.

The aim of this Master's Thesis was to enhance and develop advance bacteriophage recognition elements for a fast and reliable pathogen identification by the separation of bacteriophage's heads from their tails, thus eliminating the infection capacity, but retaining their recognition ability. The overall process consisted in *E. coli* specific T4 bacteriophage production by infection of bacterial cultures, preparation and amplification of a T4 phage stock and testing mechanical (water bath and probe sonication) and non-mechanical (osmotic shock) disruption methods for the separation of phage tails. The 25 W probe ultrasonication demonstrated to be the most promising method to achieve the proposed purpose.

Keywords: Bacteriophage, Antibiotic Resistant Bacteria, Biosensors, Advanced Recognition Elements, Bacteriophage Separation.

Resumo

Com o crescimento da população mundial, o uso de antibióticos tornou-se um tratamento médico indispensável para a prevenção de infecções bacterianas. No entanto, o uso constante, amplo e às vezes imprudente de antibióticos resultou em bactérias resistentes aos mesmos, o que representa uma preocupação para a saúde global. A falta de diagnóstico precoce e identificação do agente patogénico fortalece a causa para essa resistência. Os biossensores permitem um diagnóstico médico rápido, fiável e fácil de usar com o auxílio de elementos de reconhecimento. Neste contexto, os bacteriófagos representam promissores elementos de reconhecimento para a identificação de bactérias resistentes a antibióticos devido às suas características excepcionais. Atualmente, biossensores baseados em fagos não são eficientes dado que os fagos infetam e induzem a lise da bactéria hospedeira no seu estado natural.

Assim sendo, esta Dissertação de Mestrado teve como objetivo principal melhorar e desenvolver bacteriófagos como elementos de reconhecimento avançados para uma rápida e fiável identificação do agente patogénico através da separação das cabeças dos bacteriófagos das suas caudas, eliminando assim a capacidade de infeção, mas mantendo a capacidade de reconhecimento. O processo em geral consistiu na produção de bacteriófagos T4 específicos para *E. coli* por infeção de culturas bacterianas, preparação e amplificação de um stock de fago T4 e laboração de métodos mecânicos (sonicação em banho maria e sonicação com sonda) e não mecânicos (choque osmótico) de disrupção para a separação de caudas de fago. A ultrasonicação com sonda a 25 W demonstrou ser o método mais promissor para atingir o objetivo proposto.

Palavras-Chave: Bacteriófago, Bactérias Resistentes a Antibióticos, Biossensores, Elementos de Reconhecimento Avançados, Separação de Bacteriófagos.

Table of Contents

| | |
|---|--------------|
| Preface | III |
| Acknowledgments | V |
| Abstract | VII |
| Resumo | IX |
| List of Figures | XIII |
| List of Tables | XIX |
| List of Annex Figures | XXI |
| List of Annex Tables | XXIII |
| List of Abbreviations | XXV |
| 1. Introduction | 1 |
| 1.1. Background..... | 1 |
| 1.2. Goals and Aim of Study | 2 |
| 2. State-of-the-Art | 3 |
| 2.1. Biosensors – Basic Principles..... | 3 |
| 2.1.1. Signal Transducers | 4 |
| 2.1.2. Recognition Receptors..... | 7 |
| 2.1.3. Immobilization Techniques..... | 13 |
| 2.2. Bacteriophages..... | 15 |
| 2.2.1. Early History – Research and Discovery..... | 15 |
| 2.2.2. Bacteriophage Biology – Diversity | 16 |
| 2.2.3. Bacteriophage Biology – Morphology | 18 |
| 2.2.4. Mechanisms of Phage Proliferation | 19 |
| 2.2.5. Bacteriophages Infection Lifecycles..... | 23 |
| 2.2.6. Most Well Characterized Bacteriophages – T4 and T7..... | 25 |
| 2.3. Bacteriophage Production and Purification..... | 26 |
| 2.4. Applications of Bacteriophages | 28 |
| 2.4.1. First Practical Applications - Veterinary and Human Medicine | 28 |
| 2.4.2. Bacteriophage Therapy..... | 29 |

| | |
|--|-----------|
| 2.4.3. Bacteriophage-Based Biosensors | 30 |
| 3. Materials and Methods..... | 36 |
| 3.1. Experimental Process | 36 |
| 3.2. Cell Cultures | 37 |
| 3.2.1. Rehydration of Dried <i>E. coli</i> Cell Culture..... | 37 |
| 3.2.2. <i>E. coli</i> Bacterial Growth Curve | 38 |
| 3.3. Bacteriophage Stock..... | 38 |
| 3.3.1. Revitalization of Dried <i>E. coli</i> Bacteriophages | 38 |
| 3.3.2. Bacteriophage Stock Amplification..... | 38 |
| 3.4. Bacteriophage Separation Methods | 40 |
| 3.4.1. Osmotic Shock | 40 |
| 3.4.2. Water Bath Ultrasonication | 41 |
| 3.4.3. Probe Ultrasonic Homogenization..... | 42 |
| 3.5. Characterization of Bacteriophages..... | 42 |
| 3.5.1. SDS-PAGE and Protein Quantification | 42 |
| 3.5.2. Bradford Assay..... | 43 |
| 3.5.3. Bacteriophage Morphology Analysis..... | 43 |
| 4. Results and Discussion..... | 44 |
| 4.1. Characterization of <i>E. coli</i> Growth Phases | 44 |
| 4.2. Bacteriophage Stock Amplification | 46 |
| 4.3. Bacteriophage Dissociation Techniques..... | 48 |
| 4.3.1. Osmotic Shock | 48 |
| 4.3.2. Water Bath Sonication | 52 |
| 4.3.3. Probe Ultrasonic Homogenization..... | 55 |
| 4.4. Bacteriophage Morphology Analysis | 60 |
| 6. Final Remarks and Future Perspectives | 62 |
| 4. References | 65 |
| Annex | 70 |

List of Figures

- Figure 1** – Flowchart demonstrating the processing steps involved and relative time taken in detecting a pathogen in biological samples. Adapted from Singh et al. ¹²3
- Figure 2** – Schematic basic representation of a Biosensor System. From Innovogene.com – accessed 10th June 2020 ²⁰4
- Figure 3** – Electrochemical Biosensor electrodes configuration. (a) working electrode; (b) reference electrode; (c) counter electrode. Adapted from Campaña et al. ²³5
- Figure 4** – Principle of SPR detection. Antibodies are immobilized onto the gold surface of the sensor. When light passes through a prism onto the sensor, it reflects the angle A and its measured by a detector. A sample containing the target analyte passes through the flow cell and binds to the antibody, making a change in the refractive index, resulting in the angle B. This change in SPR angle is proportional to the mass bound to the sensor chip surface. From Damborsky´ et al. ²⁸6
- Figure 5** – Schematic representation of a typical biosensor system. (A) Sample where the target analyte is present; (B) The target analyte binds to the biorecognition element. in the biosensor electrode, which is composed by the bioreceptor, the immobilization surface and the transducer element; (C) Physicochemical reaction occurs between the analyte and the bioreceptor; (D) Signal generated is translated by the aid for a transducer. From Campaña et al. ²³7
- Figure 6** – Schematic representation of random and site-directed methods for antibody immobilization on solid transducer surfaced. (a) Random physical adsorption through hydrophobic or electrostatic interactions; (b) Random covalent binding of antibody amine groups; (c) Random affinity binding by biotin streptavidin interactions; (d) Site-directed immobilization through oxidized carbohydrate side chains over amine surfaces; (e) Site-directed immobilization through thiolated antibody fragments into gold surfaces or maleimide functional linkers; (f) Site-directed immobilization through affinity binding between protein A or G and the constant region of the antibody. From Martins et al. ³⁸11
- Figure 7** – Schematic representation of different formats of antibody fragments including single-chain Fragment variables (scFv), Minibodies, Fab, Diabodies, Fab´, Triabodies, scFv-Fc and F(ab´)₂. From BIOLOGICS International Corp – accessed 19th June 2020 ⁴¹12
- Figure 8** – Schematic representation of immobilization methods for the biological element. (a) Physical Adsorption through electrostatic interactions; (b) Covalent Binding to the transducer surface; (c)

Crosslinking immobilization; (d) Entrapment within a polymer gel; (e) Encapsulation between two semipermeable membranes. Image created in BioRender.com, adapted from Kumar and Upadhyay and Campaña et al. ^{21,23} 14

Figure 9 – Schematic representation of bacteriophages from the families Myoviridae, Siphoviridae and Podoviridae belonging to the order Caudovirales. From Kurtböke ⁸ 17

Figure 10 – Schematic representation of tail morphology of different families of bacteriophages. Green represents genetic material enclosed by the capsid. Blue indicates tails and other adsorption organelles such as tail fibers. Diagonal lines in Myoviridae tail shows its contractile capability. Pink represents lipids. Plasmaviridae are unusual budding viruses which lack of cell wall. From Schaechter ⁹ 18

Figure 11 – Schematic representation of a bacteriophage particle. The phage DNA is protected by the isosahedral protein capsid which is attached to the contractile tail. The hexagonal baseplate coordinates the movement of the tail fibers that initially senses the presence of the host. From Harada et al. ⁴⁸ 19

Figure 12 – Schematic representation of the phage proliferation mechanism. (a) Attachment of the phage to the host surface receptors; (b) Penetration and injection of the phage genetic material; (c) Biosynthesis of viral nucleic acid and proteins and structural components; (d) Maturation and assembly of the phage progeny; (e) Host cell lysis and release of phage progeny. From Quizlet.com – accessed 9th June 2020 ⁵⁸ 20

Figure 13 – Schematic representation of the different mechanisms of attachment to the host bacterial cell by Myoviridae, Siphoviridae, Podoviridae and tailless bacteriophages. The yellow lines represent the membrane bilayers. The green lines/layers represent the peptidoglycan layers of the bacterial cells. The question marks indicate unknown host factors or unclear membrane attachments and penetration mechanisms. Tape measure protein (TMP); Lipopolysaccharide (LPS). From Xu et al. ⁶³ 22

Figure 14 – Schematic representation of the two lifecycles of bacteriophages. Pink represents the lytic cycle of infection. Blue indicates the lysogenic cycle of infection. (1) Phage attaches to the host cell and injects its genomic material; (2) The DNA of the phage enters the cytoplasm of host bacteria; (3a) New phage DNA and proteins are synthesized and bacteriophages assembled; (4a) Cell lysis releasing new bacteriophages; (3b) Integration of the phage genome within the bacterial genome (prophage); (4b) Normal bacterial reproduction and division; (5) Under certain conditions, the prophage excises from the bacterial genome and initiates the lytic cycle. From Kurtböke ⁸ 24

Figure 15 – T4 bacteriophage obtained by transmission electron microscopy (TEM). From Miller et al. ⁷².
.....25

Figure 16 – T7 bacteriophage obtained by transmission electron microscopy (TEM). From Cuervo et al. ⁷⁵.
.....26

Figure 17 – Schematic representation of an affinity-based selection technique for phage display method. Phage libraries are screened against an immobilized target of interest, where the unbound phages are then washed away and the bound ones are eluted, propagated and used as probes for the target. From Singh et al. ¹²34

Figure 18 – Schematic representation of oriented phage immobilization. (a) Immobilized biotinylated phages by chemical attachment of streptavidin onto the sensor surface; (b) Attachment of bacteriophages to target bacteria in biosensing platforms for bacterial detection. Adapted from Gervais et al. ¹³34

Figure 19 – Graphic demonstration of the general experimental process developed in this Master’s Thesis for the generation of advanced recognition elements by the separation of bacteriophages’ tails. Image created in BioRender.com – accessed 5th November 2020.37

Figure 20 – Schematic representation of the osmotic shock process. Image created in BioRender.com – accessed 10th November 2020.41

Figure 21 – Schematic representation of the water bath sonication process. Image created in BioRender.com – accessed 11th November 2020.41

Figure 22 – Schematic representation of the probe sonication process. Image created in BioRender.com – accessed 11th November 2020.42

Figure 23 – E. coli growth curve. Identification of growth phases: (a) exponential phase between 0 and 220 minutes; (b) deceleration phase at 220 minutes.44

Figure 24 – E. coli colonies at different times of bacterial growth at the respective dilution. (a) 0 minutes; (b) 15 minutes; (c) 30 minutes; (d) 45 minutes; (e) 65 minutes and (f) 95 minutes.46

Figure 25 – Schematic representation of both solid and liquid medium amplifications. Image created in BioRender.com – accessed 10th November 2020.47

Figure 26 – SDS-PAGE of osmotic shock assay results for the separation of phages’ tails from the heads.

The gel was stained with Coomassie and after with Silver Nitrate. Well 1: Precision Plus Protein™ Dual Color Standards ladder; Well 2: T4 bacteriophage stock; Well 3: 2 minute osmotic shock concentrated supernatant; Well 4: 2 minute osmotic shock permeated supernatant; Well 5: 5 minute osmotic shock concentrated supernatant; Well 6: 5 minute osmotic shock permeated supernatant; Well 7: 10 minute osmotic shock concentrated supernatant; Well 8: 10 minute osmotic shock permeated supernatant. Two distinct bands can be seen in the concentrated osmotic shock samples with the following molecular weights: 63 kDa and 50 kDa.51

Figure 27 – SDS-PAGE of osmotic shock assay results for the separation of phages’ tails from the heads.

The gel was stained with Coomassie and after with Silver Nitrate. Well 1: Precision Plus Protein™ Dual Color Standards ladder; Well 2: T4 bacteriophage stock; Well 3: 15 minute osmotic shock concentrated supernatant; Well 4: 15 minute osmotic shock permeated supernatant; Well 5: 20 minute osmotic shock concentrated supernatant; Well 6: 20 minute osmotic shock permeated supernatant; Well 7: 30 minute osmotic shock concentrated supernatant; Well 8: 30 minute osmotic shock permeated supernatant. Two distinct bands can be seen in the concentrated osmotic shock samples with the following molecular weights: 63 kDa and 50 kDa.52

Figure 28 – SDS-PAGE of water bath ultrasonication assay results for the separation of phages’ tails from the heads.

The gel was stained with Coomassie and after with Silver Nitrate. Well 1: Precision Plus Protein™ Dual Color Standards ladder; Well 2: T4 bacteriophage stock; Well 3: 1 minute sonication; Well 4: 5 minutes sonication; Well 5: 10 minutes sonication; Well 6: 15 minutes sonication; Well 7: 20 minutes sonication; Well 8 :25 minutes sonication; Well 9: 30 minutes sonication; Well 10: 40 minutes sonication. Six distinct bands can be seen in all of the wells with the following molecular weight: 240 kDa, 196 kDa, 160 kDa, 96 kDa, 73 kDa and 50 kDa.54

Figure 29 – SDS-PAGE of 25W probe ultrasonication assay results for the separation of phages’ tails from the heads.

The gel was stained with Coomassie and after with Silver Nitrate. Well 1: Precision Plus Protein™ Dual Color Standards ladder; Well 2: T4 bacteriophage stock; Well 3: concentrated T4 bacteriophage stock (with Amicon® Ultra-4 100 kDa Centrifugal Filter Units); Well 4: 5 minutes sonication; Well 5: 10 minutes sonication; Well 6: 15 minutes sonication; Well 7: 20 minutes sonication; Well 8 :30 minutes sonication; Well 9: 40 minutes sonication. Ten distinct bands can be seen in all of the wells with the following molecular weight: 220 kDa, 204 kDa, 176 kDa, 82 kDa, 74 kDa, 63 kDa, 54 kDa, 24 kDa, 15 kDa and 14 kDa.57

Figure 30 – SDS-PAGE of 50W probe ultrasonication assay results for the separation of phages’ tails from the heads.

The gel was stained with Coomassie and after with Silver Nitrate. Well 1: Precision Plus

Protein™ Dual Color Standards ladder; Well 2: T4 bacteriophage stock; Well 3: concentrated T4 bacteriophage stock (with Amicon® Ultra-4 100 kDa Centrifugal Filter Units); Well 4: 5 minutes sonication; Well 5: 10 minutes sonication; Well 6: 15 minutes sonication; Well 7: 20 minutes sonication; Well 8 :30 minutes sonication; Well 9: 40 minutes sonication. Seven distinct bands can be seen in all of the wells with the following molecular weight: 178 kDa, 166 kDa, 135 kDa, 102 kDa, 89 kDa, 80 kDa and 49 kDa.59

Figure 31 – TEM images of specific E. coli T4 bacteriophages submitted to a 25 W probe ultrasonication stained with uranyless. Images obtained at 40 000x magnification at a 200nm scale in IST MicroLab. (a) phage capsid separated of their tail apparatus with 15 minutes of probe ultrasonication; (b) contracted and non-contracted tail apparatus separated from phage capsid with 15 minutes of probe ultrasonication; (c) tail apparatus with visible baseplates separated from phage capsid with 15 minutes of probe ultrasonication; (d) tail apparatus with visible tail fibers separated from phage capsid with 15 minutes of probe ultrasonication; (e) tail apparatus with visible baseplates separated from phage capsid with 20 minutes of probe ultrasonication; (f) tail apparatus with visible baseplates separated from phage capsid with 20 minutes of probe ultrasonication.61

List of Tables

| | |
|---|----|
| Table 1 – Advantages and limitations of recognition elements for biosensor systems. Adapt from Singh et al., Eggins and Justino et al. ^{12,30,31} | 13 |
| Table 2 – Comparison of the therapeutic use of phages and antibiotics. Adapted from Kutter and Sulakvelidze ⁴⁷ | 29 |
| Table 3 – E. coli growth data. Parcels with (-) symbol mean that the number of colonies were not between 30 and 300 which are the acceptable interval for the counting of PFUs. Parcels with the (*) symbol are the ones that belong to colonies counted on plate with dilution -5. The rest of the colonies were counted on plates with dilution -4..... | 45 |
| Table 4 – Osmotic shock process data for the different periods of exposure (2, 5, 10, 15, 20 and 30 minutes) to sodium acetate. Parcels with (-) symbol mean that the number of colonies were not between 30 and 300 which are the acceptable interval for the counting of PFUs. Parcels with the (*) symbol are the ones that belong to phage plaques counted on plate with dilution -5. The rest of the phage plaques were counted on plates with dilution -4..... | 48 |
| Table 5 – Protein concentrations of osmotic shock suspensions performed by the Bradford protein assay. | 50 |
| Table 6 – Water bath ultrasonication process data for the different periods of exposure (1, 5, 10, 15, 20, 25, 30 and 40 minutes). Parcels with (-) symbol mean that the number of colonies were not between 30 and 300 which are the acceptable interval for the counting of PFUs. Parcels with the (*) symbol are the ones that belong to phage plaques counted on plate with dilution -8. The rest of the phage plaques were counted on plates with dilution -7. | 53 |
| Table 7 –Protein concentrations of water bath ultrasonication samples performed by the Bradford protein assay..... | 53 |
| Table 8 – 25W probe ultrasonication process data for the different periods of exposure (5, 10, 15, 20, 30 and 40 minutes). Parcels with the (*) symbol are the ones that belong to phage plaques counted on plate with dilution -5. The rest of the phage plaques were counted on plates with dilution -6. | 55 |
| Table 9 – 50W probe ultrasonication process data for the different periods of exposure (5, 10, 15, 20, 30 and 40 minutes). Parcels with (-) symbol mean that the number of colonies were not between 30 and | |

300 which are the acceptable interval for the counting of PFUs. Phage plaques were counted on plates with dilution -6.55

Table 10 –Protein concentrations of 25W probe ultrasonication samples performed by the Bradford protein assay.56

Table 11 – Protein concentrations of 50W probe ultrasonication samples performed by the Bradford protein assay.56

List of Annex Figures

- Figure A 1** – TSA medium plate where the host bacteria was plated using the double agar overlay assay supplemented with MgCl_2 1 M. The filter paper containing the dried phage suspension is placed in the middle of the host plate with TSB medium on top. The clear zone around the filter paper is where the lysis of the host bacteria occurred.....70
- Figure A 2** – Linear calibration curve of BSA concentration in function of the absorbance at 595 nm for the osmotic shock test samples.70
- Figure A 3** – Standard curve of the log of the molecular weight (MW) of the ladder bands versus their migration distance. The tendency line allows the determination of the molecular weight (MW) of the osmotic shock gel with samples from 1 minute to 10 minutes of exposure with a band migration of 1.8 to 4.3 cm. This curve was obtained by the selection of these three values of interest for a more accurate calculation of the molecular weight.71
- Figure A 4** – Standard curve of the log of the molecular weight (MW) of the ladder bands versus their migration distance. The tendency line allows the determination of the molecular weight (MW) of the osmotic shock gel with samples from 15 minute to 30 minutes of exposure with a band migration of 1.7 to 4.1 cm. This curve was obtained by the selection of these three values of interest for a more accurate calculation of the molecular weight.71
- Figure A 5** – Linear calibration curve of BSA concentration in function of the absorbance at 595 nm for the water bath ultrasonication test samples.73
- Figure A 6** – Standard curve of the log of the molecular weight (MW) of the ladder bands versus their migration distance. The tendency line allows the determination of the molecular weight (MW) of the water bath ultrasonication gel for a band migration of 0.5 to 1.4 cm. This curve was obtained by the selection of these three values of interest for a more accurate calculation of the molecular weight....73
- Figure A 7** – Standard curve of the log of the molecular weight (MW) of the ladder bands versus their migration distance. The tendency line allows the determination of the molecular weight (MW) of the water bath ultrasonication gel for a band migration of 1.4 to 3.2 cm. This curve was obtained by the selection of these three values of interest for a more accurate calculation of the molecular weight....74

Figure A 8 – Standard curve of the log of the molecular weight (MW) of the ladder bands versus their migration distance. The tendency line allows the determination of the molecular weight (MW) of the 25 W probe ultrasonication gel for a band migration of 0.8 to 2.0 cm. This curve was obtained by the selection of these three values of interest for a more accurate calculation of the molecular weight....74

Figure A 9 – Standard curve of the log of the molecular weight (MW) of the ladder bands versus their migration distance. The tendency line allows the determination of the molecular weight (MW) of the 25 W probe ultrasonication gel for a band migration of 2.7 to 6.7 cm. This curve was obtained by the selection of these three values of interest for a more accurate calculation of the molecular weight....75

Figure A 10 – Standard curve of the log of the molecular weight (MW) of the ladder bands versus their migration distance. The tendency line allows the determination of the molecular weight (MW) of the 25 W probe ultrasonication gel for a band migration of 10.3 to 19.3 cm. This curve was obtained by the selection of these three values of interest for a more accurate calculation of the molecular weight....75

Figure A 11 – Standard curve of the log of the molecular weight (MW) of the ladder bands versus their migration distance. The tendency line allows the determination of the molecular weight (MW) of the 50 W probe ultrasonication gel for a band migration of 0,4 to 1,7 cm. This curve was obtained by the selection of these three values of interest for a more accurate calculation of the molecular weight....76

Figure A 12 – Standard curve of the log of the molecular weight (MW) of the ladder bands versus their migration distance. The tendency line allows the determination of the molecular weight (MW) of the 50 W probe ultrasonication gel for a band migration of 1,7 to 5,0 cm. This curve was obtained by the selection of these three values of interest for a more accurate calculation of the molecular weight....76

List of Annex Tables

Table A 1 – T4 bacteriophage gene products and their respective functions and molecular weights. Adapted from Clokie et al. and Miller et al.^{72,112}72

List of Abbreviations

| | |
|---------------------------|--|
| ADP | Adenosine Diphosphate |
| AEC | Anion Exchange Chromatography |
| AK | Adenylate Kinase |
| ATP | Adenosine Triphosphate |
| BDDH | Benzene Dihydrodiol Dehydrogenase |
| BED | Benzene Dioxygenase |
| BSA | Bovine Serum Albumin |
| CE | Counter Electrode |
| CFU | Colony Forming Units |
| DNA | Deoxyribonucleic acid |
| dsDNA | Double stranded DNA |
| dsRNA | Double stranded RNA |
| DTT | Dithiothreitol |
| EC | Electrochemical |
| <i>E. coli</i> | <i>Escherichia coli</i> |
| ELISA | Enzyme-Linked Immunosorbent Assay |
| ESKAPE | <i>Enterococcus faecium</i> , <i>Staphylococcus aureus</i> , <i>Klebsiella pneumoniae</i> , <i>Acinetobacter baumannii</i> , <i>Pseudomonas aeruginosa</i> and <i>Enterobacter</i> species pathogenic bacteria |
| Fab | Antigen-binding antibody fragment |
| Fc | Crystallizable antibody fragment |
| GFP | Green Fluorescent Protein |
| GOx | Glucose Oxidase |
| IgA | Immunoglobulin A |
| IgE | Immunoglobulin A |
| IEC | Ion Exchange Chromatography |
| IgG | Immunoglobulin G |
| MOI | Multiplicity Of Infection |
| MW | Molecular Weight |
| OD_{600nm} | Optical Density measured at 600nm |
| PAGE | Polyacrylamide Gel Electrophoresis |
| PCR | Polimerase Chain Reaction |
| PEG | Polyethylene Glycol |
| PFU | Plaque Forming Units |

| | |
|-----------------|---|
| PTFE | Polytetrafluoroethylene |
| RBPS | Receptor Binding Proteins |
| RE | Reference Electrode |
| RNA | Ribonucleic acid |
| scFv | Single-chain Fragment variables |
| SDS-PAGE | Sodium Dodecyl Sulfate Polyacrylamide Gel Electrophoresis |
| SEC | Separation Exchange Chromatography |
| SPR | Surface Plasmon Resonance |
| ssDNA | Single stranded DNA |
| ssRNA | Single stranded RNA |
| TEM | Transmission Electron Microscopy |
| TMPs | Tape Measure Proteins |
| TSA | Tryptic Soy Agar |
| TSB | Tryptic Soy Broth |
| WE | Working Electrode |

1. Introduction

1.1. Background

The emergence of pharmaceutical antibiotics in the mid-20th century, along with the better understanding of disease and sanitation, revolutionized healthcare and drastically improved both quality of life and life expectancy. Antibiotics uncovered a new era in medicine by rapidly becoming an indispensable medical tool ¹. However, the broad and often inconsiderate use of antibiotics in human and veterinary medicine, and also in agriculture, resulted in the widespread antibiotic resistance in a variety of microbiota in several ecological compartments. Because of this, antibiotic-resistant bacteria are a major and increasing global health concern. Among some of the highly resistant species of bacteria include the Gram-positive *Enterococcus faecium* and *Staphylococcus aureus* and the Gram-negative *Klebsiella pneumoniae*, *Acinetobacter baumannii*, *Pseudomonas aeruginosa* and *Enterobacter* species. These bacterial pathogens are commonly known by the acronym ESKAPE ². This increase of resistance is mostly due the lack of early diagnosis, which play an important role in successful identification of the infectious pathogen and its treatment.

Nowadays, the use of biosensor technology in the field of medical diagnostics has allowed a cost-effective, fast, reliable, and easy-to-use sensing platform. Biosensors are analytical devices that utilize recognition elements such as enzymes, nucleic acids and antibodies for the detection of a specific target ³. Because of obstacles like false positives, isolation and purification steps that may be time-consuming and expensive, recent evolutions in biotechnology have created the possibility to develop novel affinity-based recognition elements that overcome the limitations encounter. Bacteriophages are novel innovative recognition elements due to their exceptional characteristics, such as their high affinity and specificity for their targets, fast and cheap production, their stability and ease to be modified ^{2,3,4,5,6,7}.

As naturally-occurring bacterial parasites, bacteriophages are viruses with the capability to infect and kill bacteria. The reproduction of viral bacteriophage particles occurs only within the host cell where their machinery is available to replicate phage's own genome, making these viruses ultimately dependent on the bacterial host for survival ¹. Unlike the wide range of bacteria targeted by antibiotics, bacteriophages are highly specific for the target bacterial host and do not affect other beneficial microbes ^{8,9,10}. A renewed interest in bacteriophage potential emerged in order to control especially multidrug-resistant bacteria ².

Therefore, phage libraries, which consist of a high number of different bacteriophages, each displaying a different protein on their surface, can be used as a target specific recognition element of a biosensor, distinctively the ones with high affinity and specificity for a specie of resistant bacteria ¹¹. With all the recent developments in the enhancement of recognition elements, it becomes crucial to study and improve the current bacteriophage-based biosensors. One possible solution to consider is their

fragmentation in order to generate novel fast and cost-effective recognition elements, based on the tails of *Caudovirale* phages, similar to the generation of antibody fragments.

1.2. Goals and Aim of Study

Current phage-based biosensors for research and medical diagnosis are not completely efficient for target identification once phages, in their native structure, are capable to induce the host bacterial cell lysis upon attachment and infection. This limits bacteria identification and tracking, as well allowing the release of endotoxins and other bacterial toxins.

This Master's Thesis has the objective of generating advanced recognition elements elements for the identification of antibiotic resistant bacteria by fragmentation of bacteriophage's heads from their tails, thus eliminating the infection capacity. By isolating the tails which are the main apparatus of recognition and attachment to the target bacteria, phages would maintain their ability to identify the target without lysing it. The process should be effective and suitable to be applied in a biosensor platform in order to improve the field of medical diagnosis.

To this end, a *E. coli* host strain and a specific T4 bacteriophage were used. The first stage of this experimental study consisted in the rehydration and preparation of the biological material for all experiments, especially a working cell bank and the study of the *E. coli* host strain growth curve. A phage stock was prepared as well by inoculating a *E. coli* culture with a phage stock solution.

The second stage of the experimental plan comprised in the test of mechanical (sonication by water bath and probe sonication) and non-mechanical (osmotic shock) methods to promote the disaggregation of phage tails from their heads. In each disruption process the phages were analyzed by their titre through a double-layer plaque assay and by their protein content through SDS-PAGE and Bradford assay. In the most promising method, phages were visualized by TEM (Transmission Electron Microscopy).

2. State-of-the-Art

2.1. Biosensors – Basic Principles

Increasing public health concerns related to diseases caused by infectious bacteria, as well the need for monitoring food and water supplies, have instigated the interest in the development of low-cost practical pathogen detection systems. The detection and identification of these pathogens rely on conventional microbiological culture techniques and biochemical analysis, which are highly accurate, but unfortunately overly time consuming and cost-ineffective. These assays are based on assessing the ability of bacteria to grow in plates or tubes containing a variety of media, solid or liquid, under several conditions. While the detection of a small number of bacteria is possible by incubation, the growth of bacteria to sufficient number for identification can take various days^{12,13,14,15}.

Alternative reliable and accurate methods for pathogen detection that can overcome the limitations given by conventional methods would be of outmost importance for a quick diagnosis. Advances have been observed in immunological techniques such as Enzyme-Linked Immunosorbent Assay (ELISA), which explores antibody-antigen interactions with the target bacterial strains and can be performed within a working day. Typical ELISA assays are comprised of a number of steps, such as blocking, washing, incubation of primary and secondary antibodies and substrate development. Besides, immunological methods suffer from cross-reactivity of polyclonal antibodies, high cost of production for monoclonal antibodies and the need for sample pre-enrichment due to low sample volume which limits the detection. These can take up to 24h to be complete and may be problematic when rapid detection is a requisite. Polymerase Chain Reaction (PCR) is another technique that allows for amplification of small amounts of the genetic material from bacteria in order to detect these pathogens through nucleic acid complementarity-based specificity. Nevertheless, the process of DNA extraction and PCR techniques require sample enrichment steps, highly trained personnel, its expensive and also time-consuming (1-4h per assay)^{12,13,16,17,18}. **Figure 1** outlines the main steps involved in the analysis of a biological sample by various popular detection methods and time required to reach a conclusive pathogen identity.

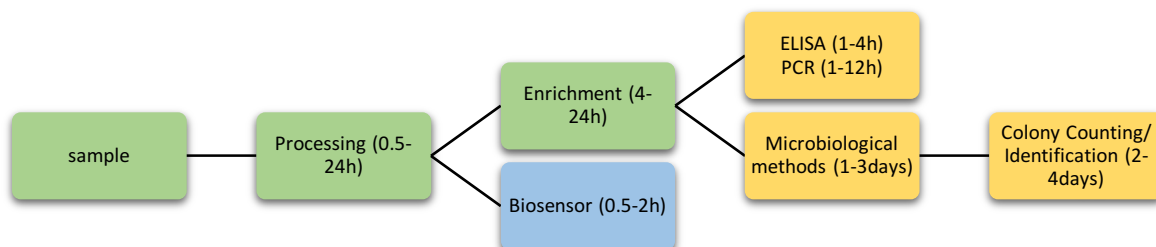


Figure 1 – Flowchart demonstrating the processing steps involved and relative time taken in detecting a pathogen in biological samples. Adapted from Singh *et al.*¹².

Therefore, the development of alternative tools for fast, accurate and sensitive detection of pathogens has raised sustained interest towards the biosensing systems, that would outgrow conventional techniques.

Biosensors are analytical devices able to translate a specific bio-recognition even into a measurable signal. Typically, a biosensor platform couples: i) a sensor platform functionalized with a biological recognition element (bioreceptor/ligand) for specificity binding to the target (analyte); ii) a physical or chemical platform (transducers) capable of convert the biochemical interactions into a measurable digital signal; and iii) a signal amplifier to provide a quantitative estimate of the analyte captured, as it is demonstrated in **Figure 2**. These devices allow for high degree of sensitivity and specificity of detection, minimal sample preparation, cost-effectiveness and reduced overall time required for detection since does not need for sample pre-enrichment. In this way, biosensors can be directly applied for the detection of pathogens^{3,12,13,17,18,19,20}.

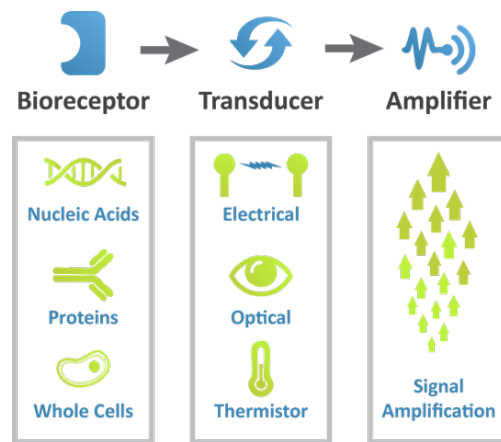


Figure 2 – Schematic basic representation of a Biosensor System. From Innovogene.com – accessed 10th June 2020²⁰.

2.1.1. Signal Transducers

According to the method of signal transduction, biosensors can be generally categorized into four types: electrochemical (EC), optical, calorimetric and piezoelectric.

Generally, the **EC biosensors** are simple devices based on the measurements of electric current (amperometric), charge accumulation or potential changes (potentiometric), or conductance changes in the medium (conductometric/impedimetric) carried out by bioelectrodes^{21,22,23}. The EC sensing normally requires a working electrode (WE), a reference electrode (RE) and a counter/auxiliary electrode (CE) as it is represented in **Figure 3**. The WE act as the transduction element when the interaction between the analyte and the recognition component occurs, whereas the CE measures current and facilitates delivery of electrolytic solution in order to transfer the current to the WE. The RE should be maintained at a distance from the site of biological recognition element and analyte interaction to establish a known and stable potential. Thus, these electrodes need to be conductive and chemically stable in order to be reliable, which is why platinum, gold, graphite and silicon compounds are the most frequently used for WE and CE, whilst the RE is typically silver or silver chloride^{22,24,25}.

An amperometric biosensor device is based on the measurement of current as a result from the ability of certain analytes to be oxidized or reduced in a biochemical reaction. This type of biosensor is most commonly used on a large scale for analytes such as glucose^{21,22,26,27}.

A potentiometric biosensor measures the potential difference between the RE and the WE when zero or no significant current flows between them, allowing the determination of ion activity in a broad range of concentrations. Most used potentiometric devices are pH electrodes, gas electrodes and ion selective electrodes^{21,22,24,25,26}.

Conductometric biosensors are based on the measure of the ability of an analyte to conduct current. Many biochemical reactions between the biomolecules and analytes result in a change in ionic strength, which can be determined by the conductometric device. This happens when the conductivity meter applies an altering current at an optimal frequency between two electrodes and measures the potential. Both the current and the potential measurements are used to calculate the conductance. This type of biosensor is generally used in different analytes such as glucose and urea. Its attractiveness is due to its enhance speed, and suitability for miniaturization^{21,22,24,25,26}.

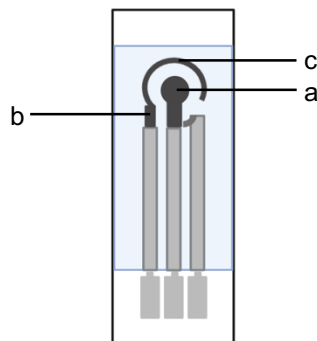


Figure 3 – Electrochemical Biosensor electrodes configuration. (a) working electrode; (b) reference electrode; (c) counter electrode. Adapted from Campaña *et al.*²³.

The **optical transducers** use an optical measurement principle based on the light emission or light absorption by the sample in the ultraviolet, visible, or near-infrared spectrum region. A response is generated when the target analyte is present in the sample and the signal intensity increases with an increasing concentration of the analyte. The working principle of optical transducers is to measure and analyse changes in the optical properties that occur when an analyte binds to the bioreceptor element.

Optical biosensors can be label-free and label-based. Labelled biosensors make use of a label and the optical signal can be generated by a colorimetric, fluorescent or chemiluminiscent method. The most explored is fluorescence quantification due to the fact that most fluorophores are sensitive to environmental changes, which is fundamental to sensing applications. In this way the detection of multiple compounds in a single device can be accomplished by monitoring different wavelengths. When the analyte is detected, the fluorescent signal is transduced and measured^{21,24,25,26,28}.

In label-free detection, the signal is generated when the analyte interacts with the transducer. The most widely used label-free detection makes use of surface plasmon resonance (SPR) which bears analytes that are not labelled to be detected in their natural form, directly and in “real time”. When the analyte interacts with the immobilized recognition element, a change in the refractive index occurs and a measurable shift in the SPR angle due to mass change is detected at the biosensor surface as it is represented in **Figure 4**^{22,28}.

Optical biosensors own a great advantage when the response is in the range of visible light, thus, these biosensors discard the need for reading results equipment, making them appealing for portability. The most common applications for optical biosensors are the determination of glucose levels in the blood, cancer detection, inflammatory, cardiovascular, and neurodegenerative diseases, viral infections, and drug screening^{21,26}.

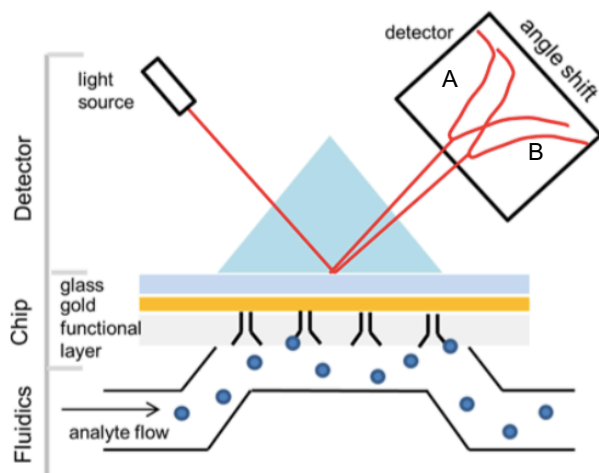


Figure 4 – Principle of SPR detection. Antibodies are immobilized onto the gold surface of the sensor. When light passes through a prism onto the sensor, it reflects the angle A and its measured by a detector. A sample containing the target analyte passes through the flow cell and binds to the antibody, making a change in the refractive index, resulting in the angle B. This change in SPR angle is proportional to the mass bound to the sensor chip surface. From Damborsky *et al.*²⁸.

The **thermal/calorimetric** type of transducer is able to detect heat differences when a biochemical reaction between the biorecognition element and the target analyte occurs with the support of a thermostat. The change in temperature can be correlated to the number of reactants consumed or products formed, hence the concentration of analyte. The major advantage of using this type of transducer is its high sensitivity where the thermostat is capable of detecting temperature changes in the range of 0.0001–0.05°C. These biosensors can also detect concentrations of sample as low as 10⁻⁵M and are very stable^{21,24,25,26}.

At last, **piezoelectric sensors** work on a principle of affinity interactions to which are sensitive to changes in mass, density or viscosity of the samples. This type of biosensor generates electrical signals in response to the applied mechanical pressure and gathers a biorecognition element with a piezoelectric component, usually a quartz crystal coated with a gold electrode. When an interaction between the

biorecognition elements and the analytes occur on the surface of the crystal, there is an increase in the mass, resulting in change of oscillation frequency. The change in frequency is proportional to the mass bound to the crystal and can be measured electrically. The most widely used devices are the quartz crystal microbalance and the surface acoustic wave. Piezoelectric biosensors are considered the most sensitive sensors when compared with others and can be used to detect pathogens, gases, pesticides and hormones, among others^{21,24,25,26,29}.

Figure 5 shows a schematic representation of the basic principles behind any biosensor device.

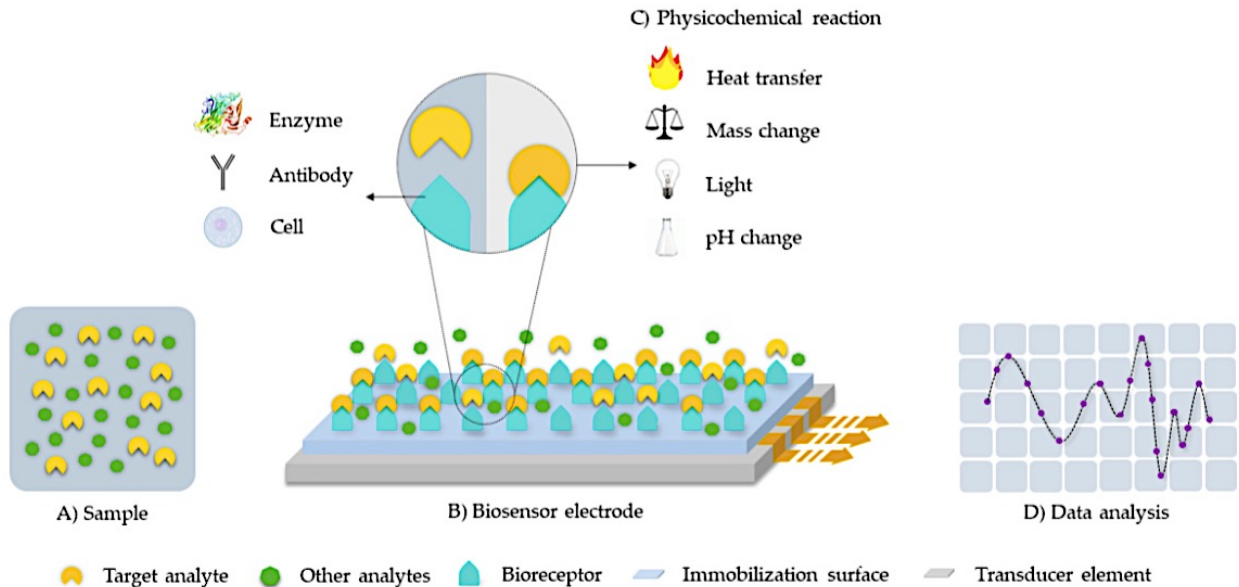


Figure 5 – Schematic representation of a typical biosensor system. (A) Sample where the target analyte is present; (B) The target analyte binds to the biorecognition element. in the biosensor electrode, which is composed by the bioreceptor, the immobilization surface and the transducer element; (C) Physicochemical reaction occurs between the analyte and the bioreceptor; (D) Signal generated is translated by the aid for a transducer. From Campaña *et al.*²³.

2.1.2. Recognition Receptors

Ideal attributes for any recognition element would be high stability, ease of immobilization on the sensor platform and recognition specificity towards the target analyte with minimum cross-reactivity interference. The classical recognition elements include enzymes, nucleic acids, whole cells and antibodies. Recent and advanced recognition elements, such as aptamers, affibodies and bacteriophages improved the analytical performance of biosensors and are mainly associated with more rapid synthesis or easiness in integrating sensor transducer^{12,30,31}.

- **Enzymes**

Enzymes are the most commonly exploited biological elements in biosensors. Enzymes are biological catalysts that can selectively react with specific substrate/target analyte^{25,30}. The substrate (S) to be detected diffuses into the enzyme layer, where the enzymatic reaction occurs, resulting in a product (P)

or consuming co-reactant (R), which can be measured by the transducer. This reaction is represented in **Equation 1**.



There are several mechanisms by which enzymes allow analyte recognition. For instance, enzymes may react directly with the analyte, generating a detectable product, but enzymes can also be inhibited by the analyte, which is associated with a decrease in enzymatic product formation^{26,31}. Enzyme-based biosensors can be either EC or optical sensors^{26,32}. The most commonly used enzyme biosensors in the clinical sector have been designed for glucose, urea, lactate, glutamate and cholesterol detection^{25,30}. The principle of glucose measurement depends on the interaction of glucose oxidase (GOx) with glucose present in the sample. GOx is considered the classic enzyme used in biosensors due to its higher selectivity towards glucose. In EC biosensors, the immobilized GOx catalyses the oxidation of glucose which results in the production of gluconic acid and hydrogen peroxide. Hydrogen peroxide is then re-oxidized and there is the release of electrons. The number of electrons transferred is proportional to the number of glucose molecules present in the blood²⁵.

- **Nucleic Acids**

The basic principle used for nucleic acid-based (DNA or RNA) detection, the basic principle is sequence complementarity. Complementary DNA or RNA strands are immobilized into a suitable transducer surface, and exposed to a sample solution that may contain the DNA or RNA fragments of interest. The specific binding between the DNA or RNA probe with its complementary target strand results in a hybridization event^{3,12,25,30,31}.

The major advantage of using DNA-based probes is the ability to amplify a desired target DNA sequence from the target pathogen using PCR and consequently increase the signal generated by the biosensor in the event of hybridization on the detection platform. RNA could also be amplified by reverse transcription PCR using RNA polymerase enzymes for the similar effect¹². These nucleic acid-based probes are highly stable in a variety of solvents and buffers, and are able to provide sensitive, selective, rapid and accurate detection of nucleic acid hybridization^{12,13,25}. However, the use of PCR technique for amplification, strongly relies on the purity of the template nucleic acid, and therefore, are prone to contaminations that would be amplified and result in false positives^{12,13}. Among the several transducers available, the ability of EC biosensors to identify nucleic acids directly in complex samples makes it the most suitable choice²⁵. For instance, the analysis of nucleic acids can be used as a valuable tool for genetic diagnostics in order to detect a complementary sequence that is specific to a particular disease^{25,30}.

- **Aptamers**

Aptamer ligands are short oligonucleotide (single stranded DNA or RNA) or peptide molecules capable of binding with high affinity and specificity to a wide range of targets, such as large and small

proteins, drugs, toxic compounds and cells^{3,25,26,31,32,33}. These ligands are produced *in vitro* by a method called Systematic Evolution of Ligands by Exponential Enrichment (SELEX) and have the ability to fold into defined three dimensional conformations, which allow and facilitate specific interactions with the target molecules by complementary shape and not their sequence^{3,26,31,32,33}. Because of these folding abilities, high binding affinity, simple synthesis, resistance to degradation and chemical stability, aptamers have become an important tool for diagnosis and therapeutics. In spite of these advantages, there is still limited availability of aptamer types and poor knowledge on their immobilization on transducer surfaces^{25,26,31,32}.

Optical and EC biosensors can both be used to detect binding events between aptamers and their target molecules^{3,33}. DNA aptamers can be used for the detection of a cancer marker related to the growth and metastasis of several tumors called angiogenin, a very promising strategy to perform a simple, rapid and sensitive diagnostic³¹.

- **Affibodies**

Affibodies are small artificial recognition elements based on proteins, engineered in the laboratory with high affinity and specificity to bind any target protein or peptide after their isolation, imitating monoclonal antibodies³¹. Affibodies were originally derived from the B-domain (the immunoglobulin G binding domain) of protein A or G and can be expressed via fusion with other protein. The B-domain was then mutated at a key position in order to enhance chemical stability, resulting in a variant denoted Z-domain. The engineered Z-domain affibody was able to retain the favourable folding and stability properties, as well the affinity for the constant region of the antibody^{31,34}.

In contrast to monoclonal antibodies that can be generated by immunization of laboratory animals combined with hybridoma technology, the isolation of affinity proteins based on non-immunoglobulin scaffolds is performed by synthetic combinatorial affibodies libraries. These libraries are composed of a large number of affibody molecule variants generated by combinatorial randomization of 13 amino acid positions. Affibody molecules are mainly used in biochemical researches for new pharmaceutical drugs, and can also be used for biorecognition in diagnostic and therapeutic applications. Affibodies may be used in EC biosensors in order to detect their respective target proteins such as IgA, IgE, IgG and insulin^{31,34,35}.

- **Whole Cells**

Living organisms such as bacteria, fungi, yeasts, animal or plant cells, also have been used as a recognition element in biosensor. These whole cell sensors are able to detect responses of cells after exposure to the sample, measuring the general metabolic status of such living organisms. In this way, growth inhibition, cell viability, respiration activity (concentrations of oxygen) and substrate uptake can be measured by the transducer^{11,26,30,36,31}. Whole cell biosensors gained interest because they are typically cheaper to obtain than isolated enzymes, they don't require purification steps and have a low cost of preparation. However, biosensors developed with this type of recognition elements tend to demonstrate longer response times and possible loss in selectivity as they often contain a mixture of enzymes^{26,30,36,31}.

Potentiometric EC sensors and optical sensors are the most commonly used to detect binding events between whole cells, particularly *Escherichia coli* bacterial strains, and their target analytes. For instance, a whole cell biosensor with two recombinant *E. coli* strains as recognition elements has been studied for the monitoring of environmental benzene contamination in air samples.^{30,31,37}

- **Antibodies**

Antibodies have long been the most popular affinity-based recognition elements used in biosensors due to their extremely high degree of specificity towards define antigens. Antibodies are Y-shaped proteins produced by living organisms, usually by a defence mechanism against invading bacteria or viruses. Based on their selective properties and synthesis protocol, antibodies can be classified as monoclonal or polyclonal; or as natural or recombinant antibodies^{3,11,25,26,31,32,38}.

A monoclonal antibody is derived of a humoral immune response from a single B-cell clone and can be produced by the hybridoma technique. Monoclonal antibodies recognize only one specific antigen region, named the epitope, with equivalent affinity, and are more selective than polyclonal antibodies^{3,11,26,31}. These antibodies may offer some drawbacks as they also suffer from physical instabilities (temperature and pH changes), chemical and enzymatic damage, and present cost-intensive methods of production, isolation and purification. Besides, monoclonal antibody production raises several ethical problems of the use and sacrifice of animals^{12,13,16,17}.

Polyclonal antibodies derive from numerous B-cell clones and are capable of recognizing multiple antigen epitopes from different locations. These antibodies are harvested from animals such as rats, rabbits or sheep, therefore is possible to develop a selective antibody for almost any antigen. These type of antibodies can easily be generated, but varying affinity specificity that may present cross-reactivity towards other species, strains and molecules, can create barriers when polyclonal antibodies are used as a probe in biosensors^{3,11,12,13,16,17,26,31,39}.

Additionally, there are recombinant antibodies that consist in genetically engineered common antibody molecules produced by expressing the antibody genes in a microbial or mammalian host cell. Both full antibodies, their fragments or engineered versions are possible to obtain. Recombinant antibodies are less expensive and time consuming to produce²⁶.

A variety of signal transducers, such as optical and EC sensors have been explored for antibody recognition element assays. These are essential for clinical diagnosis, as for the detection of cancer biomarkers, infection biomarkers, human serum albumin, and others^{3,25,31,32}. The process to which antibodies are immobilized to the transducer surface is known to influence the performance of the biosensor. A higher or lower amount of antibodies available for interaction appears to be dependent on the orientation of the immobilized molecule. A random antibody immobilization method may occur by adsorption, covalent binding using a bifunctional linker, or by biotin and streptavidin interactions. Random immobilization may lead to inaccessibility of the active binding site of the antibodies to the antigen molecules, so the best approach to avoid immunological inactivity is to address an oriented immobilization method. An oriented

antibody immobilization includes oxidation of carbohydrate side chains mostly located in the (crystallizable fragments) Fc region of the antibody, followed by a reaction with the amine groups on the support. As an alternative, disulfide bridges in the hinge region of the antibody may be reduced to active thiol groups, favoring the direct immobilization over gold surfaces or through a maleimide functional linker. Another option for site-directed immobilization is through affinity binding of immobilized protein A or G towards the constant region of the antibody, avoiding chemical modifications frequently associated with loss of immunological activity³⁸. **Figure 6** shows all methods for antibody immobilization on solid transducer surfaces.

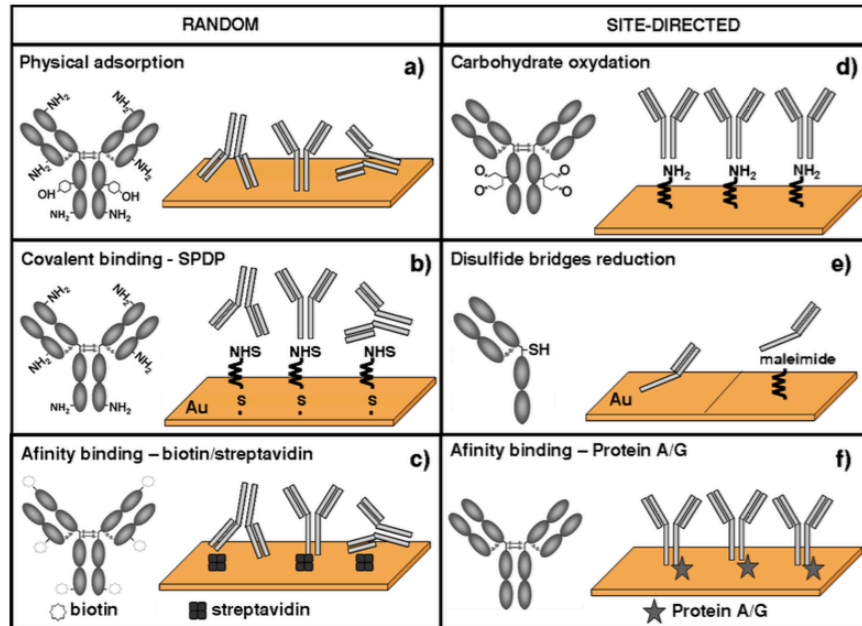


Figure 6 – Schematic representation of random and site-directed methods for antibody immobilization on solid transducer surfaced. (a) Random physical adsorption through hydrophobic or electrostatic interactions; (b) Random covalent binding of antibody amine groups; (c) Random affinity binding by biotin streptavidin interactions; (d) Site-directed immobilization through oxidized carbohydrate side chains over amine surfaces; (e) Site-directed immobilization through thiolated antibody fragments into gold surfaces or maleimide functional linkers; (f) Site-directed immobilization through affinity binding between protein A or G and the constant region of the antibody. From Martins *et al.*³⁸.

As antibodies in general are chemically and structurally complex and heterogeneous, several limitations are observable regarding their interactions with the biosensor surface. As a result, the cleavage of antibodies into different molecule fragments have been explored and optimized for affinity and/or stability to improve the development of a robust antibody-based recognition element that owns specific characteristics³⁹. Antibody fragmentation is accomplished by proteases able to cleave certain regions of the antibody structure. Antibody fragments can be divided into two main groups of interest, such as the antigen-binding fragments (Fab) and the crystallizable fragments (Fc) that interacts with the target surface receptors. **Figure 7** shows a representation of some antibody fragments, which include single-chain Fragment variables (scFv), Minibodies, Fab, Diabodies, Fab', Triabodies, scFv-Fc and F(ab')₂^{39,40,41}.

Due to their small size, antibody fragments possess several advantages over intact antibodies, especially for experimental applications and immobilization of the biosensor surface, among them the reduction of non-specific binding resulting from the Fc interactions since many targets have receptors for the Fc domain; and small fragments generally provide higher sensitivity in antigen detection as a result of reduced barrier from large protein epitopes. Although antibody fragmentation improves the recognition of biological molecules, fragmentation is laborious and requires a large supply of antibodies to make it reasonable efficient^{39,40}.

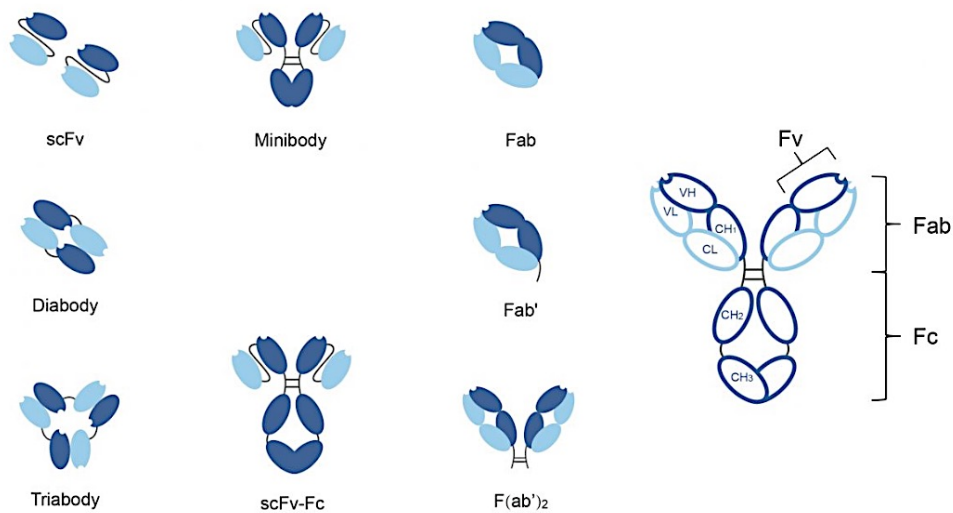


Figure 7 – Schematic representation of different formats of antibody fragments including single-chain Fragment variables (scFv), Minibodies, Fab, Diabodies, Fab', Triabodies, scFv-Fc and F(ab')₂. From BIOLOGICS International Corp – accessed 19th June 2020⁴¹.

As it was described, there are several biorecognition elements of choice for biosensor systems, each of them presenting their advantages and limitation. In **Table 1** there is represented a summarized pros and cons for all recognition elements mentioned.

Table 1 – Advantages and limitations of recognition elements for biosensor systems. Adapt from Singh *et al.*, Eggins and Justino *et al.*^{12,30,31}.

| Recognition Elements | | Advantages | Limitations |
|----------------------|-----------------------|--|--|
| Classical | Enzymes | <ul style="list-style-type: none"> - Specificity - Simple procedures | <ul style="list-style-type: none"> - Expensive isolation and purification - Efficient only at optimal pH and temperature - Time consuming |
| | Nucleic Acids | <ul style="list-style-type: none"> - Stability | <ul style="list-style-type: none"> - Limited target (only complementary nucleic acid) - Rely heavily on purify templates |
| | Whole Cells | <ul style="list-style-type: none"> - Low cost preparation - Reduced purification requirements | <ul style="list-style-type: none"> - Longer response times - Less selectivity (due to enzymes) |
| | Antibodies | <ul style="list-style-type: none"> - High affinity - High specificity | <ul style="list-style-type: none"> - Production may require the use of animals - Laborious production - Limited target (protein) - Lack of stability (pH and temperature variations) |
| | Fragmented Antibodies | <ul style="list-style-type: none"> - Reduction of non-specific binding - High specificity - High affinity | <ul style="list-style-type: none"> - Laborious production - Requires large supply of antibodies to be efficient |
| Recent | Aptamers | <ul style="list-style-type: none"> - High affinity - Ease to modify - Possibility to design structure - Thermally stable - Resistance to degradation - <i>In-vitro</i> synthesis | <ul style="list-style-type: none"> - Limited availability of aptamer types and poor knowledge on their immobilization on transducer surfaces |
| | Affibodies | <ul style="list-style-type: none"> - Lack of disulfide bonds that enable intracellular applications | |
| | Bacteriophages | <ul style="list-style-type: none"> - High specificity and affinity towards target bacteria - Able to self-reproduction - High stability | <ul style="list-style-type: none"> - Lost of detection signal in a biosensor system due to the lyse of the target cell |

2.1.3. Immobilization Techniques

In order to make a viable biosensor with efficient performance, the biological components need to be properly attached to the surface of the transducer. The process of immobilization depends on factors such as the physical and chemical properties of the analyte, nature of the biological elements, type of transducer used, and the operating environment of the biosensor²⁵. There are five methods for biomolecule immobilization as represented in **Figure 8**.

Adsorption is the simplest method of immobilization and consists in adsorption of the biological element onto the surface of the transducer. However, the bonding is weak which makes it the least stable technique. The forces linking the biorecognition element to the transducer in a physical adsorption are primarily weak van der Waals forces and electrostatic interactions, with occasionally hydrogen bonds, whereas chemical adsorption is stronger and involves the formation of covalent bonds. This method is often used for short-time and exploratory studies^{22,25,30,36}.

Crosslinking method consists in the binding of two or more molecules by covalent bonds. For this, usually the biocomponent is attached to the transducer with the support of crosslinking/bifunctional agents in order to increase the attachment. The involved functional groups are $-NH_2$, $-COOH$, $-OH$ and $-SH$. This type of immobilization needs to be performed under mild conditions such as low temperatures, low ionic strengths and pH in the physiological range^{21,22,23,25,30,36}.

Entrapment procedure involves the preparation of a polymeric gel solution containing the biorecognition element that is to be “entrapped” within the gel matrix. The most commonly used polymers are polyacrylamide, starch gels, nylon and conductive polymers. However, this method can give rise to barriers in the diffusion of the analyte, leading to a delay in the reaction and hence the response time of the sensor. Also, there may be a loss of bioactivity occurring through the pores in the gel^{21,22,25,30}.

Encapsulation method works by confining the biological element between two semipermeable membranes. The most common types of membranes used are the polytetrafluoroethylene (PTFE), also known as Teflon, and cellulose acetate membrane. This technique allows a close attachment between the biomaterial and the transducer, there is a high degree of specificity, good stability to changes in temperature, pH and ionic strengths, and also a minimal contamination and biodegradation occurring^{22,23,30}.

The choice of the appropriate method of immobilization onto the surface of the biosensor depends on the bioreceptor to be used, as well as its characteristics.

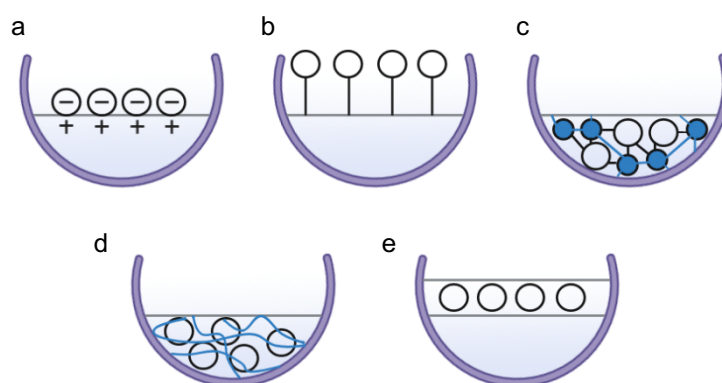


Figure 8 – Schematic representation of immobilization methods for the biological element. (a) Physical Adsorption through electrostatic interactions; (b) Covalent Binding to the transducer surface; (c) Crosslinking immobilization; (d) Entrapment within a polymer gel; (e) Encapsulation between two semipermeable membranes. Image created in BioRender.com, adapted from Kumar and Upadhyay and Campaña *et al.*^{21,23}.

Recent evolutions in biotechnology and nanotechnology have created the possibility to develop novel affinity-based recognition elements to be used in biosensors. Bacteriophages offer an enormous potential as alternative probe for specific biosensing due to their exceptional characteristics, such as their high affinity and specificity for their targets, especially bacterial pathogens; their fast, cheap and animal-free production; their stability and their easy modification. Bacteriophages possess a significant advantage over antibodies and other biorecognition elements since they are able to self-reproduce themselves inside a host cell during the infection process. These properties make bacteriophages a unique class of recognition molecules that can be explored not only for bacterial pathogen detection, identification and binding on a biosensor system, but also as potential vehicles for diagnostics and therapeutics of bacterial diseases^{11,12,13,16,17,42}.

2.2. Bacteriophages

Viruses are tremendously small infectious particles in which they exist in a vast variety of forms and are able to infect almost all living systems, such as animals, plants, insects and bacteria. All viruses are composed by a nucleic acid genome (DNA, RNA or both) surrounded by a protective stable capsid and occasionally by additional complex layers. To insulate the capsid, viruses can have an envelope around the protein capsid (enveloped viruses) or only have a protein coat (“naked” or non-enveloped viruses)⁸. To complete their life cycle and proliferation process, viruses have two major phases, one in which they are qualified to live outside the host cells and other within them. The reproduction of viral particles occurs only within the host cell where their machinery is available to replicate their own genome and essential proteins, so, once outside, the viruses stay inert for long periods of time even on harsh conditions^{8,9}.

The study of viruses’ morphology allowed to distinguish them by size, shape and structure, which became the key characteristics for their description. Viruses may have a circular or oval shape, and some of them possess a distinctive heads and a tail. The smallest viruses are around 20 nm in diameter and the largest around 500 nm⁸. Depending on the organism to infect, viruses take different classifications. Bacteriophages for instant, are bacterial viruses with strongly efficient nanomachines able to specifically and effectively infect bacteria⁴³. Bacteriophages, also known as phages, cover a unique position in biology since they are the most abundant microorganisms in the biosphere with 4.8×10^{31} phage particles estimated⁴⁴. These viruses can be found in very large numbers wherever their hosts lives – in sewage, soils, deep thermal vents and in natural bodies of water^{45,46}. All bacteria in general are susceptible to the infection of the bacteriophages, while for all of the remaining organisms, including humans, phages are inoffensive^{47,48}.

2.2.1. Early History – Research and Discovery

Bacteriophages gone unnoticed for almost 40 years after the beginning of serious bacteriological studies in Europe and America. In 1896, the British bacteriologist Ernest Hanbury Hankin, reported that the waters of the Jumna and Ganges Rivers in India had unexpected antibacterial properties against many kinds of bacteria such as the *Vibrio cholera*⁸. Hankin verified that this antiseptic activity would persist after

water filtration but was destroyed by boiling⁴⁷. Some years later, in 1901, the German bacteriologists Emmerich and Löw, reported as well that some substance present in their cultures was able to cause not just the lysis of several cultures, but also to cure experimental infections and provide immunity to subsequent inoculations^{47,49}. At those times it was difficult to provide reliable interpretations on what that substance was, making it difficult to be completely sure if those observations in the early studies were compatible with the action of bacteriophages.

Phages were first discovered and initially characterized by the English microbiologist Frederick Twort in 1915 when he discovered a small agent that was able to kill colonies of *Staphylococcus* bacteria in growing cultures, creating zones of clearance in his *Staphylococcus* plates, as he described⁴⁷. Twort could not explain the observed event and provided his own description as “the eaten edges of the colonies of *Staphylococcus*”¹⁰. His interesting observed colonies appeared to be mucoid watery colonies. This event could be induced in other colonies by inoculation of fresh bacteria with a portion of those watery colonies, and could be propagated indefinitely⁴⁷. With his findings he hypothesized that the observable antibacterial activity could be due to a virus (phage)⁵⁰.

The “bacteriophage phenomenon” era continued independently with the French-Canadian microbiologist Felix d’Herelle in 1917, as he discovered a microbe that experienced the bacteriophage behavior on severe hemorrhagic dysentery⁵¹. The main observation that d’Herelle made was that cultures of the dysentery disease bacteria disappeared with the addition of a bacteria-free filtrate from sewage⁴⁷. He conceived of these invisible microbes as ‘bacteriophages’, a word derived from the fusion of ‘bacteria’ and ‘phagein’, in which stains for eaters in Greek⁵². Thus, bacteriophages are also called ‘bacteria eaters’ given the fact that they are capable of naturally injecting their genome into the bacteria’s cytoplasm, infect and hijack the bacteria’s metabolic mechanisms in order to replicate, and lead to the death of the host cell⁴⁴. Consequently, bacteriophages were primarily described by Twort and d’Herelle bearing in mind their three predominant features: formation of holes (zones of clearance) in bacterial lawns, dissolution of bacterial and clarification of bacterial culture broths⁹.

2.2.2. Bacteriophage Biology – Diversity

As it was mentioned, bacteriophages are viruses that only infect specific bacteria. They present themselves with high morphological diversity, each carrying its genome from one susceptible bacterial cell to another in which it can direct the production of more phages^{47,53}.

Despite the large diversity of phages, about 96% (around 5360) of all reported phages in the scientific literature to date carry a tail and possess dsDNA as genetic material^{54,55}. Phage tails can either be short, long, contractile or non-contractile^{8,9}. These tailed phages belong to the *Caudovirales* order and constitute the largest and most widespread group of bacterial viruses^{8,47,55}. The *Caudovirales* order can be grouped in three phylogenetic related families according to their type of tail: *Podoviridae*, *Myoviridae*, and *Syphoviridae* as demonstrated in **Figure 9**. Regarding the *Podoviridae* phages which represent 14% of tailed phages, possess short non-contractile tails. The family of *Myoviridae*, phages comprise a long

contractive tail consisting of a sheath and a central tube, representing 25% of tailed phages. At last *Siphoviridae* family is composed by 61% of all tailed phages, comprising long and non-contractile tail^{8 47}. Phage particles that belong to the *Caudovirales* order (tailed phages) are also not enveloped, their genome is enclosed in an icosahedral (polyhedral with 20 faces) capsid and their tails are helical⁴⁷.

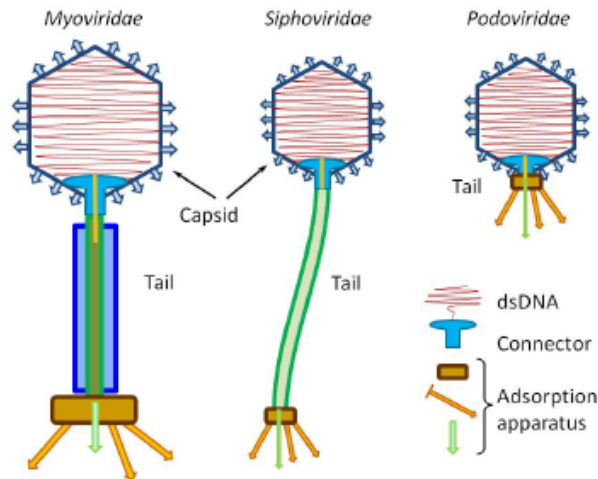


Figure 9 – Schematic representation of bacteriophages from the families *Myoviridae*, *Siphoviridae* and *Podoviridae* belonging to the order *Caudovirales*. From Kurtböke⁸.

Tailless phages only include about 190 known viruses, corresponding to less than 4% of all reported phages. They are classified into 10 small families which sometimes include only a single genus and species. These families may differ in crucial properties and constitute several independent phylogenetic groups⁵⁶. Tailless phages include enveloped and non-enveloped ones and can be grouped in three types: Polyhedral, Filamentous and Pleomorphic phages⁴⁷. Polyhedral phages may have a DNA or RNA genome and are composed by icosahedral capsid shape and cubic symmetry. This group include 5 families: *Microviridae* (ssDNA), *Corticoviridae* (dsDNA), *Tectiviridae* (dsDNA), *Leviviridae* (ssRNA), *Cystoviridae* (dsRNA)⁴⁷. Filamentous phages comprise helical symmetry with only 3 families: *Inoviridae* (ssDNA), *Lipothrixviridae* (dsDNA), *Rudiviridae* (dsDNA)⁴⁷. Pleomorphic phages present themselves in variable shapes without obvious symmetry axes, which are composed of a small number of known phages, can be divided in 2 families: *Plasmaviridae* (dsDNA), *Fuselloviridae* (dsDNA)⁴⁷.

Figure 10 demonstrates an illustration of all types of bacteriophages according to their tail morphology.

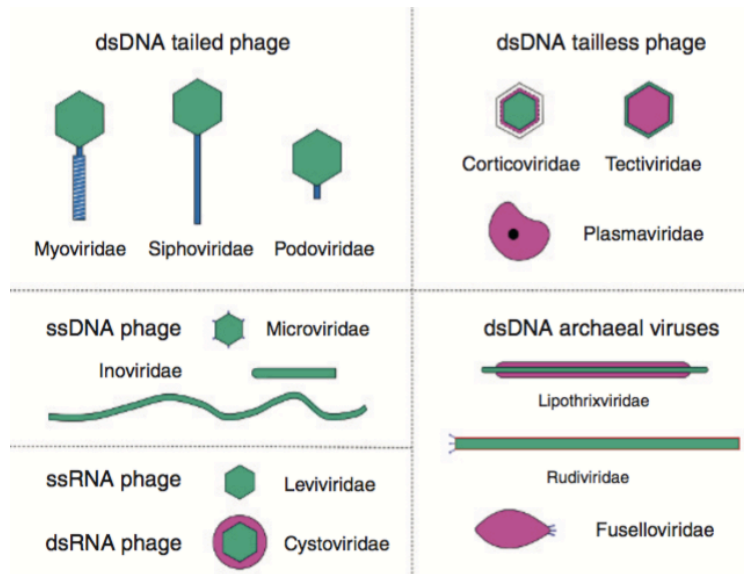


Figure 10 – Schematic representation of tail morphology of different families of bacteriophages. Green represents genetic material enclosed by the capsid. Blue indicates tails and other adsorption organelles such as tail fibers. Diagonal lines in *Myoviridae* tail shows its contractile capability. Pink represents lipids. *Plasmaviridae* are unusual budding viruses which lack of cell wall. From Schaechter⁹.

2.2.3. Bacteriophage Biology – Morphology

The *Caudovirales* order is the largest and most widespread group of bacterial viruses, which each phage particle is typically a well-defined three dimensional structure containing the nucleic acid genome (DNA or RNA) enclosed in a protein or lipoprotein isosahedral capsid, a highly specialized and extremely efficient phage component required for infecting its hosts. The capsid is composed of many copies of one or several different proteins and have a very stable organization.

In order to provide interaction with bacteria and release of its genetic material, the bacteriophage owns additional structures such as a spiral contractile tail (or sheath) and usually six tail fibers connected to a baseplate, presenting the receptor-binding proteins as it is demonstrated in **Figure 11**. The tail is attached to the capsid though a connector which serves as an adaptor between these two crucial components of the phage. The baseplate hub is responsible for recognition of specific molecules at the surface of the bacterial membrane. The tail serves both as a signal transmitter and as a pipeline through which DNA is delivered into the bacteria during the infection process^{8,47,48,57}.

The target host for each phage is a specific group of bacteria. This group is often a subset of one species, but several species can sometimes be infected by the same phage. Estimates suggest about 10 different bacteriophages for every bacterial cell, some of which are highly specific for their bacterial host. Therefore, bacteriophages can either be monophages if they recognize only one type of receptor in the bacteria membrane, or polyphages if they display of a wide host range and recognize more than one type of receptor^{8,9,47,48}.

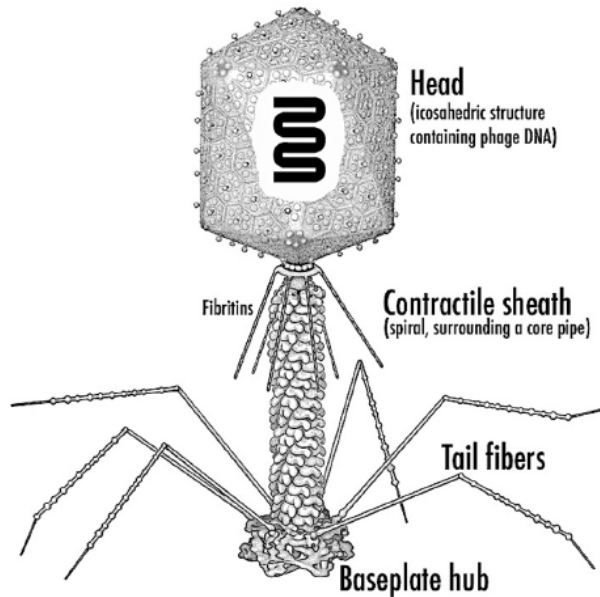


Figure 11 – Schematic representation of a bacteriophage particle. The phage DNA is protected by the isosahedral protein capsid which is attached to the contractile tail. The hexagonal baseplate coordinates the movement of the tail fibers that initially senses the presence of the host. From Harada *et al.* ⁴⁸.

2.2.4. Mechanisms of Phage Proliferation

Specific receptors on the surface of the host bacteria are required for the phage to recognize and infect them. Due to this specificity between the receptor present on the bacteria cell surface and the bacteriophage, bacteriophages can infect specific host only. Since bacteriophages do not have specific structures responsible for virion motion and, consequently, they cannot move independently, the attachment process is the result of random phage-cell collision. The infection process itself involves several detailed and tightly programmed steps in which its efficiency and timing are affected by the host metabolic state ⁴⁷. **Figure 12** outlines the main steps involved in phage proliferation mechanism ⁵⁸.

- **Attachment**

The process is initiated with the attachment on the host surface. A specific bacteriophage strain is known to be able to infect a narrow host range of microbial species and thus, such specificity in interaction is determined by specificity of adsorption, which is the key mechanism in virus recognition to attach onto the host cell surface. Because of its specificity, the attachment is dependent on the nature and structural characteristics of bacterial cell surface receptors ⁵⁹.

Adsorption by tailed phages starts when specialized adsorption structures (fibers) bind to specific surface molecules localized in the target host bacteria. This phage-bacteria interaction differs accordant to type of bacteria. In Gram-negative bacteria, the phage genome must pass through the outer membrane, periplasmic space, peptidoglycan layer and inner membrane in order to inject its genetic material and replicate. The outer membrane of Gram-negative bacteria has an external lipopolysaccharide layer and

embedded outer membrane proteins (OMPs) for transport and diffusion of nutrients, which are able to act as phage receptors. As for Gram-positive bacteria, peptidoglycan interspersed with acid polysaccharides and teichoic acids which can act as receptors for their specific phages as well ^{55,59,60,61,62}.

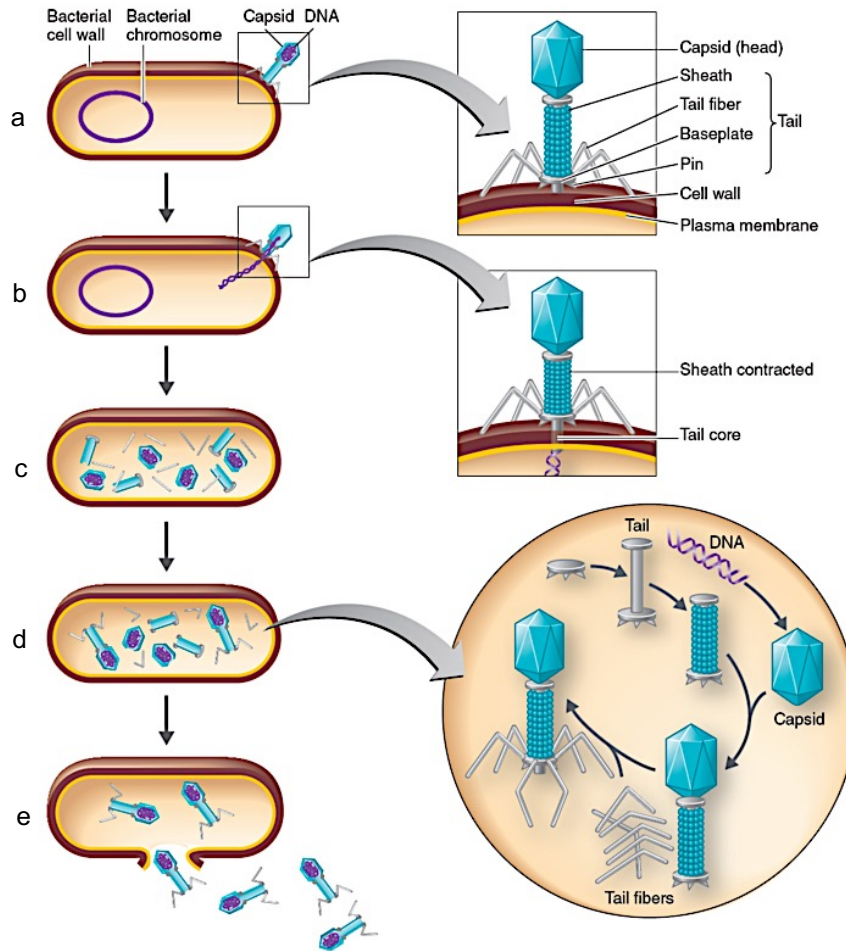


Figure 12 – Schematic representation of the phage proliferation mechanism. (a) Attachment of the phage to the host surface receptors; (b) Penetration and injection of the phage genetic material; (c) Biosynthesis of viral nucleic acid and proteins and structural components; (d) Maturation and assembly of the phage progeny; (e) Host cell lysis and release of phage progeny. From Quizlet.com – accessed 9th June 2020 ⁵⁸.

- **Penetration**

Bacteriophages, like any other viruses are obligate intracellular parasites, so successful penetration into the host bacterial cell is an essential condition for continuation of their lifecycle ⁴⁷. The process of penetrating the bacteria cell varies in different phage groups. Typically, *Caudovirales* bacteriophages insert their genetic material into the host's intracellular environment by using a syringe-like movement of their tail. When the surface binding is irreversible, with the help of ATP, the contraction of the phages' tail takes place, along with the injection of the genetic material. On other hand, tailless phages, which have no tail present,

insert its genetic material after enzymatically degrading a portion of the bacterial cell membrane through their small tail fibers^{55,60}.

Since the morphology of each bacteriophage can differ from long contractile, long non-contractile, short non-contractile tailed phages to tailless phages, the strategies of attachment and penetration to the host bacteria also varies, as represented in **Figure 13**⁶³.

T4 bacteriophage, which belongs to the *Myoviridae* family, has a long contractile tail and is able to infect Gram-negative *E. coli* cells. During the attachment process to the cell surface receptors, the T4 tail baseplate undergoes a change in shape from hexagon-to-star shape, and a contraction signal is transferred from the baseplate to the sheath, triggering sheath contraction. The force of this contraction leads to the penetration of the tail tube in the inner membrane of the bacterial host cell^{63,64}.

The non-contractile tailed T5, HK95 and λ phages, belong to the *Syphoviridae* family and comprise the largest group of bacteriophages, which infect both Gram-negative and Gram-positive bacteria. T5, HK95 and λ bacteriophages, specifically infect *E. coli* cells. Some studies refer that the tape measure proteins (TMPs) present in the tail of these phages, assemble to form a channel that bridges the outer and inner membranes of the host cell for genome release by interacting with the host membrane channel proteins. The similar process has been suggested for non-contractile tailed phages that infect Gram-positive bacteria.

The ϕ 29 bacteriophage infects Gram-positive *Bacillus subtilis* cells and belongs to the *Podoviridae* family. Their short non-contractile tail comprises an enlarged end knot and is long enough to span the cell wall and membrane. The tail knot is composed of a long loop of gp9 proteins which block the tube structure. Structural analysis show that once the phage is attached to the host, the loop of gp9 exits and the DNA injection is allowed^{63,65}.

The T7 phage belong to the *Podoviridae* family and infects Gram-negative *E. coli* cells. These phages have a short non-contractile tail that is not long enough to span the cell wall and membranes. Structural studies suggested that encapsulated viral gp14, gp15 and gp16 proteins are ejected from the phage head after the disruption of the outer membrane and support the formation of a channel in the periplasmic space of the host cell, allowing the release of viral genetic material^{63,66}.

The encapsulated viral H protein of the tailless phage $\phi\chi$ 174 that infects Gram-negative *E. coli* cells, is referred to form a long channel between the periplasmic space and the inner membrane of the host, wide enough to allow the circular ssDNA genome to be transported^{63,67}.

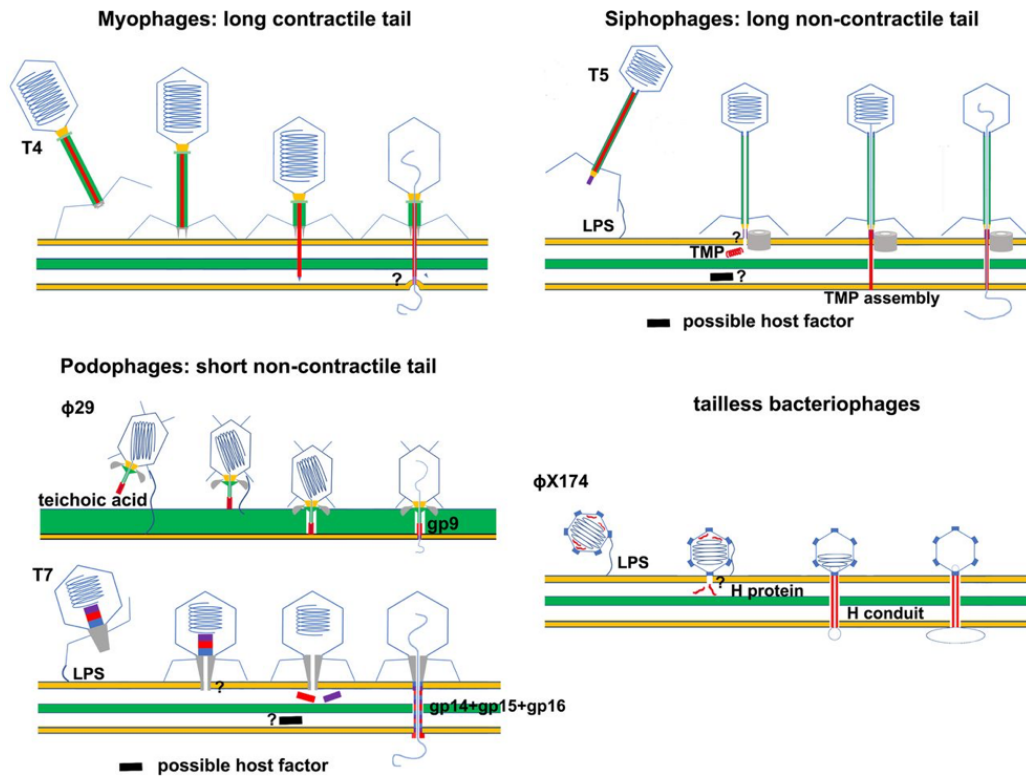


Figure 13 – Schematic representation of the different mechanisms of attachment to the host bacterial cell by *Myoviridae*, *Siphoviridae*, *Podoviridae* and tailless bacteriophages. The yellow lines represent the membrane bilayers. The green lines/layers represent the peptidoglycan layers of the bacterial cells. The question marks indicate unknown host factors or unclear membrane attachments and penetration mechanisms. Tape measure protein (TMP); Lipopolysaccharide (LPS). From Xu *et al.*⁶³.

- **Biosynthesis – Transition from Host to Phage-Directed Metabolism**

After the entry of the bacteriophages' genetic material into the cytoplasm of the bacterial cell, it starts the recognition of very strong phage promoters by the host's RNA polymerase, leading to the transcription and expression of immediate early genes. The products of these expressed genes contribute for the reprogramming of the cell for the synthesis of new phages, by conferring a certain protection to the phage genome and restructure the host appropriately for the needs of the bacteriophages. This restructure can possibly include the degradation of the host genome, the inactivation of host proteases and blocking of restriction enzymes, the destruction of host proteins and inhibition the host transcription and translation mechanisms⁴⁷. To initiate the phage genome replication and associated functions, is necessary for the middle or delayed-early genes expression. Once phages are able to encode their own DNA or RNA polymerases, they are able to begin the synthesis of one of those enzymes. In this step, bacteriophages are able of guiding and directing the bacterial metabolism to, not only, replicate their genome, but to generate structural components⁹.

- **Maturation**

Subsequently, with the structural components produced, it is the turn to assemble the phages' particles. The process of assembly is often described as 'self-assembly' given the fact that the complex structures are able to self-assemble independently in a define order. In this way, different phage components such as the head, tail fibers, and if present, tail, self-assemble and join together⁹. The tail assembly system begins with the baseplate. Once the baseplate has assembled, the short tail fibers attach to it. Only after this step is completed the tail tube can be formed, assembling onto the baseplate. The replicated phage genome produced is packaged into pre-assembled icosahedral capsid. During packaging, the head expands with the movement of dsDNA into the capsid. This process stops when the maximum amount of DNA fills up the capsid space of the bacteriophage^{8,9,47}. Finally, the tail assembly is only finished by the addition of the connector proteins that will link the complete tail to the head^{9,47}.

- **Host Cell Lysis**

The final step of phage proliferation is the lysis oh the bacterial host cell. Phage-induced bacterial lysis allows rapid release of large numbers of the phage progeny, but comes at expense of ending intracellular phage progeny production^{9,47}.

Tailed phage-induced lysis involve the release of intracellular bacterial enzymes, and other molecules. The two components associated with the lysis mechanism are the protein holin and the enzyme endolysin. When accumulated in the inner membrane of infected bacteria, holin creates small pores in the bacterial cytoplasmic membrane to allow the exposure of the peptidoglycan layer to the phage endolysin. Endolysin is capable of cleaving the most crucial and essential bonds in the peptidoglycan matrix of the cell wall. Hense, the pores created in the cell wall induce the lysis of the bacteria with the simultaneous release of the new progeny of bacteriophages to the outside environment^{9,47,48}.

Tailless phages have a different mechanism for the lysis of bacteria through the production and export of a cell wall synthesis inhibitors. These inhibitors eventually cause the failure of the cell wall, promoting the osmotic lysis of the bacteria cell and consequently the release of intracellular phage progeny^{9,47}.

At last, there is one more type of lysis which is the lysis from without where the adsorption happens by multiple of phages to a single host cell. This process will eventually weaken the cell wall due to lytic enzymes found in the phage tail, contributing to the failure and disruption of the host cell wall. This mechanism serves to increase lysis possibilities by the phages during growth within cultures that contain high densities of phage-infected bacteria⁹.

2.2.5. Bacteriophages Infection Lifecycles

Phage life cycles dictate their role in bacterial and *archaeal* biology. Depending on the type of bacteriophage, the bacterial infection can either occur by a lytic or lysogenic cycle as it is represented in **Figure 14**.

The lytic pathway is carried by the lytic or virulent bacteriophages. This infection process is characterized by the hijack of the host bacteria and converting it into a bacteriophage-producing factory. The bacterial host's metabolic machinery is taken over and re-targeted to the reproduction of new bacteriophage particles. The cycle initiates with the attachment of the phage on the membrane surface of the bacteria and the genetic material of the bacteriophage is injected. This event causes the lysis and, consequently death of the host minutes or hours later, with the release of newly formed bacteriophages. The lytic lifecycle is considered productive since the burst size corresponds to the number of phages produced per infected host cell. The phages characterized by following this type of lifecycle are the T4, T7 (most well studied), T1, T2, T6, SPP1, LP65, K and RB69^{8,47,44,48,55,68,69,70}. Additionally, lytic type of infection is considered a process very much dependent on the host metabolic machinery, so in most cases it is highly affected by what the host is experiencing shortly prior to infection, as well by the energetic state, nutrients and conditions that are present during the infection process itself⁴⁷.

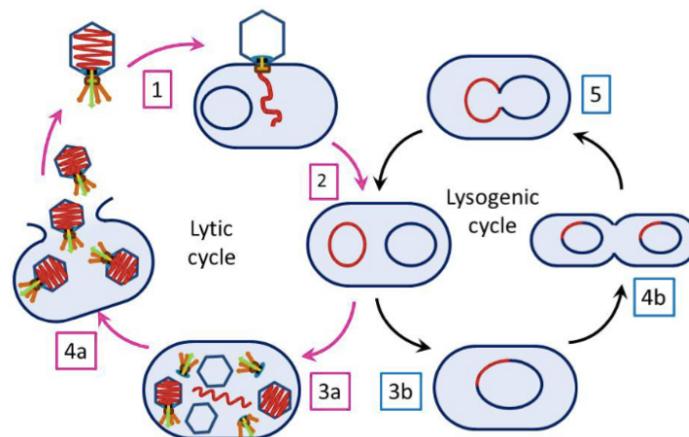


Figure 14 – Schematic representation of the two lifecycles of bacteriophages. Pink represents the lytic cycle of infection. Blue indicates the lysogenic cycle of infection. (1) Phage attaches to the host cell and injects its genomic material; (2) The DNA of the phage enters the cytoplasm of host bacteria; (3a) New phage DNA and proteins are synthesized and bacteriophages assembled; (4a) Cell lysis releasing new bacteriophages; (3b) Integration of the phage genome within the bacterial genome (prophage); (4b) Normal bacterial reproduction and division; (5) Under certain conditions, the prophage excises from the bacterial genome and initiates the lytic cycle. From Kurtböke⁸.

The lysogenic cycle results in the integration of the viral material within the bacterial genome (called prophage), which causes the phage propagation slower. In this case, the replication of the bacteriophage is ensured without any fatal consequences to the infected host bacterial cell and could occur through several generations. The prophage remains in a latent state until is activated by stress or cellular damage processes of the host bacteria. These factors turn the bacteriophage cycle of replication via lytic pathway, after excision from the bacterial genome. Afterwards the induction of lysis of the host occurs and, consequently release of new phages. The lysogenic lifecycle is characteristic of the M13, Mu, P1, P7, HK97 and λ phages^{8,9,47,44,48,55,68,70}.

2.2.6. Most Well Characterized Bacteriophages – T4 and T7

In spite of the great abundance of tailed bacteriophages, studies and details of their organizations and modes of operating have emerged only during the last decade. The support of new and improved imaging systems such as the electron microscopy, allowed to obtain information on the relative amount of different protein components, protein localization, structure determination at high resolution and viral titre monitoring ⁸.

The T-even bacteriophages, also known as the *Escherichia coli* bacteriophages, are a group of complex dsDNA phages belonging to the family *Myoviridae* which are considered the most well studied model organisms. Model organisms are usually required to be simple and with as few as five genes. However, T-even phages are in fact among the largest and highest complex viruses. Coincident with their complexity, T-even viruses are found to have unique features: regulated gene expression; transduction process responsible for transfer of drug resistance and random insertion into the host bacterial genome ⁷¹. Since the 1940s, T-even phages have been major model systems in the development of modern genetics and molecular biology. Many studies took advantage of their useful degree of complexity and ability to derive detailed genetic and physiological information with simple experiments. These group of phages include the T4 bacteriophages that are most known for their genetic engineering studies. T4 bacteriophages (*Myoviridae*) were used for the formulation of many fundamental biological concepts including: recognition of nucleic acids as the genetic material; definition of gene; demonstration that the genetic code is triplet; discovery of the mRNA; the importance of recombination in DNA replication, and many others. The T4-type phages own an icosahedral head and a long contractile tail as demonstrated in **Figure 15**, are approximately 200nm long, with a dsDNA genome of 168,903bp, encoding 289 proteins. It has served to elucidate mechanisms of not only T-even phages but of large isosahedral viruses in general, including the widely distributed eukaryotic viruses (e.g. the herpes virus) ^{8,72,73}.



Figure 15 – T4 bacteriophage obtained by transmission electron microscopy (TEM). From Miller *et al.* ⁷².

The T-odd phages were later discovered to share morphological and biochemical features that distinguish them from the T-even phages. However, due to their lytic mode of infection, the T4 and T7 bacteriophages share genetic similarities that allow them to infect the same specific bacterial hosts (*E. coli*). For this reason, the T7 bacteriophages can also be considered as model phages⁷⁴. T7 bacteriophages (*Podoviridae*) also possess several properties that make them ideal for phage experiments. Some of the assays made with T7 phages include: purification and concentration processes that have produced consistent values in chemical analysis of substances; and phage display to clone RNA binding proteins. The T7 promoter sequence is extensively used in molecular biology due to its extremely high affinity for T7 RNA polymerase and thus, high level of expression. This type of phage is characterized for having an icosahedral head, a short non-contractile tail as demonstrated in **Figure 16**, is approximately 60nm in diameter and a dsDNA genome of 39977bp^{75,76,77}.

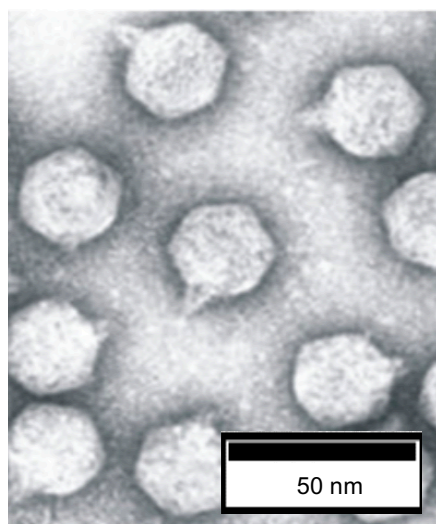


Figure 16 – T7 bacteriophage obtained by transmission electron microscopy (TEM). From Cuervo *et al.*⁷⁶.

2.3. Bacteriophage Production and Purification

The production of bacteriophages requires viable bacterial host cells. The culture medium should also be taken in consideration as it is the one that allows the proper support for the growth of their hosts which enables the growth and propagation of bacteriophages under any conditions. To maximize the production of bacteriophages, the bacterial host to be targeted must be used, nevertheless the purification and decontamination processes for the pathogenic bacteria should be carefully accomplished specially if the purpose of use is therapeutic applications. The use of contaminated phage solutions that contain cell debris can be dangerous for administration. Simply removing the live bacterial cells along with larger bacterial cell debris via filtration or other purification methods may be sufficient for some cases^{12,47,70,78}.

For relatively small volumes of phage lysate (<10L) used at a laboratory scale, the methods of separation depend on the desired purity and quantity of the final product. In these cases, the downstream process is normally composed by a few purification steps, each of them with distinct finalities. The first step is composed by broth clarification, accomplished either by low-speed centrifugation or the combination of low-speed centrifugation followed by filtration through a suitable sized membrane, which allows the removal of cells and cellular debris from the media. For many applications, the clarified lysate can be directly used after the first purification step, however if the intent is to use bacteriophages for therapeutic applications or diagnosis, further purification steps are required. The second stage in downstream purification, phage preparations could involve the concentration of the phages and removal of impurities either through i) precipitation with polyethylene glycol (PEG); ii) ultracentrifugation; iii) centrifugation with a density gradient such as the cesium chloride; or iv) ultrafiltration by tangential flow. A diafiltration step can also be added in order to exchange the phage media into a suitable buffer, if a chromatographic step is desired ^{12,47,70,78}.

For larger volumes and regardless the field of use, it is important that phages are purified to a high level, preserving their high capacity to infect the target bacteria. When high purity product and scalable to industrial settings is required, chromatography is a frequent method of choice. Chromatography is also substantially faster, more consistent, and allows for system automation. Chromatography presents several different modes of operation: ion-exchange based on the charge of the particles being separated; size exclusion which the separation is based on the particles size; and affinity chromatography based on the high binding potential between the molecule of interest and a specific ligand present in the medium ^{79,80,81}.

The purity achieved by ion-exchange chromatography (IEC) is one of the most promising and used modes of operation for bacteriophages as they typically exhibit a negative charge, consequently being retained in a positive charged anion-exchange resin. Adriaenssens *et al.* used anion-exchange chromatography (AEC) as an alternative method to concentrate and purify several bacteriophages with different morphologies and hosts. Their results showed that the recovery of each phage varied between 35 and 99% of the original phage titre which confirms that AEC is an alternative to traditional cesium chloride purification methods, however requires more extensive optimizations ⁸². One limitation which this type of chromatography presents is that it cannot remove empty phage capsids and other impurities that can also bind to the anion exchange resin ⁸¹.

Size exclusion chromatography (SEC) is typically used as a polishing step in order to remove final contaminants. However, this method of purification is not capable of removing large impurities. Farkas *et al.* used SEC to purify a phage MS2 lysate. The method successfully removed non-encapsidated phages and other impurities contained in the culture which enabled the accurate estimation of viral particles ⁸³.

Affinity chromatography allows the separation of the interest molecule from the undesired molecules which does not interact and elutes first in the column. The desired products with high purity only elute in the presence of a solvent of higher salt concentration. In the study of Ceglarek *et al.* used affinity chromatography not only to purify bacteriophages from the bacterial contaminants, but also to separate phages from other phages. The authors transformed the producing bacterial cells with a plasmid, expressing a recombinant phage capsid protein, which contained a His-Tag. During phage capsid assembly, the wild-

type capsid proteins compete with the recombinant capsid proteins and produce virions expressing the affinity tag. This tag was used as a molecule to separate the phages from the contaminants in the preparations^{79,84,85}.

2.4. Applications of Bacteriophages

Enzymology research concerning phages was a big focus during the 1980s for the development of brand new technologies exploiting bacteriophages and their enzymes (e.g. phage enzymes and vectors that made genetic engineering possible; phage display technologies – which a desired protein gets genetically engineered into the viral genome for display in the surface of the phage; and the use of phages to detect bacterial pathogens)⁴⁷. Nowadays, due to their attractive characteristics, bacteriophages have been used for a wide variety of applications in agriculture, food safety, health, veterinary and human medicine, biology, biotechnology and molecular biology. Among the large diversity of applications, such as phage-based vaccines, food biopreservation and phage-display, phage therapy and phage-based biosensors, these viruses regained a whole new purpose^{9,52,47,48,55}.

2.4.1. First Practical Applications - Veterinary and Human Medicine

Since the discovery of phages by Frederick Twort and Felix d'Herelle in 1915 and 1917, respectively⁴⁷, bacteriophages have participated at various studies in laboratories worldwide in order to better understand and use them in several practical applications¹⁰. Phages became prospective therapeutic agents and targets for modern biotechnology studies once bacteria are a major cause of diseases worldwide. Thus, bacteriophages have been contributing for a wide range of fields such as molecular biology (e.g. as genetic vectors), biotechnology (e.g. for the development of phage-delivered vaccines, as delivery vehicles for gene therapy), medical diagnostics (e.g. use of specific phage for bacteria typing), phage display (where proteins, peptides or antibodies are displayed on the phage surface) and phage therapy (e.g. use of bacteriophages as anti-bacterial agents)^{50,86}.

The first therapeutic use of phages was reported by Bruynoghe and Maisin in 1921, where they treated a *Staphylococcus aureus* infection with the injection of a preparation of specific staphylococcal phages in the local region of cutaneous boils. It was reported both reduction in swelling and in pain, as well some reduction in fever. At the same time, d'Herelle carried out experiments on phages against the natural infection of chickens by *Bacillus gallinarum*, the bacteria that causes gastrointestinal diseases. He reported that the chickens treated with specific *B. gallinarum* phages presented a high degree of protection^{10,47,87}. Phage treatments were also evaluated in field trials against bovine hemorrhagic septicemia in Indochina. In this case it was also reported that inoculation of specific phages for this causative bacteria also protected the water buffaloes against infectious *Pasteurella multocida*⁸⁸. With effective evidences that phages can be used for therapeutic uses in both gastrointestinal and septicemic diseases, d'Herelle extended his trials to humans. The work that attracted the most attention of phage activity was d'Herelle's report of four patients with bubonic plague he treated with antiplague specific phages⁵⁰.

Despite the breakthroughs, with the discovery of antibiotics in the 1940s, the research for the therapeutic applications of bacteriophages decreased drastically in Europe and in the USA, although it continued in the Soviet Union ^{10,43}.

2.4.2. Bacteriophage Therapy

Bacteriophages have been presented as natural antimicrobial agents to attack bacterial infections in humans, animals (veterinary medicine), agricultural important crops or hygiene measures in food production facilities (food microbiology) and hospital centers ⁵².

Due to the emergence of pharmaceutical antibiotics in the mid-20th century, the treatment and attenuation of infectious diseases caused by pathogenic bacteria had been exclusively held by the use of these antibiotics. However, the abusive, incorrect and indiscriminate use of antibiotics in clinical, agricultural and animal settings resulted in the widespread antibiotic resistance in a variety of microbiota in several ecological compartments ^{9,10,89}. Because of this, antibiotics started to become less effective and antibiotic-resistant bacteria started to increase, leading to a major global health concern. Among some of the highly resistant species of bacteria include the Gram-positive *Enterococcus faecium* and *Staphylococcus aureus* and the Gram-negative *Pseudomonas aeruginosa*, *Klebsiella pneumoniae*, *Acinetobacter baumannii* and *Enterobacter* species ^{2,43}.

Therefore, due to the extremely prevalence and increase of antibiotic-resistant bacterial strains, it became necessary to synthesize new antibiotics or explore new effective and viable strategies for the treatment of infectious diseases, as a complement or even replacement to antibiotic therapy. One of the most promising alternative agents whom can be used for medicinal and biological control purposes are bacteriophages ^{2,4,5,6,7}. Phage therapy uses lytic bacteriophages in order to reduce or eliminate pathogenic bacteria that cause infectious diseases as an alternative to antibiotics ^{8,43}.

2.4.2.1. Comparison between Bacteriophages and Antibiotics

Bacteriophages as therapeutic agents reveal multiple advantages that make them an attractive alternative over tradition antibiotic-based therapy. Regarding the clinical applications of bacteriophages, these agents can be used as antimicrobial agents, or simply just use the phage products or phage lysins.

The most important distinctions between the use of phages and antibiotics is represented and summarized in **Table 2** ^{2,4,8,10,47,44,50,86,90,91,92}.

Table 2 – Comparison of the therapeutic use of phages and antibiotics. Adapted from Kutter and Sulakvelidze ⁴⁷.

| Bacteriophages | Antibiotics |
|---|--|
| Phages are highly effective in killing their targeted bacteria. | Some antibiotics are bacteriostatic; i.e., they inhibit the growth of bacteria rather than killing them. Antibiotics attack not only the disease-causing bacteria, but also all susceptible microorganisms, |

| | |
|---|--|
| <p>The high selectivity of bacteriophages permits the targeting of specific pathogens, without affecting desirable bacterial flora.</p> | <p>including the normal - and often beneficial - microflora of the host. Thus, their non-selective action affects the patient's microbial balance, which may lead to various side effects.</p> <p>Multiple side effects, including intestinal disorders, allergies, and secondary infections have been reported for antibiotics.</p> |
| <p>In the case of bacteria become resistant to the phage, by changing surface receptors, this one is capable of evolve naturally in order to infect the resistant bacteria, therefore reducing the chances of bacteria escape.</p> | <p>Because of their broad spectrum of activity, antibiotics may select for resistant mutants of many pathogenic bacterial species, not just for resistant mutants of the targeted bacteria.</p> <p>Developing a new antibiotic (e.g., against antibiotic-resistant bacteria) is a time-consuming process and may take several years to accomplish.</p> |
| <p>The pharmacokinetics of bacteriophage therapy is such that the initial dose increases exponentially if the susceptible bacterial host is available. In such cases, there is no need to administer the phages repeatedly.</p> | <p>Repeated doses of antibiotic are required to cure the bacterial disease.</p> |
| <p>Humans are exposed to phages throughout their life, and tolerate them. Only a few minor side effects have been reported for therapeutic phages, and they may have been due to the liberation of endotoxins from bacteria lysed <i>in vivo</i> by the phages.</p> | <p>The liberation of endotoxins by bacteria can also be observed when antibiotics are used.</p> |
| <p>Because of phages' specificity, their successful use for preventing or treating bacterial infections requires identification of the agent and determining its <i>in vitro</i> susceptibility to the phage preparation prior to initiating phage treatment.</p> | <p>Antibiotics have a higher probability of being effective when administered before the identification of the agent.</p> |
| <p>The cost of phage therapy is lower than conventional antibiotic treatment. Production of phage by infection of the host is simple and cheaper.</p> | <p>Production is complex and expensive because may involve toxic compounds and organic solvents for extraction.</p> |

2.4.3. Bacteriophage-Based Biosensors

Wild-type phages have been studied for functionalization of biosensors and subsequent pathogen detection. Phage-based biosensors are considered to be more robust and simpler than immunosensors since phages present valuable properties that makes them potentially promising recognition elements for diagnostics and therapeutics of bacterial diseases. Besides all of the characteristics that have been mentioned in favor of bacteriophages over other bioelements, these viruses have a long-term survivability

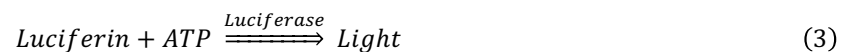
in harsh conditions and can be stored for long periods of time in the cold with minimal loss of binding affinity toward the target ^{17,31,93}.

Several bacteriophages have already been explored as a probe for a rapid and accurate detection and recognition of bacterial pathogens in complex conditions based on the release of intracellular components during the host cell lysis; indirect detection based on the inhibition of metabolism and growth; direct detection through cell wall recognition; and recognition by engineered phages ^{16,17,93}.

- **Detection based on the release of intracellular components during bacterial lysis**

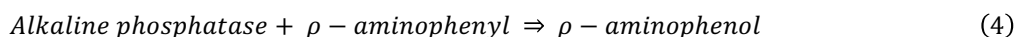
The lysis of bacterial cells by intact bacteriophages culminates in the release of intracellular materials of the host and the phage progeny ⁹³.

The most popular method measures the bacterial intracellular adenosine triphosphate (ATP). The firefly luciferase/luciferin enzyme system allows to determine the total number of bacterial cells by the release of intracellular ATP following cell death and disruption. This enzyme system permits the production of light which is directly proportional to the quantity of ATP in the assay. However, this system does not allow the detection of specific pathogens. The desired specificity can only be achieved by specific cell lysis, which can be accomplished by phages. Therefore, pathogen specific bacteriophages must be added to the sample, where only target bacteria will be infected. Blasco *et al.* developed the phage adenylate kinase (AK) assay. AK is an enzyme that directs the conversion of ADP to ATP. During bacterial infection and lysis by phage specific activity, AK is released. Excess of ADP is added to the sample which leads the reaction towards the generation of ATP. Similarly, the quantity of light produced by the firefly luciferase/luciferin enzyme system is proportional to the quantity of ATP, and therefore, to the number of bacterial cells in the sample. **Equation 2** and **Equation 3** express this conversion assay. With this assay, Blasco *et al.* was able to detect 10^3 CFU/mL of *E. coli* and *Salmonella* within less than 2h ^{16,17,93,94,95}.



Besides ATP and AK, there are other intracellular constituents that can be used to monitor phage-cell interaction and pathogen quantification such as β -galactosidase that is produced during phage replication and release progeny from the bacterial cells. Neufeld *et al.* used an amperometric biosensor in order to measure changes in the medium due to phage-mediated cell lysis. Infection of *E. coli* with a lytic specific bacteriophage leads to the release of many components such as β -D-galactosidase, which can be measured amperometrically with the addition of a specific substrate. This assay was able to detect 1 CFU/mL of *E. coli* within 6-8h ^{16,93,95}. However, a single phage would likely be insufficient to infect across the large spectrum of target bacteria and false negative signals could arise or naturally lysing bacterial cells could also give false positives. To overcome these concerns, Neufeld *et al.* used in his assays a phage-

encoded alkaline phosphatase enzyme that had to be delivered during infection to the target bacterial host in order to be expressed. In this way, only after infection the enzyme would be synthesized and then released during lysis. **Equation 4** expresses the reaction between this enzyme and the substrate p-aminophenyl generates p-aminophenol as a product, which is then oxidized and measured amperometrically. This assay was able to detect 1 CFU/mL of *E. coli* within less than 3h^{93,95}.



- **Indirect detection based on the inhibition of metabolism and growth**

Typically, lytic phages infect their host cells leading to inhibition or decrease of cell growth and afterwards to cell lysis. Various studies have demonstrated the monitoring of metabolic activity and microbial growth of bacterial populations with amperometric, conductimetric and optical biosensors⁹³.

Chang *et al.* was based on the understanding that growth in a microbial culture could be monitored electrochemically by measuring electrical changes in the media due to the breakdown of substrates, increasing conductivity. He hypothesized that with the presence of bacteriophages in the bacterial cell culture, culture growth would decrease or cease, directly affecting the media conductivity. Thus, by comparing conductance between phage-free samples and phage-supplemented samples or between phage-specific and phage-non specific bacterial cultures, Chang *et al.* was able to screen for samples with phage-specific pathogens. Resulting conductance curves were able to discriminate between two different strain cultures of *E. coli* with 10⁶ CFUs/mL within a 24h period^{93,96}.

- **Direct detection through cell wall recognition**

Immobilization of bacteriophages onto transducer platforms has been explored using different techniques including physical adsorption and covalent immobilization, which are widely employed for a vast range of biological elements^{17,93}.

Optical biosensors have been extensively applied as means to detect bacterial pathogens, specially the SPR sensors as it is designed for real-time monitoring of all dynamic processes without the need for labeling samples. Detection and quantification is performed by the binding event between the immobilized recognition element and the pathogen in solution, which results in a refractive index change in the SPR angle^{16 93}. Balasubramanian *et al.* employed an SPR-based sensor for the detection of *Staphylococcus aureus* using specific lytic bacteriophages adsorbed on gold surface as recognition elements. This assay was able to detect 10⁴ CFU/mL of *S. aureus*^{17,42,93}.

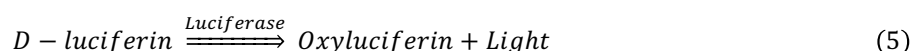
- **Recognition by engineered phages**

Intact phages are biologically active and thus result in lysis of the host bacterial cell upon infection. This process can lead to lost of signal on the biosensor platform. Additionally, intact phages can have relatively large sizes and limit the detection activity. For these reasons, engineered bacteriophages,

including reporter phages and phage display technology, are typically used for detection of antibiotic-resistant bacteria^{12,13,16,17,93}. Reporter phages are genetically modified phages with reporter genes that when transmitted by infection events to the host bacteria can easily be expressed and visualized. The measured optical signals often take the form of bioluminescence, fluorescence, colorimetric via luciferase/luciferin enzyme system, green fluorescent protein (GFP), and β -galactosidase. The ability to distinguish between live and dead bacteria is the biggest advantage of reporter phages since the phages will be unable to infect and express the reporter gene in dead bacteria^{12,16,17,93}.

Several studies have used reporter phages with the luxAB gene alone, which generates a bioluminescent signal after the addition of a specific reagent. Thouand *et al.* adapted the concept of reporter phages to a commercially viable kit-like format that consisted in only four steps in order to identify *Salmonella Typhimurium* pathogens: i) addition of only the luxAB reporter phages to the culture for 12-14h; ii) incubation of 1h to allow the contact between *S. Typhimurium* and the specific phages; iii) incubation of 4h with fresh growth medium; and iv) addition of a reagent allowing light measurement. This assay detected a bacterial concentration of 10^6 CFU/mL in 16h^{17,93,97}.

On the other hand, the luc firefly luciferase catalyzes the two-step conversion of D-luciferin to oxyluciferin to generate a bioluminescent light signal as represented in **Equation 5**. Carriere *et al.* used luc reporter phages in order to detect and assess the drug susceptibility in *Mycobacterium tuberculosis*. Susceptibility to anti-mycobacterial drugs was determined by comparing the bioluminescence from the reporter phages added to antibiotic-free or antibiotic-supplemented *M. tuberculosis* cultures. In the cultures where the drug was effective, fewer host *M. tuberculosis* cells were available for phage infection, thus less light was emitted as compared to antibiotic-free cultures^{93,98}. Bardarov *et al.* performed a similar experiment and was able to detect 10^4 CFU/mL in antibiotic-free *M. tuberculosis* cultures^{93,99}.



GFP-reporter phages are also very commonly used for bacterial pathogen detection since the GFP is easily activated and visible in ultraviolet or blue light. Funatsu *et al.* used specific *E. coli* reporter phages genomically incorporated with the GFP gene and combined them with a mixed culture of *E. coli* and *M. smegmatis*. Under an epifluorescent microscope, Funatsu *et al.* observed fluorescent *E. coli* cells that had been infected with the specific phages, while non-infected *M. smegmatis* cells were not fluorescing^{93,100}.

Furthermore, there are also reports about the incorporation of the lacZ gene, that encodes for β -galactosidase enzyme which catalyzes the hydrolysis of β -galactosides. These β -galactosides are possible to be optically observed by the addition of a fluorescent, luminescent or a chemiluminescent substrate. Goodridge and Griffiths describe the incorporation of the lacZ reporter gene into T4 phages for the detection of *E. coli* and subsequent addition of a chemiluminescent substrate for posterior visualization. This assay detected a bacterial concentration of 10^2 CFU/mL within 12h^{93,101}.

Bacteriophages also have a unique ability to display proteins or peptides on their surface which enables the screening of molecules with affinity to a variety of targets (proteins, molecules or an entire cell). Phage display method is characterized by the fusion of a gene that encodes for a peptide or protein of interest which results in the expression of the hybrid protein in the phage surface. M13, T4 and T7 phages have the most widely been used for these type of technique, whereby is represented in **Figure 17**^{12,14,15}.

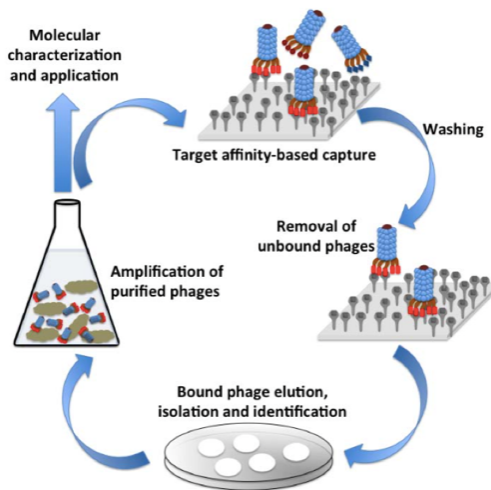


Figure 17 – Schematic representation of an affinity-based selection technique for phage display method. Phage libraries are screened against an immobilized target of interest, where the unbound phages are then washed away and the bound ones are eluted, propagated and used as probes for the target. From Singh *et al.*¹².

Gervais *et al.* demonstrated immobilization of T4 genetically modified phages using the biotin-streptavidin recognition assay. The phages expressed biotin on their capsid, potentially allowing the oriented attachment of the phage onto a streptavidin coated gold surface. This oriented attachment facilitated the tails exposure enabling a more efficient capture of the target bacteria, as demonstrated in **Figure 18**.

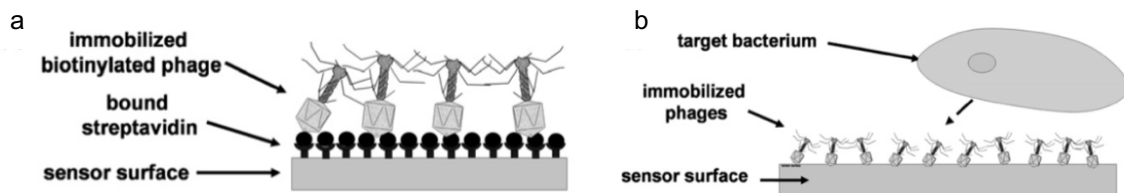


Figure 18 – Schematic representation of oriented phage immobilization. (a) Immobilized biotinylated phages by chemical attachment of streptavidin onto the sensor surface; (b) Attachment of bacteriophages to target bacteria in biosensing platforms for bacterial detection. Adapted from Gervais *et al.*¹³.

The attachment of modified phages to the target bacteria significantly delayed their growth, indicating that phages were efficiently bound to the sensor surface and infecting bacteria. Bacterial growth was monitored by conductometric biosensors by tracking the increase in impedance of ion current induced

by such growth. Thus, the conductances of biotinylated phages and wild-type samples were measured and compared. Immobilized modified phages lysed their targets with greater efficiency in comparison to unmodified phages. With this assay it was possible to detect pathogen attachment to the bacteriophages through cell wall recognition of target bacterial cells and their decreased growth. The main limitation of this method is the time-consuming process of phage modification^{13,16,17,93}. Tolba *et al.* reported the use of phage display technique for the introduction of affinity tags on the heads of T4 phages and was able to detect almost 10^3 CFU/mL of *E. coli* in 2h. The displayed proteins can be any protein and act as a recognition element, which makes this system highly versatile^{12,14}.

3. Materials and Methods

3.1. Experimental Process

The experimental process developed in this Master's Thesis for the separation of an *E. coli* specific bacteriophage tails towards the production of advanced recognition elements can be described by the flowchart presented in **Figure 19**.

Initially, an *E. coli* host strain was rehydrated, a working cell bank was prepared and the bacterial growth was studied in shake flasks. Specific *E. coli* phages were revitalized and a phage stock was prepared by amplification. Bacteriophages were then subjected to mechanical (sonication by water bath and probe sonication) and non-mechanical (osmotic shock) separation processes to promote the disaggregation of phage tails from their heads. After each method phages were accessed by their titre through a double-layer plaque assay, protein content through SDS-PAGE and Bradford assay. The most promising fragmentation methods were visualized and analyzed by TEM.

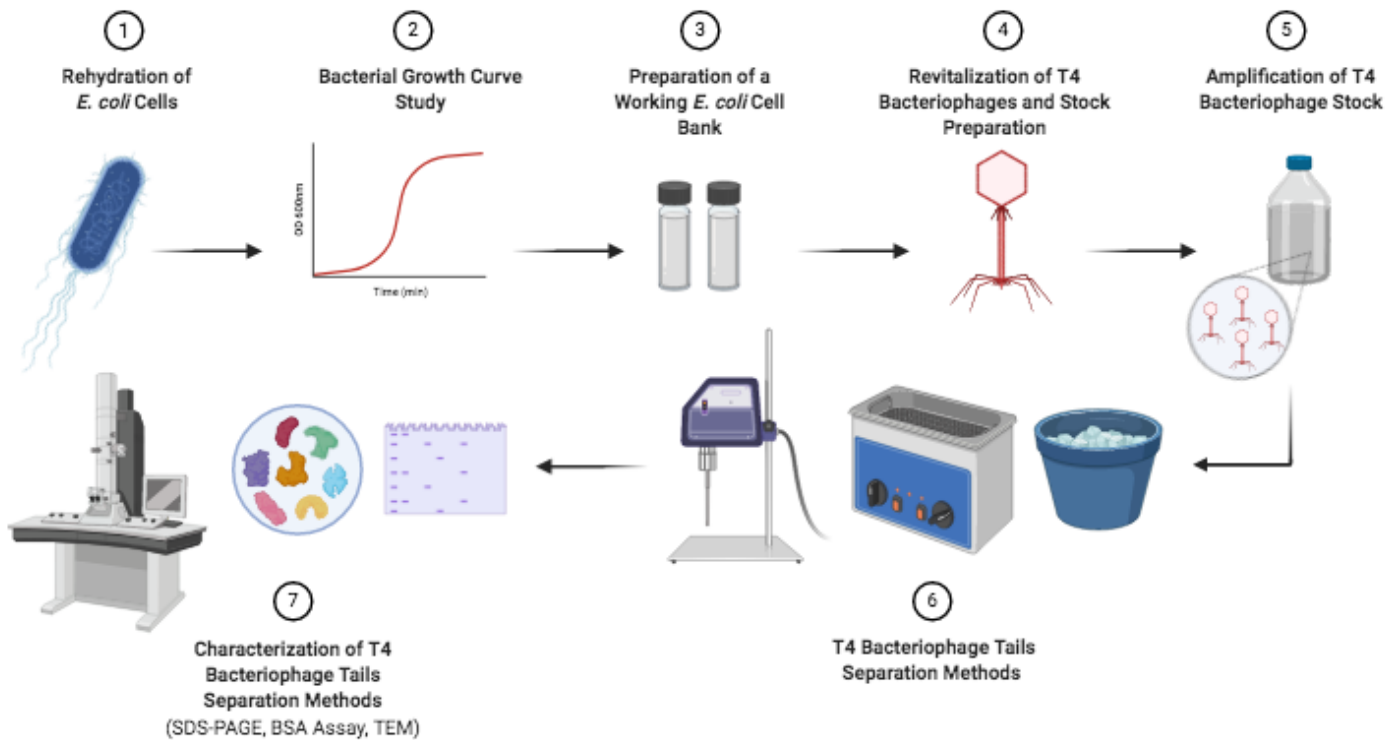


Figure 19 – Graphic demonstration of the general experimental process developed in this Master’s Thesis for the generation of advanced recognition elements by the separation of bacteriophages’ tails. Image created in BioRender.com – accessed 5th November 2020.

3.2. Cell Cultures

The *E. coli* dried bacterial content was supplied in an ampoule by the German Institute DSMZ – German Collection of Microorganisms and Cell Cultures with the designation *E. coli* DSM 613 strain B,B (Luria).

3.2.1. Rehydration of Dried *E. coli* Cell Culture

The dried bacterial cells were kept inside an ampoule. The ampoule glass was carefully broken and the inner vial was taken out. 0.5 mL of tryptic soy broth (TSB) medium was added to the dried pellet inside of the vial and let to rehydrate up to 30 minutes. The content was gently mixed with an inoculation loop to homogenize the suspension. About 100 μ L of suspension was plated in an agar plate and incubated overnight at 37 °C. The rest of suspension fraction was transferred into a sterilized eppendorf®, mixed with 50% glycerol and stored at -80 °C.

3.2.2. *E. coli* Bacterial Growth Curve

A fresh culture of bacterial cells was grown in TSB medium at 250 rpm and 37 °C overnight. A new inoculum was prepared in shake flasks with 500 mL of TSB medium and agitated at 250 rpm at 37 °C. The culture growth was followed for a period of 4h and every period of 15-30 minutes two samples were taken. The first sample was used to measure the OD at 600 nm and the second sample was used to determine the number of viable cells by plating 100 µL of the appropriate dilutions of each sample. After incubation of the plates overnight at 37 °C, the colonies of *E. coli* were counted in order to obtain *E. coli* growth data.

3.3. Bacteriophage Stock

Specific *E. coli* T4 bacteriophages dried content was supplied in an ampoule by the German Institute DSMZ – German Collection of Microorganisms and Cell Cultures with the designation Phage T4 DSM 4505.

3.3.1. Revitalization of Dried *E. coli* Bacteriophages

An agar plate was prepared and the *E. coli* host was plated using the top agar layer method containing 4 mL of top agar, 100 µL of fresh grown host culture and 40 µL MgCl₂ 5 mM. The ampoule containing the phages was carefully broken and the inner vial was taken out. Inside the vial there was a filter paper containing the dried phage suspension, which was placed in the middle of the host plate. 0.1 mL of TSB medium was added on the surface of the filter paper and the plate was incubated at 37 °C overnight. The next day it was possible to visualize a clear zone around the filter paper which was where the lysis occurred (see **Figure A 1** in Annex I). For preparing a phage stock suspension, 2-5 mL of 1x SM buffer (10x SM buffer is composed of 1 M NaCl; 0.5 M Tris-HCl pH 7.4; 100 mM MgSO₄•7H₂O; 0.3 g of gelatin and milliQ H₂O) was added to the plate and left at room temperature while slowly rotating on a shaker for at least 4h. Afterwards the phage suspension was harvested and centrifuged (Eppendorf® 5810R Centrifuge) at 8000 g at 4 °C for 10 minutes. The supernatant was collected and filtered in a 0.45 µm Nalgene™ Rapid-Flow™ sterile disposable Bottle Top Filter PES membrane to remove the remaining bacteria. The revitalized phage suspension was stored at 4 °C.

3.3.2. Bacteriophage Stock Amplification

In order to have sufficient quantities of bacteriophage stock for the experiments it was necessary to perform both solid and liquid medium amplifications.

Solid medium amplification starts with a titration assay which involves the preparation of a pre inoculum where a fresh culture of bacterial cells was grown in TSB medium at 37 °C overnight. Cells were then diluted into a 5 mL TSB medium inoculum to achieve an optical density (OD) of 0.1 and incubated at 35-38 °C with agitation (200-300 rpm). The bacterial growth was followed until an OD of 0.16-0.25 was reached. MgCl₂ 1 M was then added to the inoculum (100 µL of MgCl₂ to 10 mL of solution). MgCl₂ is a chemical compound that helps the connection of bacteriophages to the bacterial host receptors. 10-fold

serial dilutions of the bacteriophage stock were performed with 900 μL of 1x SM buffer. Since the concentration in the phage suspension was unknown, it was decided to make dilutions up to -9. It was added 200 μL of inoculum to each falcon and 100 μL of phage dilution to the correspondent falcon as well. The falcons were incubated at 35-38 $^{\circ}\text{C}$ without agitation for 15-30 minutes to promote the connection between the bacteria receptors and the bacteriophages. Top agar with MgCl_2 was melted and 3mL were mixed to each suspension in the falcons and added to the correspondent tryptic soy agar (TSA) plate following the double agar overlay plaque assay. The overlays were allowed to solidify for 15 minutes and then the plates were incubated at 35-38 $^{\circ}\text{C}$ overnight. The next day 5-10 mL of 1x SM buffer was added to the -2 and -3 plates since the number of plaque forming units (PFUs) was uncountable (higher than 300). These plates were incubated at 35-38 $^{\circ}\text{C}$ for 3 h. Afterwards the phage suspension was harvested and centrifuged (Eppendorf® 5810R Centrifuge) at 7500-8500 g at 4 $^{\circ}\text{C}$ for 10 minutes. The supernatant was collected and filtered in a 0.45 μm Nalgene™ Rapid-Flow™ sterile disposable Bottle Top Filter PES membrane to remove the remaining bacteria. The phage stock suspension was stored at 4 $^{\circ}\text{C}$. The following day the process of titration was repeated in order to determine the titre of the solid amplification phage stock. Phage titre was then determined by using the **Equation 6**:

$$\text{number of plaques} \times 10 \times \text{reciprocal of counted dilution} = \text{PFUs}/_{\text{mL}} \quad (6)$$

Since the titre of the phage stock was yet not with the desired titre, a liquid medium amplification was also performed. Once more a fresh culture of bacterial cells was grown in TSB medium at 200-300 rpm and 35-38 $^{\circ}\text{C}$ overnight. Cells were then diluted into shake flasks with 500 mL TSB medium to achieve an OD of 0.1 and agitated at 200-300 rpm at 35-38 $^{\circ}\text{C}$. The culture growth was followed for a period of 4 h and every period of 15-30 minutes one sample of 100 μL was taken. When bacterial growth reached an OD between 0.16-0.25 corresponding to the exponential phase, a certain volume of phage stock and MgCl_2 1 M was added to start the infection process. This volume of phage stock depends on the titre of the previous stock solution, in this case the titre obtained from the solid medium amplification, the number of bacteria present in the TSB medium volume and the MOI (Multiplicity of Infection). The MOI was calculated using the number of phages particles (PFUs) against host bacteria colony forming units (CFUs) as the following **Equation 7** suggests:

$$\text{MOI} = \frac{\text{PFUs}}{\text{CFUs}} = 0.1 \quad (7)$$

At last, when the OD of the bacterial culture declines and achieves values close to 0.1, a final lysate was obtained and centrifuged (Eppendorf® 5810R Centrifuge) at 7500-8500 g for 20 minutes at 4 $^{\circ}\text{C}$. The pellet was discard and the supernatant fraction was filtered with Nalgene™ Rapid-Flow™ sterile disposable

Bottle Top Filters with PES membrane, first with a 0.45 μm and then with a 0.22 μm membrane. The lysate was then subjected to a processes of concentration and diafiltration using a 500 kDa microfiltration membrane module with 140 cm^2 (GE Healthcare). The concentration process allowed to concentrate the lysate 10x and remove medium particles and other small molecules. The final permeate was discard. The concentrated bacteriophage particles were then collected and thoroughly diafiltrated against Tris-HCl 25 mM pH 9 buffer. Finally, the bacteriophage stock was obtained and stored at 4 °C. For the determination of infectious phage particles (PFUs), titration was accomplished using double agar overlay plaque assay.

3.4. Bacteriophage Separation Methods

To generate new recognition elements for the identification of antibiotic resistant bacteria, T4 bacteriophages were submitted to three different approaches. The methods used are commonly applied to disrupt cells, however these techniques were implemented on phages in order to dissociate their tails from the rest of the virus. For this detachment, both mechanical (water bath sonication and probe sonication) and non-mechanical (osmotic shock) methods were tested.

3.4.1. Osmotic Shock

An osmotic shock causes lysis by a rapid change in the concentration of solutes, such as salts and glucose, in the medium. For this sodium acetate 5 M was used for the dissociation of phage tails. The experiment was always carried on ice where 500 μL of phage stock were mixed to 500 μL of sodium acetate for different periods of exposure (2, 5, 10, 15, 20, 30 minutes). After each time of subjection 1:100 volumes of milliQ H_2O were added. A sample of 1mL was collected for each time and stored at 4 °C. Afterwards the suspensions were centrifuged (Eppendorf® 5810R Centrifuge) at 3500 g for 30 minutes at 4 °C. Both pellets and supernatants were collected and stored at 4 °C for further testing. Pellets were resuspended in 5m L of 1x SM buffer. The process of osmotic shock was adapted from the literature as described by Herriott *et al.* and Liu *et al.* ^{102,103}. These authors were trying to obtain ghost phages by osmotic shock and actually observed that the technique caused the separation of heads from tails. **Figure 20** describes the experimental process for the osmotic shock applied on T4 bacteriophages.

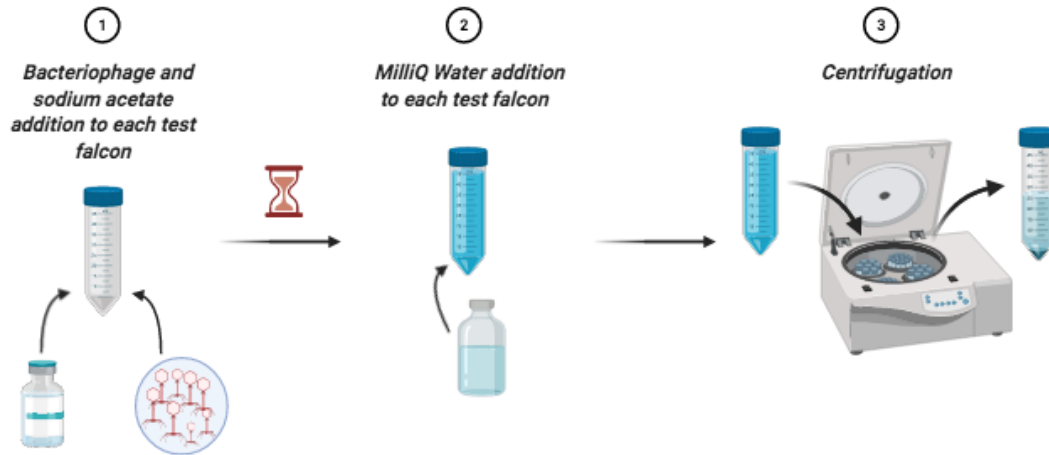


Figure 20 – Schematic representation of the osmotic shock process. Image created in BioRender.com – accessed 10th November 2020.

3.4.2. Water Bath Ultrasonication

A VWR Ultrasonicator bath operating at 45 kHz and 80 W was used to perform the disruption test on phages during a period of 40 minutes. Samples of 500 μ L were collected at 1, 5, 10, 15, 20, 25, 30 and 40 minutes of exposure to the ultrasonic waves and stored at 4 °C for further experiments. The water bath was filled with 800 mL of water and always carried at 10 °C throughout the sonication procedure. The experimental process is described in **Figure 21**.

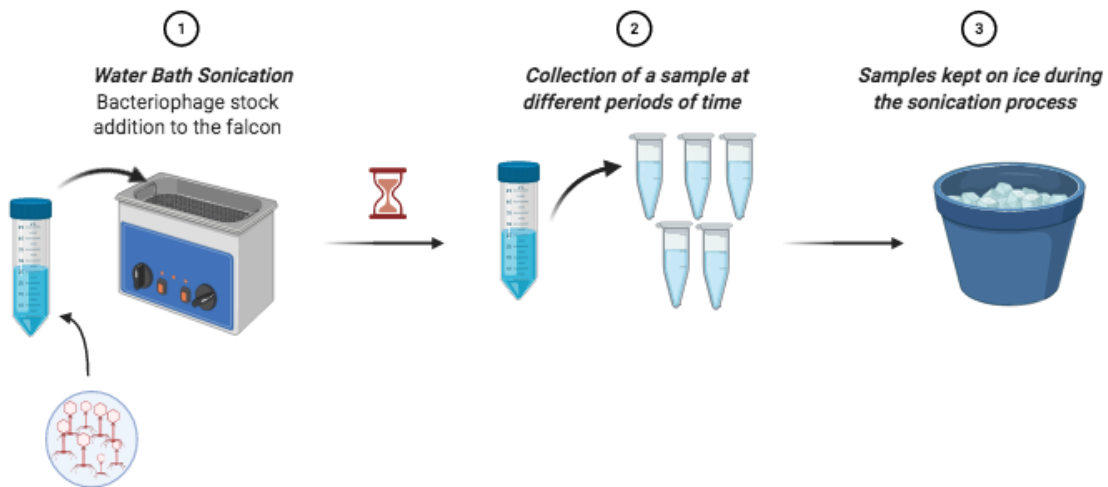


Figure 21 – Schematic representation of the water bath sonication process. Image created in BioRender.com – accessed 11th November 2020.

3.4.3. Probe Ultrasonic Homogenization

A Bandelin Sonopuls Ultrasonic Homogenizer HD 3200 operating at 20 kHz was used to carry out the disruption test on phages using a MS 72 probe. Sonication was performed at 25 and 50 W for 10 cycles of 4 minutes of exposure and 1 minute of pause. Samples of 1 mL were collected at 5, 10, 15, 20, 30 and 40 minutes of sonication and stored at 4 °C for further experiments. Both processes were adapted from the literature described by Anderson *et al.* and Pinto *et al.*^{104,105}, and the experimental process is described in **Figure 22**.

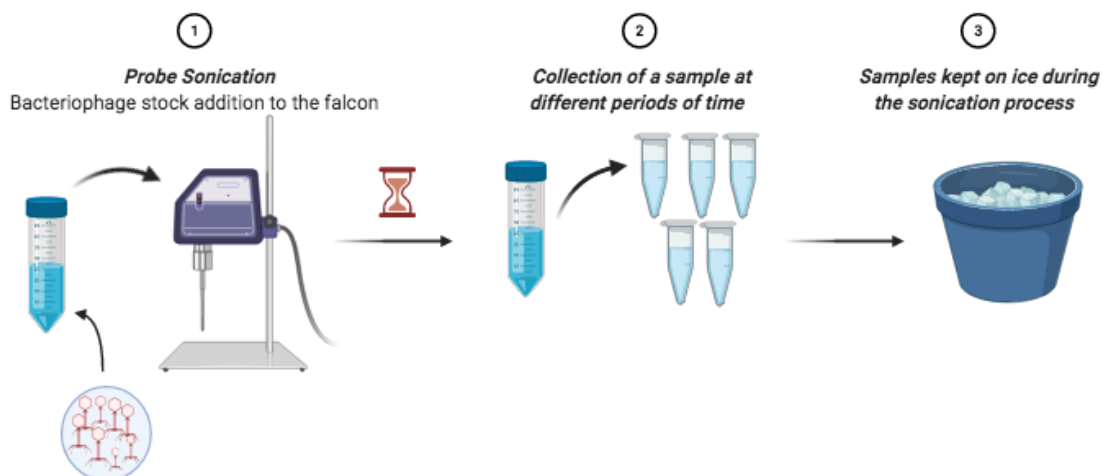


Figure 22 – Schematic representation of the probe sonication process. Image created in BioRender.com – accessed 11th November 2020.

3.5. Characterization of Bacteriophages

For each disruption process, T4 phages were analyzed and characterized by their titre through a double-layer plaque assay, their protein content through SDS-PAGE and Bradford assay. *E. coli* T4 bacteriophages submitted to fragmentation methods with the most promising outcomes were analyzed by TEM.

3.5.1. SDS-PAGE and Protein Quantification

The protein content of phages was determined by Sodium Dodecyl Sulfate Polyacrylamide Gel Electrophoresis (SDS-PAGE). The SDS-PAGE analysis was done on polyacrylamide gels with 12% T (total monomer concentration), 3.3% C (weight percentage of crosslinker) for the resolving layer and 4% T, 3.3% C for the stacking layer. 20 μ L of phage samples were added to 25 μ L of 2x Laemmli Sample buffer (Bio-Rad) and denatured by addition of 5 μ L of dithiothreitol (DTT, 1 M, Sigma). The samples were then heated in a water bath at 100 °C for 10 minutes. 20 μ L of phage samples and 2 μ L of the Bio-Rad Precision Plus Protein™ Standards Dual Color Marker were then loaded into the gel. Electrophoresis was conducted at 90

V, with the gels submerged in 1x running buffer (10x running buffer composed of 250 mM Tris-HCl, 1% SDS, 1.92M glycine, pH 8.3). Staining was performed with Coomassie Brilliant Blue and afterwards with silver nitrate. Silver staining protocol included a fixation step with 30% ethanol + 10% acetic acid for at least 2h, a wash step with 30% ethanol for 10 minutes, a second wash step with milliQ H₂O for 2x10 minutes, a sensibilization step with 0.02% of sodium thiosulfate for 10 minutes, a third wash step with milliQ H₂O 3x30 seconds, a staining step with 0.15% silver nitrate for 30 minutes, a development step with 3% sodium carbonate + 0.05% formaldehyde, and a stop step with 5% acetic acid for 15 minutes. Images of the gels were obtained with a GS-800 Calibrated Densitometer (Bio-Rad). Osmotic shock phage samples were purified and concentrated with Amicon® Ultra-4 100 kDa Centrifugal Filter Units (Merck), before sample preparation and lead into the gel, in order to remove the sodium acetate, which could interfere with the running of the gel.

3.5.2. Bradford Assay

The protein quantification present in the phage samples submitted to the disruption methods was determined by the Bradford protein assay (Pierce Coomassie Bradford Protein Assay Kit, Thermo Fisher Scientific™) and compared with the protein content in the stock phage solution. A set of protein standards was prepared by diluting the contents of one Bovine Serum Albumin (BSA) standard ampoule (2 mg/mL) five times into clean eppendorfs®, in Tris-HCl 25 mM pH 9 buffer. It was pipetted 50 µL of each standard, control and testing samples into a 96 microwell plate well. Duplicates were made. 200 µL of Coomassie solution was added to each well and the plate was mixed on a plate shaker for 30 seconds and then incubated for 10 minutes at room temperature. Absorbance was read at 595 nm with a Multiskan™ FC Microplate Photometer (Thermo Fisher Scientific™).

3.5.3. Bacteriophage Morphology Analysis

The morphology of *E. coli* T4 bacteriophages submitted to fragmentation processes were analyzed with TEM at the MicroLab facilities in Instituto Superior Técnico.

For the analysis of T4 bacteriophages submitted to fragmentation methods, the staining process with uranyless was performed as described by *Electron Microscopy Sciences*¹⁰⁶. The grid was deposited on a sample drop of these phage samples and then a droplet of uranyless solution was added on top and let to absorb for 1 minute. The excess of dye was removed with a tissue paper. The grid was then deposited on the uranyless solution for 1 minute and let to dry for another 5 minutes. Afterwards the grid was placed in the TEM device to visualize the samples.

4. Results and Discussion

The aim of this work is to develop new and advanced recognition elements for the tracking and identification of antibiotic resistant bacteria based on the dissociation of bacteriophages' tails from their heads. In the first section (4.1) of this chapter, *E. coli* bacteria are characterized in terms of their proliferation phases. The titre of bacteria in the exponential phase is also presented. Section 4.2 presents a scheme with details about the experimental processes involving bacteriophage amplification in both solid and liquid mediums. Phage titre in the prepared stock solution is also revealed. The methods applied in the stock phages for the separation of their tails from the rest of their bodies are described in section 4.3 and include non-mechanical (osmotic shock) and mechanical (water bath sonication and probe sonication) procedures. The final section (4.4) presents and describes TEM images of the T4 phages that went through the dissociation tests.

4.1. Characterization of *E. coli* Growth Phases

E. coli is a robust, gram-negative and high versatile bacterium that is characterized by its ease of maintenance and rapid growth in laboratory conditions. These qualities make *E. coli* one of the model organisms in the field of microbiology studies. The proliferation of a bacterial population and its rate of growth are limited by its genetics and environmental condition such as temperature, acidity (pH), oxygen levels, water, micro and macro nutrients and toxins. In a batch system, viable bacterial cells cultivated in TSB medium and incubated at a constant optimal temperature of 37 °C, with agitation of 250 rpm and pH 7, are capable of reproducing quickly and their dynamics of population proliferation can be measured periodically by the increase in the number of cells as a function of the incubation time^{107,108,109}. This relation makes it possible to obtain a growth curve of *E. coli* cells as present in **Figure 23**.

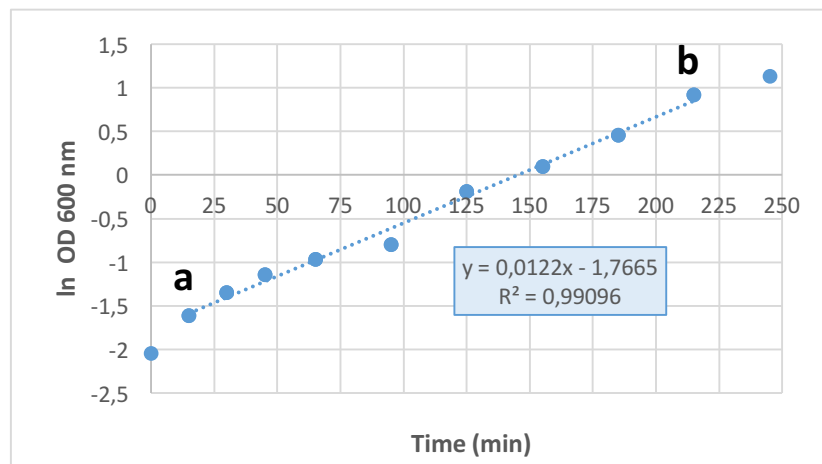


Figure 23 – *E. coli* growth curve. Identification of growth phases: (a) exponential phase between 0 and 220 minutes; (b) deceleration phase at 220 minutes.

When the microbial growth of the culture is carried out in batch, the culture goes through 4 distinct phases. Initially, when bacteria are inoculated, despite being metabolically active, cell division does not occur immediately since they need a period of adaptation to the medium where they are inserted. This adaptation period is called the latency phase in which the culture tends to synthesize enzymes and co-enzymes for its physiological activities in order to benefit from environmental changes¹⁰⁸. Due to this, the latency phase occurs in the pre-inoculum and for that reason, this state does not appear in the determined *E. coli* growth curve. When bacteria are fully adapted to the environment and all of the nutrients necessary for their growth are available, cells start to multiply continuously and at a constant rate, being this state denominated the exponential phase. The exponential phase can be characterized in the growth curve by the letter (a) between 0 and 220 minutes. After the depletion of the limiting nutrient or accumulation of toxic products by bacteria, cells enter a deceleration phase which can be characterized in the growth curve by the letter (b) at 220 minutes. Further, cells enter in the stationary phase, where the proliferation rate becomes zero^{107,108}.

By taking a sample of bacteria from the culture at every 15-30 minutes, it was possible to determine the number of viable cells through the plating the dilutions of those samples. This information in addition to the determination of the different phases of *E. coli* proliferation through the measuring of the OD, is crucial to understand the bacteria growth data, especially the exponential phase since it when the bacteria receptors are more exposed and available for the bacteriophage recognition and attachment. Data is showed in **Table 3**.

Table 3 – *E. coli* growth data. Parcels with (-) symbol mean that the number of colonies were not between 30 and 300 which are the acceptable interval for the counting of PFUs. Parcels with the (*) symbol are the ones that belong to colonies counted on plate with dilution -5. The rest of the colonies were counted on plates with dilution -4.

| Total time of bacterial growth (minutes) | 0 | 15 | 30 | 45 | 65 | 95 |
|--|----------------------|----------------------|----------------------|----------------------|----------------------|------|
| OD 600nm | 0.13 | 0.20 | 0.26 | 0.33 | 0.36 | 0.45 |
| Number of colonies (CFUs) | 188 | 191 | 113 | 168 | 132 | 10* |
| Titre (CFUs/mL) | 1.88x10 ⁷ | 1.91x10 ⁷ | 1.13x10 ⁷ | 1.68x10 ⁷ | 1.32x10 ⁷ | - |

In **Figure 24** it can be observed the counted colonies of *E. coli* at each time of bacterial growth which allow to determine that there were 1.52x10⁷ CFU/mL of bacteria in the exponential phase (between 15 and 30 minutes characterized by an OD of 0.20 and 0.26 respectively).

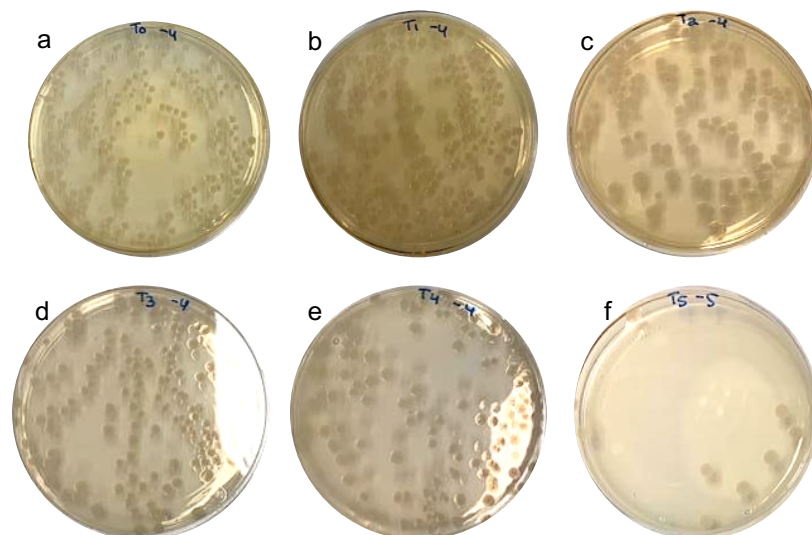


Figure 24 – *E. coli* colonies at different times of bacterial growth at the respective dilution. (a) 0 minutes; (b) 15 minutes; (c) 30 minutes; (d) 45 minutes; (e) 65 minutes and (f) 95 minutes.

4.2. Bacteriophage Stock Amplification

After the knowledge on bacteria content it was necessary to know the phage content. A titration assay showed that the revitalized phage suspension had 4.32×10^7 PFUs/mL which is low taking into account that a typical phage lysate contains approximately 10^8 to 10^{11} PFUs/mL. Due to this, it was necessary to perform both solid and liquid medium amplifications in order to have sufficient quantities of bacteriophage stock for all of the experiments. A quick and easy way to increase an order or two of revitalized phage suspension is to perform a solid medium amplification. This type of amplification basically consists in a titration assay but after the incubation of the plates overnight, a 1x SM buffer solution is added to the uncountable plates, usually the -2 and -3, and the phage suspension is harvested and posteriorly filtrated. The harvested phage suspension was subjected to a new titration assay which showed an increase of two orders of magnitude in the phage content with 2.38×10^9 PFUs/mL.

Although the phage content was already satisfactory to proceed on the experiments, it was not yet the desire titre. In this case, a liquid medium amplification was performed. For this the growth of an *E. coli* culture was followed in shake flasks containing the appropriate medium and when the OD achieved values between 0.16 and 0.25, the infection process started. In the infection step, 319 μ L of phage suspension (amplified by solid amplification method) and 5 mL of $MgCl_2$ 1 M were added to the bacterial culture. This volume of phage suspension was determined for a MOI of 0.1 by the following calculations (**Equation 8**, **Equation 9**, **Equation 10**, **Equation 11** and **Equation 12**):

$$\text{Solid amplification phage titre} = 2.38 \times 10^9 \text{ PFUs/mL} \quad (8)$$

$$\text{Bacteria content} = 1.52 \times 10^7 \text{ CFUs/mL} \quad (9)$$

$$\text{Number of bacteria} = 1.52 \times 10^7 \text{ CFUs/mL} \times 500 \text{ mL TSB medium} = 7.6 \times 10^9 \text{ CFUs} \quad (10)$$

$$\text{MOI} = \frac{\text{PFUs}}{\text{CFUs}} = 0.1 \Leftrightarrow \text{PFUs} = 0.1 \times 7.6 \times 10^9 \text{ CFUs} = 7.6 \times 10^8 \text{ PFUs} \quad (11)$$

$$\text{Volume of phage suspension to add to the bacterial culture} = \frac{7.6 \times 10^8 \text{ PFUs}}{2.38 \times 10^9 \text{ PFUs/mL}} = 0.319 \text{ mL} \quad (12)$$

Finally, *E. coli* cells start to be infected when bacterial growth reaches an OD between 0.16 and 0.25, and lyse originating a final lysate which contains rests of lysed bacteria and the multiplied phages. The final lysate goes through processes of centrifugation and filtration and then subjected to processes of concentration and diafiltration in a 500 kDa membrane module for the removal of medium and small molecules, rests of bacteria and to exchange the medium for a stable buffer. In this way a final stock phage suspension was obtained with a titre of 2.86×10^{10} PFUs/mL. **Figure 25** shows a schematic representation of both amplification processes.

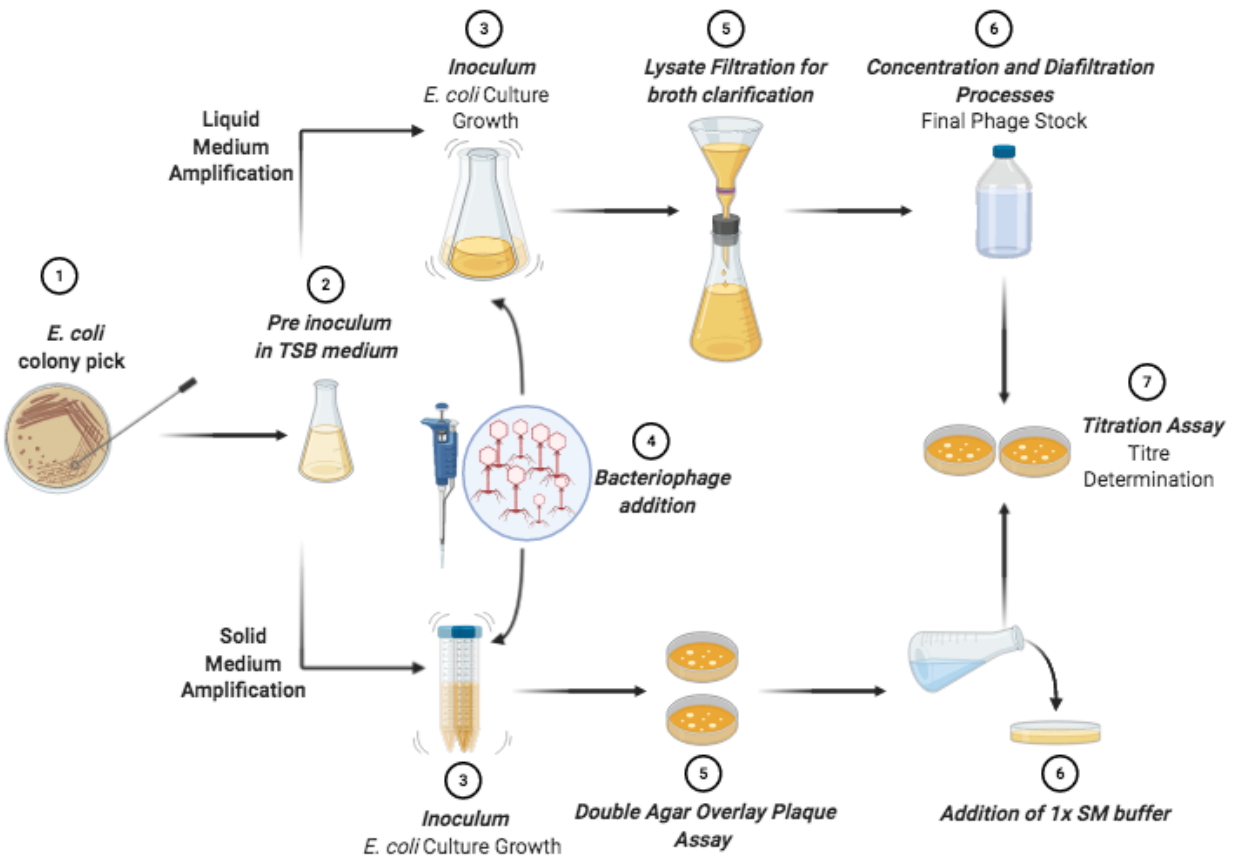


Figure 25 – Schematic representation of both solid and liquid medium amplifications. Image created in BioRender.com – accessed 10th November 2020.

4.3. Bacteriophage Dissociation Techniques

During their infection process, bacteriophages attach to the receptors in the surface of the specific bacterial cell and inject their genetic material inside them in order to create new progeny. This action leads to the rupture of the bacterial cell and release of the phage progeny. Although this is a fast and efficient way to amplify and produce new phages, it compromises the recognition of target cells when used in biosensors. Due to this, the generation of phages with only their tails (recognition and attachment portion) and lack of their heads (transmission of genetic material portion) could allow the identification of bacterial targets without lysing them. In this section it is presented three different approaches are presented to achieve the creation of phages as a new recognition element, commonly used to disrupt cells.

4.3.1. Osmotic Shock

When a rapid change in the concentration of solutes around the cell occurs, causes a quick change in the movement of water across its cell membrane leading the cell to lyse. This osmotic pressure can be promoted by salts, glucose or other substrates. In this case, the salt sodium acetate 5 M was used to cause the dissociation of the tails of phages when submitted to 100 volumes of water for different periods of time (2, 5, 10, 15, 20, and 30 minutes).

The fastest way to understand the effect of the osmotic shock process is to test and analyze the infection ability of the resulting phages. If the osmotic shock resulted in physical changes in the phages, a decrease in their infection capacity would be detected. For this, a titration assay was conducted. Data related to the titration of osmotic shock samples are presented in **Table 4**.

Table 4 – Osmotic shock process data for the different periods of exposure (2, 5, 10, 15, 20 and 30 minutes) to sodium acetate. Parcels with (-) symbol mean that the number of colonies were not between 30 and 300 which are the acceptable interval for the counting of PFUs. Parcels with the (*) symbol are the ones that belong to phage plaques counted on plate with dilution -5. The rest of the phage plaques were counted on plates with dilution -4.

| minutes | | Time of exposure to sodium acetate | | | | | |
|-----------------------|----------------------|------------------------------------|--------------------|--------------------|--------------------|--------------------|--------------------|
| | | 2 | 5 | 10 | 15 | 20 | 30 |
| Before centrifugation | Volume (mL) | 50 | | | | | |
| | Phage plaques (PFUs) | 183 | 147 | 132 | 233 | 118 | 56* |
| | Titre (PFUs/mL) | 1.83×10^7 | 1.47×10^7 | 1.32×10^7 | 2.33×10^7 | 1.18×10^7 | 5.6×10^7 |
| | Nº of phages (PFUs) | 9.15×10^8 | 7.35×10^8 | 6.60×10^8 | 1.17×10^9 | 5.90×10^8 | 2.80×10^9 |
| Pellet | Volume (mL) | 5 | | | | | |
| | Phage plaques (PFUs) | 294 | 71* | 76 | - | 163 | 132* |
| | Titre (PFUs/mL) | 2.94×10^7 | 7.1×10^7 | 7.6×10^6 | - | 1.63×10^7 | 1.32×10^8 |

| | | | | | | | |
|--------------------|----------------------|----------------------|----------------------|----------------------|----------------------|----------------------|----------------------|
| | N° of phages (PFUs) | 1.47x10 ⁸ | 3.55x10 ⁸ | 3.80x10 ⁷ | - | 8.15x10 ⁷ | 6.60x10 ⁸ |
| Supernatant | Volume (mL) | 50 | | | | | |
| | Phage plaques (PFUs) | 189 | 207 | 245 | 71* | - | 173 |
| | Titre (PFUs/mL) | 1.89x10 ⁷ | 2.07x10 ⁷ | 2.45x10 ⁷ | 7.1x10 ⁷ | - | 1.73x10 ⁷ |
| | N° of phages (PFUs) | 9.45x10 ⁸ | 1.04x10 ⁹ | 1.23x10 ⁹ | 3.55x10 ⁹ | - | 8.65x10 ⁸ |

Since the phage stock has a titre of 2.86x10¹⁰ PFUs/mL and 500 µL were used in the osmotic shock tests, it means that each suspension contained a total maximum of 1.43x10¹⁰ PFUs.

By the analysis of the titration assay on the osmotic shock samples, is possible to observe a decrease on the titre on all of the dilutions tested for the samples before centrifugation, pellet and supernatant. The samples before centrifugation show an average of 1.14x10⁹ PFUs obtained after the osmotic shock, the pellets show an average of 2.56x10⁸ PFUs and the supernatant show an average of 1.52x10⁹ PFUs. This means that all of the tested phage suspensions decreased the infection capacity by an order or two of magnitude comparing to the initial phage content, which is a positive indicative that the osmotic shock damaged in some way the bacteriophages.

To further evaluate if the fragmentation of phages was conducted, an assay based on measuring protein concentration before and after centrifugation of the samples was performed. The development of color in Bradford protein assay is associated with the presence of three basic amino acids in the proteins – arginine, lysine and histidine. When the proteins bind to the Coomassie dye, the number of dye ligands bound to each protein molecule is approximately proportional to the number of positive charges found on the protein. This results in a spectral shift from the brown form of the dye to the blue form of the dye. Free amino acids, peptides and low molecular weight proteins do not produce color with Coomassie dye reagents. It was reported by Guerlava *et al.* and Spiden *et al.* that protein content appears to be higher after mechanical or non-mechanical cell disruption techniques^{110,111}. In this context, if phage separation was successful, more phage proteins were expected to appear when compared to the intact phage protein concentration since more proteins would be exposed after the mechanical or non-mechanical applied methods. By varying the the initial concentration of BSA, it was possible to plot a linear calibration curve (**Figure A 2** in Annex II).

The Bradford assay showed a protein concentration of 64 $\mu\text{g/mL}$ in the phage stock. In the phage suspensions before centrifugation and suspensions of the supernatant was not detected any concentration of proteins, probably due to the high dilution (100x) that was made to perform the osmotic shock. Experiments using higher concentrations of phages in the initial osmotic shock process or less diluted samples could be a way to obtain a correct appraisal of the real protein content. In the pellet suspensions, low protein concentrations were detected, which could be due to the deposition of proteins in the suspension falcons and poor homogenization before taking the sample to analysis. However, this data does not allow significant conclusions to be drawn. Information about the protein content are presented in **Table 5**.

Table 5 – Protein concentrations of osmotic shock suspensions performed by the Bradford protein assay.

| | | Time of exposure to sodium acetate | | | | | |
|------------------|-----------------------|------------------------------------|----|----|----|----|----|
| | | minutes | 2 | 5 | 10 | 15 | 20 |
| $\mu\text{g/mL}$ | Before centrifugation | 0 | | | | | |
| | Pellet | 7 | 14 | 11 | 7 | 15 | 17 |
| | Supernatant | 0 | | | | | |
| | Phage Stock | 64 | | | | | |

To determine what proteins were detectable, all of the suspensions were subjected to a denaturing SDS-PAGE, in order to resolve the different proteins of the phages from the stock and the ones exposed to the osmotic shock/separation process. SDS-PAGE technique allows for a quick analysis of the gels because enables to estimate the molecular weight of each phage corresponding protein band.

By the construct of a standard curve that plots the log of the molecular weight from the ladder versus the migration of each ladder band, it was possible to calculate the molecular weight for all of the phage bands (see **Figure A 3** and **Figure A 4** in Annex II for further details).

The gels are showed in **Figure 26** and **Figure 27** after staining with Coomassie and Silver Nitrate. Gel images were edited (contrast and brightness) in order to increase band distinction and visibility to optimize results. A purification and concentration with 100 kDa Amicon® Ultra-4 was performed before the preparation of the samples for salt removal, which could interfere with the running of the gel. A titration assay allowed to confirm that there was no loss of phages in the process of purification/concentrations with the amicons® (data not shown). Samples before centrifugation and from the pellet samples were also run in SDS-PAGE but the results were not conclusive due to protein blur (data not shown).

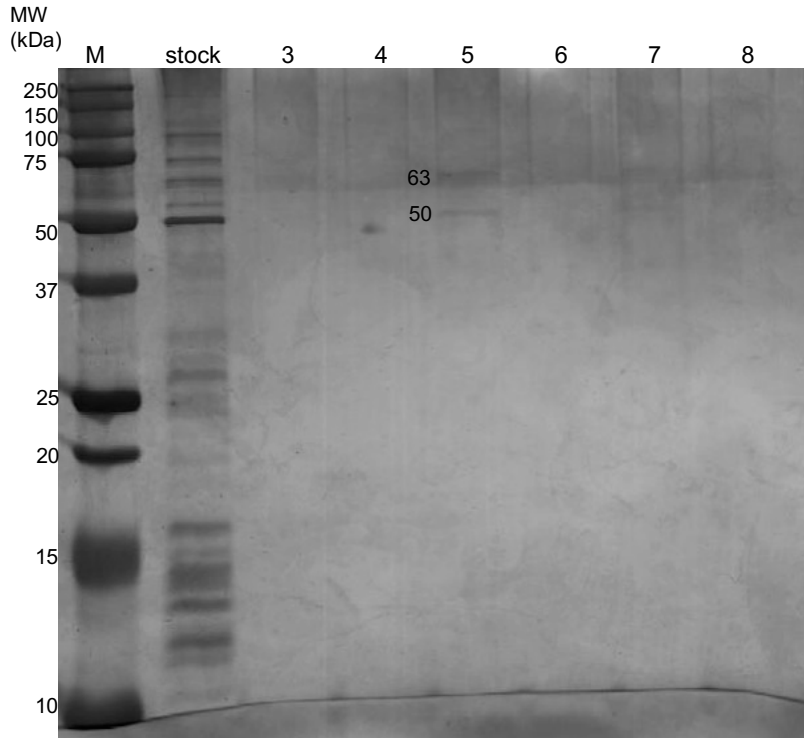


Figure 26 – SDS-PAGE of osmotic shock assay results for the separation of phages' tails from the heads. The gel was stained with Coomassie and after with Silver Nitrate. Well 1: Precision Plus Protein™ Dual Color Standards ladder; Well 2: T4 bacteriophage stock; Well 3: 2 minute osmotic shock concentrated supernatant; Well 4: 2 minute osmotic shock permeated supernatant; Well 5: 5 minute osmotic shock concentrated supernatant; Well 6: 5 minute osmotic shock permeated supernatant; Well 7: 10 minute osmotic shock concentrated supernatant; Well 8: 10 minute osmotic shock permeated supernatant. Two distinct bands can be seen in the concentrated osmotic shock samples with the following molecular weights: 63 kDa and 50 kDa.

Both gels show two distinct bands with 63 and 50 kDa respectively. The molecular weight of the osmotic shock test phage bands was calculated through the standard curve of the ladder bands and posteriorly compared to literature about T4 bacteriophages. According to Clokie *et al.* and Miller *et al.* a protein with 56kDa corresponds to the major capsid protein of the T4 phage, or to the short tail fibre, and a protein with 63kDa corresponds to the baseplate hub subunit^{112,72}. With this, the 63 kDa and 50 kDa bands presented in the gels could correspond to the baseplate hub subunit and the major capsid protein or the short tail fibre, respectively. All of the proteins show an accurate migration in the gels, according to the molecular weight maker. A reliable way to know if the osmotic shock was indeed successful is to analyze the samples in TEM. All information about T4 bacteriophage protein mass and their function reported by Clokie *et al.* and Miller *et al.* can be found in **Table A 1** in Annex II).

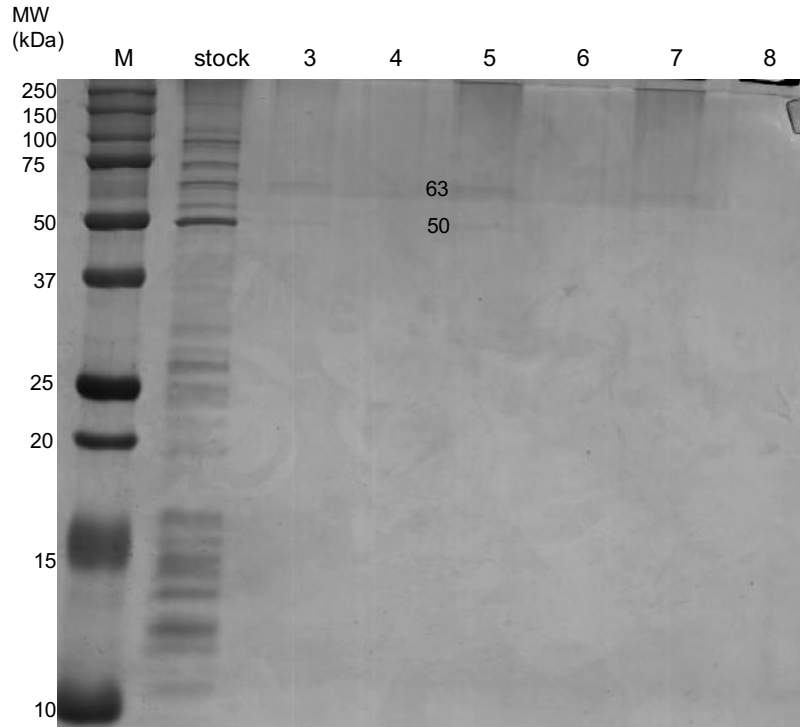


Figure 27 – SDS-PAGE of osmotic shock assay results for the separation of phages’ tails from the heads. The gel was stained with Coomassie and after with Silver Nitrate. Well 1: Precision Plus Protein™ Dual Color Standards ladder; Well 2: T4 bacteriophage stock; Well 3: 15 minute osmotic shock concentrated supernatant; Well 4: 15 minute osmotic shock permeated supernatant; Well 5: 20 minute osmotic shock concentrated supernatant; Well 6: 20 minute osmotic shock permeated supernatant; Well 7: 30 minute osmotic shock concentrated supernatant; Well 8: 30 minute osmotic shock permeated supernatant. Two distinct bands can be seen in the concentrated osmotic shock samples with the following molecular weights: 63 kDa and 50 kDa.

4.3.2. Water Bath Sonication

The basic principle of a sonication is the application of sound energy to promote the agitation of particles in a sample. This agitation is caused by the transmission of ultrasonic frequencies (>20 kHz) to the suspension sample create alternating high-pressure and low-pressure cycles. During these cycles, bubbles are formed and expand until they collapse. Cells disintegrate when the violent shock waves produced by the collapse of bubbles propagate through the suspension and collide to them¹¹³. For this experimental test, a water bath sonication was performed to cause the separation of phages’ tails when submitted to ultrasonic frequencies of 45 kHz for different periods of time (1, 5, 10, 15, 20, 25, 30 and 40 minutes). The water bath was kept at a constant 10 °C.

Once more, the tested phages were analyzed to check if they were able to conserve their infection capability through a titration assay. Data related to the titration assay of the water bath sonication is presented in **Table 6**.

In the start of the experiment, the phage stock had a titre of 2.86×10^{10} PFUs/mL and 5 mL were used for the water bath sonication, which means that the phage suspension in the falcon contained a total of 2.86×10^{10} PFUs/mL.

Table 6 – Water bath ultrasonication process data for the different periods of exposure (1, 5, 10, 15, 20, 25, 30 and 40 minutes). Parcels with (-) symbol mean that the number of colonies were not between 30 and 300 which are the acceptable interval for the counting of PFUs. Parcels with the (*) symbol are the ones that belong to phage plaques counted on plate with dilution -8. The rest of the phage plaques were counted on plates with dilution -7.

| | Time of exposure to water bath ultrasonicator | | | | | | | |
|----------------------|---|---|-----------------------|-----------------------|-----------------------|-----------------------|-----------------------|----|
| minutes | 1 | 5 | 10 | 15 | 20 | 25 | 30 | 40 |
| Volume (mL) | 0.5 | | | | | | | |
| Phage plaques (PFUs) | 289 | - | 273 | 65* | 174 | 278 | 291 | - |
| Titre (PFUs/mL) | 2.89×10^{10} | - | 2.73×10^{10} | 6.5×10^{10} | 1.74×10^{10} | 2.78×10^{10} | 2.91×10^{10} | - |
| N° of phages (PFUs) | 1.46×10^{10} | - | 1.37×10^{10} | 3.25×10^{10} | 8.70×10^9 | 1.39×10^{10} | 1.46×10^{10} | - |

The titration results show an average of 3.26×10^{10} PFUs/mL able to infect the target bacteria. The results show a slightly increase in the phage titre after the water bath ultrasonication, which may be due to the disaggregation of phages that were clumped in the phage stock. These aggregates in the stock solution could result in the counting of just one plaque in the titration assays. The disaggregation caused by the water bath ultrasonication originated different plaques, justifying the slightly increase presented. Given the fact that the phage titre after this sonication is of the same order of magnitude as the titre of the phage stock and there was no significant decrease in the phages' infection capacity, it can be assumed that this process was not effective in order to separate phage tails from the heads. Additionally, the energy applied during the process was 6.67×10^{-2} KW.h/dm³.

To help comprehend the results from the titration assay, a Bradford protein assay was conducted in order to measure protein concentration. For this, a linear calibration curve of the varying BSA initial concentration was accomplished (**Figure A 5** in Annex II).

The BSA protein assay presented a protein concentration of 62 µg/mL in the phage stock. The tested water bath ultrasonication samples showed an average of 57 µg/mL of protein concentration in the performed Bradford assay, which is a very approximate value comparing to the phage stock. However, no specific conclusions could be taken. Only a TEM analysis could verify if the separation of tails occurred. Details about the protein concentrations for the water bath ultrasonication are presented in **Table 7**.

Table 7 –Protein concentrations of water bath ultrasonication samples performed by the Bradford protein assay.

| | | Time of exposure to water bath ultrasonicator | | | | | | | |
|---------|-------------|---|----|----|----|----|----|----|----|
| minutes | | 1 | 5 | 10 | 15 | 20 | 25 | 30 | 40 |
| µg/mL | Sonication | 54 | 54 | 58 | 56 | 57 | 57 | 60 | 60 |
| | Phage Stock | 62 | | | | | | | |

To further explore the water bath ultrasonication process, the different time samples were subjected to a denaturing SDS-PAGE. The resulting gel allowed to distinguish the different proteins from the phages exposed to the experiment and compare them to the proteins resolved from the phage stock. For this gel, a standard curve plotting the molecular weight from the ladder versus the migration of each ladder band was created in order to estimate the molecular weight for all of the sonicated phage bands (see **Figure A 6** and **Figure A 7** in Annex II for further details). The gel is showed in **Figure 28** after staining with Coomassie and Silver Nitrate. The gel image was edited (contrast and brightness) in order to increase band distinction and visibility to optimize results.

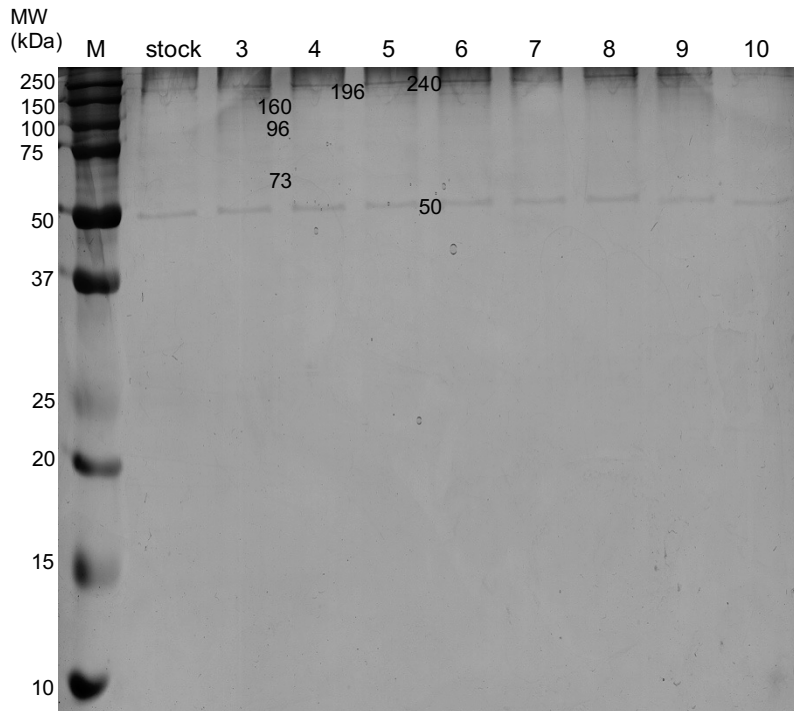


Figure 28 – SDS-PAGE of water bath ultrasonication assay results for the separation of phages' tails from the heads. The gel was stained with Coomassie and after with Silver Nitrate. Well 1: Precision Plus Protein™ Dual Color Standards ladder; Well 2: T4 bacteriophage stock; Well 3: 1 minute sonication; Well 4: 5 minutes sonication; Well 5: 10 minutes sonication; Well 6: 15 minutes sonication; Well 7: 20 minutes sonication; Well 8 :25 minutes sonication; Well 9: 30 minutes sonication; Well 10: 40 minutes sonication. Six distinct bands can be seen in all of the wells with the following molecular weight: 240 kDa, 196 kDa, 160 kDa, 96 kDa, 73 kDa and 50 kDa.

The gel presented six bands corresponding to 240 kDa, 196 kDa, 160 kDa, 96 kDa, 73 kDa and 50k Da which were calculated using the standard curve of the ladder bands and posteriorly compared to literature about T4 bacteriophages. It was reported by Clokie *et al.* and Miller *et al.*, only T4 proteins with molecular weights below 140 kDa, thus the first three bands with 240 kDa, 196 kDa and 160 kDa were not considered for protein function characterization. However, these three bands belong to the T4 bacteriophage since the phage stock well contain those same bands. The band with 96 kDa may correspond to the tail fibre component (described in literature with 109 kDa) or phage baseplate wedge subunit (described in literature with 119 kDa). As for the band with a molecular weight of 73 kDa likely corresponds

to the phage baseplate wedge subunit (described in literature with 66 kDa or 74 kDa) or to the phage head component (described in literature with 75 kDa). The last band on this gel may correspond to the major capsid protein or the short tail fibre since the estimated 50 kDa with the standard curve is close to the 56 kDa reported by Clokie *et al.* and Miller *et al.* ^{112,72}. All of the proteins show an accurate migration in the gels, according to the molecular weight maker.

4.3.3. Probe Ultrasonic Homogenization

In laboratory, probe ultrasonication is commonly applied to disrupt cells. However, this type of sonication provokes a large generation of heat which can compromise biological samples. For this reason, phage samples were kept on ice through the all experiment. Probe sonication was performed at a constant frequency of 20 kHz for two different powers, 25 and 50 W and carried to periods of 5, 10, 15, 20, 30 and 40 minutes.

To easily and rapidly analyze the consequence of the probe ultrasonications, a titration assay was conducted. The probe ultrasonication at 25 and 50 W titration data is presented in **Table 8** and **Table 9**, respectively. The titre of the initial phage stock was 2.86×10^{10} PFUs/mL and 7 mL were used for each experiment, which makes a total of 2.86×10^{10} PFUs/mL per falcon available for each ultrasonication.

Table 8 – 25W probe ultrasonication process data for the different periods of exposure (5, 10, 15, 20, 30 and 40 minutes). Parcels with the (*) symbol are the ones that belong to phage plaques counted on plate with dilution -5. The rest of the phage plaques were counted on plates with dilution -6.

| | Time of exposure to the probe ultrasonicator at 25W | | | | | |
|----------------------|---|-------------------|--------------------|-------------------|-------------------|--------------------|
| minutes | 5 | 10 | 15 | 20 | 30 | 40 |
| Volume (mL) | 1 | | | | | |
| Phage plaques (PFUs) | 125 | 83 | 266* | 31 | 30 | 173* |
| Titre (PFUs/mL) | 1.25×10^9 | 8.3×10^8 | 2.66×10^8 | 3.1×10^8 | 3.0×10^8 | 1.73×10^8 |
| N° of phages (PFUs) | 1.25×10^9 | 8.3×10^8 | 2.66×10^8 | 3.1×10^8 | 3.0×10^8 | 1.73×10^8 |

Table 9 – 50W probe ultrasonication process data for the different periods of exposure (5, 10, 15, 20, 30 and 40 minutes). Parcels with (-) symbol mean that the number of colonies were not between 30 and 300 which are the acceptable interval for the counting of PFUs. Phage plaques were counted on plates with dilution -6.

| | Time of exposure to the probe ultrasonicator at 50W | | | | | |
|----------------------|---|--------------------|--------------------|--------------------|-------------------|----|
| minutes | 5 | 10 | 15 | 20 | 30 | 40 |
| Volume (mL) | 1 | | | | | |
| Phage plaques (PFUs) | 200 | 102 | 141 | 152 | 74 | - |
| Titre (PFUs/mL) | 2.00×10^9 | 1.02×10^9 | 1.41×10^9 | 1.52×10^9 | 7.4×10^8 | - |
| N° of phages (PFUs) | 2.00×10^9 | 1.02×10^9 | 1.41×10^9 | 1.52×10^9 | 7.4×10^8 | - |

As the results present, probe ultrasonications with 25 and 50 W showed, respectively, an average of 5.22×10^8 PFUs/mL and 1.34×10^9 PFUs/mL that were able to maintain their infectiveness. Both experiments exhibit a decrease by one and two orders of magnitude in the number of phages able to infect, which is a strong evidence that phage separation occurred. Additionally, the energy applied during the processes were 2.38 KW.h/dm^3 and 33.3 KW.h/dm^3 for the 25 and 50 W probe sonication respectively.

To complement these promising titration results, a Bradford protein assay was performed. The linear calibration curve of the varying BSA initial concentration is presented in **Figure A 5** in Annex II, the same one used for the water bath ultrasonication experiment.

The phage stock presented a protein concentration of $62 \text{ }\mu\text{g/mL}$ in the BSA protein assay. The tested samples for the probe sonication at 25 W showed an average of $58 \text{ }\mu\text{g/mL}$, while the samples for probe sonication at 50 W presented an average of $27 \text{ }\mu\text{g/mL}$. When compared to the protein concentration of the phage stock, 25 W ultrasonication exhibit more reliable outcomes since the concentration values are close to each other. Although reported by Guerlava *et al.* and Spinden *et al.* that after disruption there is an increase in protein concentration, it does not necessary mean that the same results should be obtained in this case since the authors based their studies on bacterial and yeast cells. The aim of the cell disruption was to release metabolic and protein content, however in this experimental work the objective is not to burst the phages but to dissociate their structure^{110,111}. Consequently, the level of protein content in the Bradford assay analysis would not be mandatorily much higher than the protein content of the stock. In this case, 25 W probe ultrasonication is shown promising for phage separation. As for the protein contents of 50W ultrasonication, results show a decrease in the protein content which coincides with protein degradation. The fact that the sonicator performed at 50W allows a rapid and high increase of temperature that may compromise biological samples and destroy protein molecules. Details about the protein concentrations for the probe ultrasonication at 25 and 50 W are presented in **Table 10** and **Table 11**, respectively.

Table 10 –Protein concentrations of 25W probe ultrasonication samples performed by the Bradford protein assay.

| | | Time of exposure to the probe ultrasonicator at 25W | | | | | |
|------------------|-------------|---|----|----|----|----|----|
| minutes | | 5 | 10 | 15 | 20 | 30 | 40 |
| $\mu\text{g/mL}$ | Sonication | 61 | 60 | 60 | 57 | 56 | 55 |
| | Phage Stock | 62 | | | | | |

Table 11 – Protein concentrations of 50W probe ultrasonication samples performed by the Bradford protein assay.

| | | Time of exposure to the probe ultrasonicator at 50W | | | | | |
|------------------|-------------|---|----|----|----|----|----|
| minutes | | 5 | 10 | 15 | 20 | 30 | 40 |
| $\mu\text{g/mL}$ | Sonication | 52 | 39 | 29 | 12 | 14 | 14 |
| | Phage Stock | 62 | | | | | |

Further, the samples of both probe ultrasonications were tested to acquire more information about their effect on phages. In this way, the different time samples were subjected to a denaturing SDS-PAGE with the purpose of resolving the distinct proteins of the tested phages. For both gels, 25 and 50 W probe sonication, a standard curve plotting the the molecular weight from the ladder versus the migration of each ladder band was created in order to estimate the molecular weight for all of the sonicated phage bands (see **Figure A 8, Figure A 9, Figure A 10, Figure A 11 and Figure A 12** in Annex II for further details). The gels concerning the 25 and 50 W probe ultrasonication are presented in **Figure 29** and **Figure 30**, respectively after staining with Coomassie and Silver Nitrate. Gel images were edited (contrast and brightness) in order to increase band distinction and visibility to optimize results. A purification and concentration with 100 kDa Amicon® Ultra-4 was performed to the T4 bacteriophage stock for a better visualization of the bands in the SDS-PAGE. A titration assay allowed to confirm that there was no loss of phages in the process of purification/concentrations with the amicons® (data not shown).

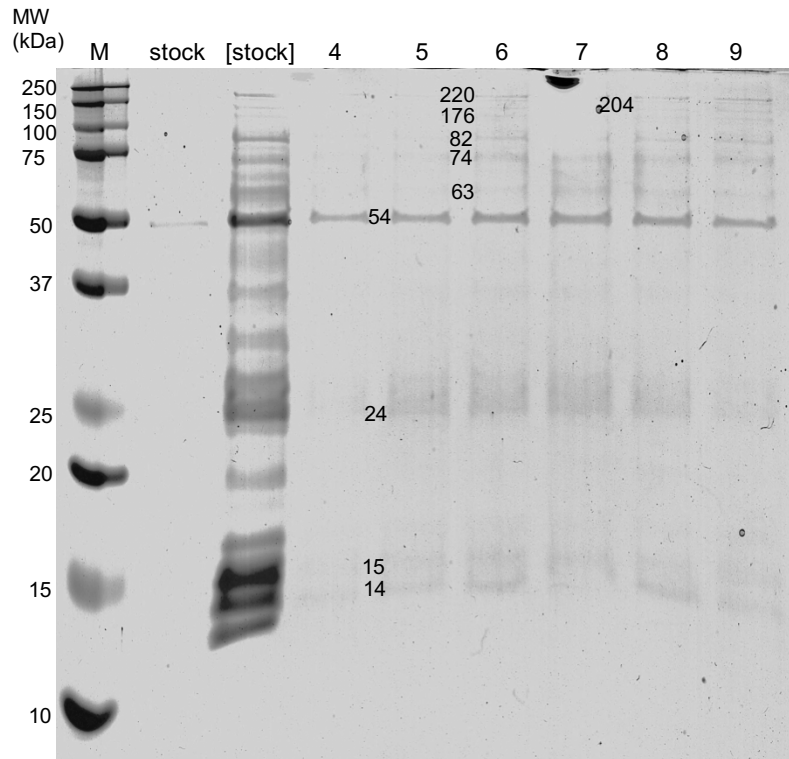


Figure 29 – SDS-PAGE of 25W probe ultrasonication assay results for the separation of phages’ tails from the heads. The gel was stained with Coomassie and after with Silver Nitrate. Well 1: Precision Plus Protein™ Dual Color Standards ladder; Well 2: T4 bacteriophage stock; Well 3: concentrated T4 bacteriophage stock (with Amicon→Ultra-4 100 kDa Centrifugal Filter Units); Well 4: 5 minutes sonication; Well 5: 10 minutes sonication; Well 6: 15 minutes sonication; Well 7: 20 minutes sonication; Well 8 :30 minutes sonication; Well 9: 40 minutes sonication. Ten distinct bands can be seen in all of the wells with the following molecular weight: 220 kDa, 204 kDa, 176 kDa, 82 kDa, 74 kDa, 63 kDa, 54 kDa, 24 kDa, 15 kDa and 14 kDa.

The 25 W probe ultrasonication gel reveals ten distinguishing bands, all of them matching with bands from the concentrated phage stock, which means its proteins corresponding to the T4 bacteriophage. All of the protein bands were determined by the standard curves of the ladder bands according to their migration distance. The first three protein bands presented in the gel were not considered for any conclusion regarding their protein function since it has only been reported by Clokie *et al.* and Miller *et al.*, T4 proteins with molecular weights below 140 kDa. In spite of that fact, these bands (220 kDa, 204 kDa and 176 kDa) belong to the T4 bacteriophage genome. As for the next band with 82 kDa it may correspond to the phage head component, described in literature by 75 kDa. Considered as a baseplate wedge subunit with 74 kDa described by Clokie *et al.* and Miller *et al.*, the band with 74 kDa is the one that most certainly characterizes this function. The protein band in the gel presenting a 63 kDa may correspond to the baseplate hub subunit (described in literature with 63 kDa) or the baseplate wedge subunit (described in literature with 66 kDa). The most visible band is determined to have 54 kDa and can own either the be a major capsid protein (56 kDa) or be a short tail fibre (56 kDa) according to the authors, respectively ^{112,72}. Characterized in literature as the internal head protein (21 kDa) and the long tail fibre component (23 kDa), are proximate enough to classify the gel band of 24 kDa with one of these functions. The last two bands in the gel (15 kDa and 14 kDa) have similar values to 18 kDa that is reported by Clokie *et al.* and Miller *et al.* as a tail tube protein. All of the proteins show an accurate migration in the gels, according to the molecular weight maker. Thus, the results show a promising indicative that the 25 W probe ultrasonication was able to separate the capsid from the baseplate and tails of the phages based on the visible gel bands. A TEM session would be crucial to validate these results.

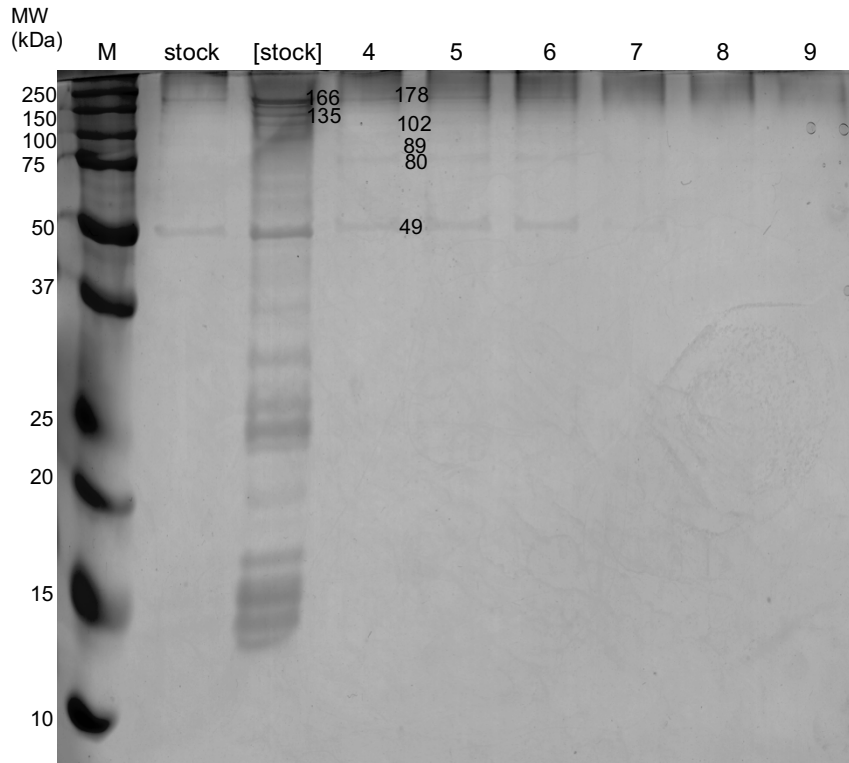


Figure 30 – SDS-PAGE of 50W probe ultrasonication assay results for the separation of phages’ tails from the heads. The gel was stained with Coomassie and after with Silver Nitrate. Well 1: Precision Plus Protein™ Dual Color Standards ladder; Well 2: T4 bacteriophage stock; Well 3: concentrated T4 bacteriophage stock (with Amicon→Ultra-4 100 kDa Centrifugal Filter Units); Well 4: 5 minutes sonication; Well 5: 10 minutes sonication; Well 6: 15 minutes sonication; Well 7: 20 minutes sonication; Well 8 :30 minutes sonication; Well 9: 40 minutes sonication. Seven distinct bands can be seen in all of the wells with the following molecular weight: 178 kDa, 166 kDa, 135 kDa, 102 kDa, 89 kDa, 80 kDa and 49 kDa.

The 50W probe ultrasonication gel shows seven distinct bands with 178 kDa, 166 kDa, 135 kDa, 102 kDa, 89 kDa, 80 kDa and 49 kDa. As it been referred by Clokie *et al.* and Miller *et al.*, proteins with molecular weights higher than 140 kDa are not characterized so the first two bands in the gel (with 178 kDa and 166 kDa) were not classified by their function. According to the authors, the bands with 135 kDa, 102 kDa and 80kDa are most likely to have the function of long tail fibre component (described in literature with 140 kDa), tail fibre component (described in literature with 109 kDa) or baseplate wedge subunit (described in literature with 119kDa) and phage head component (described in literature with 75 kDa), respectively. The most visible band in the gel, corresponding to 49 kDa may be characterized by a head phage protein, as it has a molecular weight close to what’s been reported (46 kDa). With 89 kDa it has not yet been reported characterization for its function^{112,72}. All of the proteins show an accurate migration in the gels, according to the molecular weight maker. These results show a promising indicative that the 50 W probe ultrasonication may have been able to separate the capsid from the baseplate and tails of the phages based on the visible gel bands, however presented less bands comparing to the 25 W probe ultrasonication, which can reinforce the idea that some of the proteins were degraded along with the process. A TEM session

session would be crucial to understand all of the results together.

4.4. Bacteriophage Morphology Analysis

The *E. coli* T4 bacteriophages submitted to a 25 W probe ultrasonication were visualized by TEM since it was the fragmentation process with the most promising and reliable results. Intact T4 bacteriophages were reported by Miller *et al.* to be composed of a long contractile tail and an icosahedral head. These characteristics indicate that these phages belong to the T-even bacteriophages from the *Myoviridae* family⁷². **Figure 31** presents images of a sample of T4 phages submitted to a 25 W probe ultrasonication at 40 000x magnification.

The submitted T4 phages appear to be with their tails separated from their respective capsids and their baseplate and tail fibers are also visible, which indicated that the recognition portion may be intact and functionalized. These observations may be an evidence that the 25 W probe ultrasonication was effective for the generation of bacteriophages comprising only the recognition apparatus suitable to be applied in a biosensor platform in order to improve the field of medical diagnosis. Even with no images visualized of the intact T4 bacteriophage, the morphology of the capsid and tails analyzed appear to be in accordance to Miller *et al.*⁷².

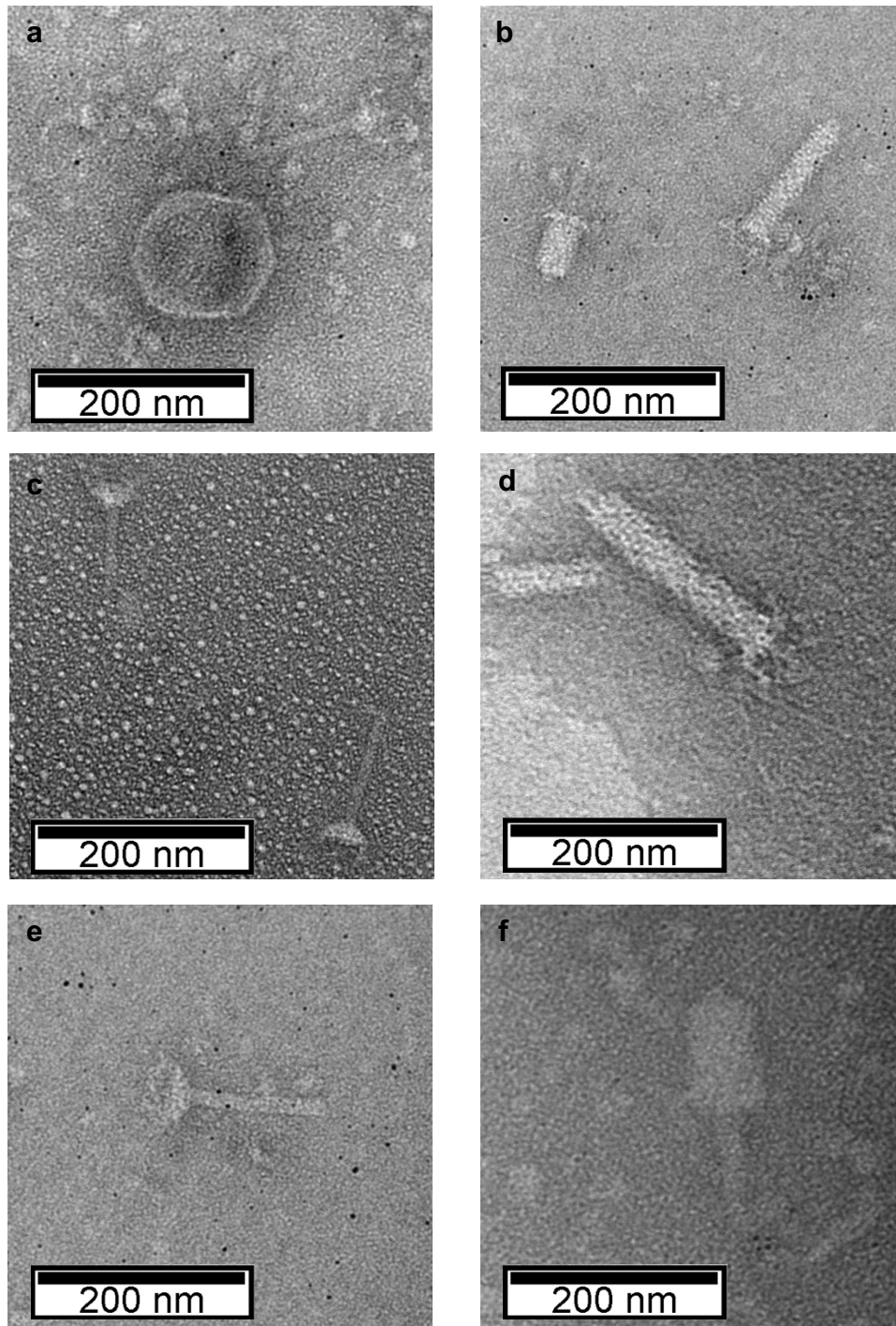


Figure 31 – TEM images of specific *E. coli* T4 bacteriophages submitted to a 25 W probe ultrasonication stained with uranylless. Images obtained at 40 000x magnification at a 200nm scale in IST MicroLab. (a) phage capsid separated of their tail apparatus with 15 minutes of probe ultrasonication; (b) contracted and non-contracted tail apparatus separated from phage capsid with 15 minutes of probe ultrasonication; (c) tail apparatus with visible baseplates separated from phage capsid with 15 minutes of probe ultrasonication; (d) tail apparatus with visible tail fibers separated from phage capsid with 15 minutes of probe ultrasonication; (e) tail apparatus with visible baseplates separated from phage capsid with 20 minutes of probe ultrasonication; (f) tail apparatus with visible baseplates separated from phage capsid with 20 minutes of probe ultrasonication.

6. Final Remarks and Future Perspectives

This Master's Thesis aimed to enhance and develop advance bacteriophage recognition elements for a fast and reliable pathogen identification by the separation of bacteriophage's heads from their tails, thus eliminating the infection capacity, but retaining their recognition ability. The overall process consisted in the production, preparation and amplification of *E. coli* specific T4 bacteriophages stock and testing of disruption methods for the separation of phage tails.

The concentration and diafiltration procedures, referent to the amplification process, appeared to be important for phage stability since only small losses in phage titre were detected when storing the stock for three months. When the lysate was stored in the culture media after centrifugation, without concentration and diafiltration processes, a phage precipitation showed up, leading to a large loss in the titre.

For further experiments it was crucial to work with a well-known and characterized T4 bacteriophage suspension. The working cell bank and a T4 phage stock were prepared from dried suspensions and used in all performed testing and analytical experiments. The *E. coli* host strain growth study provided an understanding of the behavior of these bacterial cells, and also important information such as OD_{600nm} (to know when the exponential phase occurs) and CFUs for the infection assays. The exponential phase was crucial to determine because its in that interval when bacteria receptors are more exposed and available for the bacteriophage recognition, attachment and infection.

After having a functional cell bank and phage stock, the second stage of this study consisted in the attempt to separate the tails of the phages from their heads to prevent the infection and subsequent lysis of the host cells, which compromises the recognition of target cells when used in biosensors. The experimental approaches used to achieve the generation of phages as new recognition elements are commonly used to disrupt and release intracellular components of cells. However, they were applied in the T4 phages. For this, mechanical (water bath ultrasonication and probe ultrasonication) and non-mechanical (osmotic shock) disruption techniques were tested. The submitted phages of each disruption process were analyzed and characterized by their titre, their protein content through SDS-PAGE and Bradford assay.

The fastest way to understand the effect of the fragmentation processes was to analyze the infection capacity of the submitted phages. All of the assays demonstrated a decrease in the ability to maintain infectiveness by one to two orders of magnitude in comparison to the initial phage content that was used in the beginning of each procedure, in exception for the water bath ultrasonication which was not effective. These results showed a positive indicative that the osmotic shock and the 25 and 50 W probe ultrasonication separation techniques damaged in some way the bacteriophages. Despite these results, the decline of the infection capacity could be due to: i) burst of the phages capsids;; ii) generation of openings in the capsid of the phages, which may have lead to the escape of the genetic material; and iii) actual separation of phage tails from their heads. Nevertheless, PFU counting plaques does not differentiate between undamaged intact phages and damaged "leaky" phages which are technically whole, however may have openings in the

capsid which may or not allow the escape of the DNA, as so they can still infect the bacterial host as long as they own enough genetic material for that process ¹¹¹. Furthermore, the plaque counting methods is not an exact method due to possible dilution and plaquing associated errors.

To further evaluate if the phage fragmentation by the disruption methods was conducted, an assay based on measuring protein concentration was performed. This content is reported to be higher in bacterial cells or yeasts after mechanical or non-mechanical cell disruption techniques ^{110,111}, so theoretically, it would be expected to obtain the same outcome for phages. The Bradford assay on the osmotic shock samples demonstrated zero or very low protein contents when compared to the protein concentration on the phage stock. This result could be explained by the high dilutions that were made to perform the osmotic shock. The analyzed protein samples from the water bath ultrasonication and 25 W probe ultrasonication presented high values of protein concentration that almost reached the content of the phage stock. Although reported in literature that after disruption there is an increase in protein concentration ^{110,111}, it does not necessary mean that the same results should be obtained for two reasons: i) this experimental work is done with phages which are much resistant and robust than bacterial cells or yeasts, and ii) the main objective is to separate body parts of the phages, not disrupt them, so in theory, the protein content would be less than the protein content released by burst phages. Consequently, the level of protein content in the Bradford assay analysis would not be mandatorily much higher than the protein content of the stock. Additionally, the Bradford assay is only applicable to differentiate between whole undamaged phages and phages which have released their metabolites. It is not applicable to distinguish between phages which are ruptured and more extreme levels of fragmentation ^{110,111,114}. The 50 W probe ultrasonication presented very low values of protein concentrations which is compatible to protein degradation by the rapid increase of temperature at the tip of the probe ¹¹⁵.

All of the phage samples submitted to the fragmentation processes were also subjected to a denaturing SDS-PAGE. The resulting gels allowed to distinguish several bands which belong to T4 bacteriophage stock. The bands were identified by their molecular weight and specific function and characterized as proteins which belong to the head, tail and tail fibres ^{112,72}.

Taking into account all of the four dissociation methods, the one that showed more promising results was the 25W probe ultrasonication, phage samples were analysed in TEM. TEM images showed a successful fragmentation of the phage tails from their capsids during 15 and 20 minutes of ultrasonication. The other three disruption methods were not analysed by TEM, however it would be a way to take more detailed conclusions on the fragmentation of the bacteriophages.

For future work, supplementary disruption assays could be performed by changing or adding some of parameters such as temperature or power in probe ultrasonication or different salt concentrations for the osmotic shock. dDNA quantification assay such as PicoGreen® could also be strategy to measure the concentration of nucleic acids after the fragmentation processes once a high concentration of DNA would indicate the release of genetic material in consequence of the detachment of the phage heads from the tails.

Furthermore, enzymatic digestion could also be performed as a disruption technique to separate phage heads in the specific aminoacids.

Additionally, a two-phase separation assay with PEG (Polyethylene Glycol) or a column chromatography would be approaches worth to try in order to separate and purify phages tails from the heads. PEG separation would allow for the majority of the tails to rest on the upper phase since they have lower density and the heads, which have higher density due to the DNA encapsulation, to rest in the lower phase. Afterwards, a diafiltration step could also be added in order to exchange the phage media into a suitable buffer. Separation of the tails from the heads in the medium could also be achieved by chromatography which is substantially faster, more consistent, and allows for system automation when compared to the PEG two-phase system. Ion-exchange chromatography (IEC) is the most promising mode of operation that could be used once the heads appear to be more negatively charged than the tails, consequently being retained in a positive charged anion-exchange resin. Size-exclusion chromatography (SEC) is another possibility to consider for this attempt of separation in order to remove non-encapsidated phages (just with tail apparatus) that would elute in last due to their smaller size in comparison to intact phages. At last affinity chromatography could be another way to separate the tails from the heads, however in this case the tails required to be expressing a protein in order to interact with the affinity molecule present in the column. The heads would not interact with the column and elute first. The desire recombinant tails would only elute in the presence of a solvent of higher salt concentration. For instant, it could be produced bacterial cells with a plasmid expressing a His-tag in the proteins of the tail fibers. Thus, during phage assembly, phages with a His-tag in their tail fibers would be present. After phage fragmentation processes, this tag could be used to capture the tails that bind to the column coated with immobilized metal ions such as nickel or copper. In the same way, a biotin-streptavidin recognition assay could be used to separate the tails from the heads. Once again bacterial cells with a plasmid expressing biotin in the tail fibers could be produced and after phage assembly, phages with biotin attach to their tail fibers would be present. After this, the capture could proceed with a column coated with streptavidin. Besides that, the bacterial cells could simply be immobilized in the column to be recognized by the tail fibers and be captured without engineer the phages. After confirmation of phage tail separation and purification, trials for the functionalization of the tails to biosensors could start in order to provide a fast reliable pathogen identification and improve the medical diagnosis field.

4. References

1. Lin, D. M., Koskella, B. & Lin, H. C. Phage therapy: An alternative to antibiotics in the age of multi-drug resistance. *World J. Gastrointest. Pharmacol. Ther.* **8**, 162 (2017).
2. Chanishvili, N. & Aminov, R. Bacteriophage therapy: Coping with the growing antibiotic resistance problem. *Microbiol. Aust.* **40**, 5–7 (2019).
3. Altintas, Z. *Biosensors and Nanotechnology: Applications in Health Care Diagnostics. Biosensors and Nanotechnology* (John Wiley & Sons, Inc., 2018).
4. Wittebole, X., De Roock, S. & Opal, S. M. A historical overview of bacteriophage therapy as an alternative to antibiotics for the treatment of bacterial pathogens. *Virulence* **5**, 209–218 (2014).
5. Frieri, M., Kumar, K. & Boutin, A. Antibiotic resistance. *J. Infect. public Heal.* **10**, 369–378 (2017).
6. Aminov, R. *et al.* Application of bacteriophages. *Microbiol. Aust.* **38**, 63–66 (2017).
7. Kakasis, A. & Panitsa, G. Bacteriophage therapy as an alternative treatment for human infections. A comprehensive review. *Int. J. Antimicrob. Agents* **53**, 16–21 (2019).
8. Kurtböke, I. *Bacteriophages. Bacteriophages* (InTech, 2012).
9. Schaechter, M. *The Desk Encyclopedia of Microbiology. Encyclopedia of Microbiology* (Elsevier Inc., 2010).
10. Chanishvili, N. *Phage Therapy-History from Twort and d’Herelle Through Soviet Experience to Current Approaches. Advances in Virus Research* vol. 83 (Elsevier Inc., 2012).
11. Van Dorst, B. *et al.* Recent advances in recognition elements of food and environmental biosensors: A review. *Biosens. Bioelectron.* **26**, 1178–1194 (2010).
12. Singh, A., Poshtiban, S. & Evoy, S. Recent advances in bacteriophage based biosensors for food-borne pathogen detection. *Sensors (Switzerland)* **13**, 1763–1786 (2013).
13. Gervais, L. *et al.* Immobilization of biotinylated bacteriophages on biosensor surfaces. *Sensors Actuators, B Chem.* **125**, 615–621 (2007).
14. Tolba, M., Minikh, O., Brovko, L. Y., Evoy, S. & Griffiths, M. W. Oriented immobilization of bacteriophages for biosensor applications. *Appl. Environ. Microbiol.* **76**, 528–535 (2010).
15. Edgar, R. *et al.* High-sensitivity bacterial detection using biotin-tagged phage and quantum-dot nanocomplexes. *Proc. Natl. Acad. Sci. U. S. A.* **103**, 4841–4845 (2006).
16. Tawil, N., Sacher, E., Mandeville, R. & Meunier, M. Bacteriophages: Biosensing tools for multi-drug resistant pathogens. *Analyst* **139**, 1224–1236 (2014).
17. Sorokulova, I., Olsen, E. & Vodyanoy, V. Bacteriophage biosensors for antibiotic-resistant bacteria. *Expert Rev. Med. Devices* **11**, 175–186 (2014).
18. Byrne, B., Stack, E., Gilmartin, N. & Kennedy, R. O. Antibody-Based Sensors: Principles, Problems and Potential for Detection of Pathogens and Associated Toxins. *Sensors* **9**, 4407–4445 (2009).
19. Mehrotra, P. Biosensors and their applications - A review. *J. Oral Biol. Craniofacial Res.* **6**, 153–159 (2016).
20. InnovoGENE Biosciences. <https://www.innovogene.com/store/pc/viewcontent.asp?idpage=11> (2020).
21. Kumar, N. & Upadhyay, L. S. B. *Polymeric gels for biosensing applications. Polymeric Gels: Characterization, Properties and Biomedical Applications* (Elsevier Ltd, 2018).
22. Moran, K. L. M., Fitzgerald, J., McPartlin, D. A., Loftus, J. H. & O’Kennedy, R. *Biosensor-Based Technologies for the Detection of Pathogens and Toxins. Comprehensive Analytical Chemistry* vol. 74 (Elsevier Ltd, 2016).
23. Campaña, A. L. *et al.* Enzyme-based electrochemical biosensors for microfluidic platforms to detect pharmaceutical residues in wastewater. *Biosensors* **9**, 41 (2019).
24. Lakshmipriya, T. & Gopinath, S. C. B. *An Introduction to Biosensors and Biomolecules. Nanobiosensors for Biomolecular Targeting* (Elsevier Inc., 2019).
25. Malhotra, B. D. & Pandey, C. M. *Biosensors: Fundamentals and Applications.* (Smithers Rapra, 2017).
26. Pereira, A., Sales, M. & Rodrigues, L. *Biosensors for Rapid Detection of Breast Cancer Biomarkers. Advanced Biosensors for*

- Health Care Applications* (Elsevier Inc., 2019). doi:10.1016/b978-0-12-815743-5.00003-2.
27. Pohanka, M. & Skládal, P. Electrochemical biosensors - Principles and applications. *J. Appl. Biomed.* **6**, 57–64 (2008).
 28. Damborský, P., Švitel, J. & Katrlík, J. Optical biosensors. *Essays Biochem.* **60**, 91–100 (2016).
 29. Pohanka, M. Overview of piezoelectric biosensors, immunosensors and DNA sensors and their applications. *Materials (Basel)*. **11**, (2018).
 30. Eggins, B. R. *Biosensors: an Introduction*. (Wiley, 1996, 1996).
 31. Justino, C. I. L., Freitas, A. C., Pereira, R., Duarte, A. C. & Rocha Santos, T. A. P. Recent developments in recognition elements for chemical sensors and biosensors. *Trends Anal. Chem.* **68**, 2–17 (2015).
 32. Chambers, J. P., Arulanandam, B. P., Matta, L. L., Weis, A. & Valdes, J. J. Biosensor recognition elements. *Curr. Issues Mol. Biol.* **10**, 1–12 (2008).
 33. Vidal, J. C. *et al.* Electrochemical affinity biosensors for detection of mycotoxins: A review. *Biosens. Bioelectron.* **49**, 146–158 (2013).
 34. Löfblom, J. *et al.* Affibody molecules: Engineered proteins for therapeutic, diagnostic and biotechnological applications. *FEBS Lett.* **584**, 2670–2680 (2010).
 35. Ståhl, S. *et al.* Affibody Molecules in Biotechnological and Medical Applications. *Trends Biotechnol.* **35**, 691–712 (2017).
 36. Ronkainen, N. J., Halsall, H. B. & Heineman, W. R. Electrochemical biosensors. *Chem. Soc. Rev.* **39**, 1747–1763 (2010).
 37. Di Gennaro, P. *et al.* Development of microbial engineered whole-cell systems for environmental benzene determination. *Ecotoxicol. Environ. Saf.* **74**, 542–549 (2011).
 38. Martins, S. S. A., Martins, V. C., Cardoso, F. A., Freitas, P. P. & Fonseca, L. P. *Waterborne Pathogen Detection Using a Magnetoresistive Immuno-Chip. Molecular Biological Technologies for Ocean Sensing* (Humana Press, 2012).
 39. Saerens, D., Huang, L., Bonroy, K. & Muyldermans, S. Antibody fragments as probe in biosensor development. *Sensors* **8**, 4669–4686 (2008).
 40. Thermo Scientific, P. *Antibody Production and Purification Technical Handbook. Antibody Handbook* (2010).
 41. Corp, Biologic. I. Antibody Engineering. <https://www.biologicscorp.com/scfv-antibody-production/#.XvIFz5NKh-U> (2020).
 42. Balasubramanian, S., Sorokulova, I. B., Vodyanoy, V. J. & Simonian, A. L. Lytic phage as a specific and selective probe for detection of Staphylococcus aureus-A surface plasmon resonance spectroscopic study. *Biosens. Bioelectron.* **22**, 948–955 (2007).
 43. Mendes, J. J. *et al.* In vitro design of a novel lytic bacteriophage cocktail with therapeutic potential against organisms causing diabetic foot infections. *J. Med. Microbiol.* **63**, 1055–1065 (2014).
 44. Stone, E., Campbell, K., Grant, I. & McAuliffe, O. Understanding and Exploiting Phage-Host Interactions. *Viruses* **11**, 1–26 (2019).
 45. Veesler, D. & Cambillau, C. A Common Evolutionary Origin for Tailed-Bacteriophage Functional Modules and Bacterial Machineries. *Microbiol. Mol. Biol. Rev.* **75**, 423–433 (2011).
 46. Brüssow, H. & Hendrix, R. W. Phage Genomics: Small is beautiful. *Cell* **108**, 13–16 (2002).
 47. Kutter, E. & Sulakvelidze, A. *BACTERIOPHAGES: Biology and Applications*. (Raton London New York Washington, Boca: CRC Press, 2005).
 48. Harada, L. K. *et al.* Biotechnological applications of bacteriophages: State of the art. *Microbiol. Res.* **212–213**, 38–58 (2018).
 49. Abedon, S. T., Thomas-Abedon, C., Thomas, A. & Mazure, H. Bacteriophage prehistory: Is or is not Hankin, 1896, a phage reference? *Bacteriophage* **1**, 174–178 (2011).
 50. Haq, I. U., Chaudhry, W. N., Akhtar, M. N., Andleeb, S. & Qadri, I. Bacteriophages and their implications on future biotechnology: a review. *Viol. J.* **9**, 1–23 (2012).
 51. Cisek, A. A., Dąbrowska, I., Gregorczyk, K. P. & Wyżewski, Z. Phage Therapy in Bacterial Infections Treatment: One Hundred Years After the Discovery of Bacteriophages. *Curr. Microbiol.* **74**, 277–283 (2017).
 52. Hermoso, J. A., García, J. L. & García, P. Taking aim on bacterial pathogens: from phage therapy to enzybiotics. *Curr. Opin. Microbiol.* **10**, 461–472 (2007).
 53. Black, L. W. & Thomas, J. A. Condensed Genome Structure. *Adv. Exp. Med. Biol.* **726**, 469–487 (2012).

54. Azeredo, J. & Sutherland, I. The Use of Phages for the Removal of Infectious Biofilms. *Curr. Pharm. Biotechnol.* **9**, 261–266 (2008).
55. Sharma, S. *et al.* Bacteriophages and its applications: an overview. *Folia Microbiol. (Praha)*. **62**, 17–55 (2017).
56. Ackermann, H. W. Frequency of morphological phage descriptions in the year 2000. *Arch. Virol.* **146**, 843–857 (2001).
57. Clokie, M. R. J., Millard, A. D., Letarov, A. V. & Heaphy, S. Phages in nature. *Bacteriophage* **1**, 31–45 (2011).
58. Quizlet. <https://quizlet.com/306553685/the-lytic-cycle-figure-1311-diagram/>.
59. Rakhuba, D. V., Kolomiets, E. I., Dey, E. S. & Novik, G. Bacteriophage receptors, mechanisms of phage adsorption and penetration into host cell. *Polish J. Microbiol.* **59**, 145–155 (2010).
60. León, M. & Bastías, R. Virulence reduction in bacteriophage resistant bacteria. *Front. Microbiol.* **6**, 1–7 (2015).
61. Molineux, I. J. & Debabrata, P. Popping the cork: mechanisms of phage genome ejection. *Nat. Rev. Microbiol.* **11**, 194/204 (2013).
62. Cumby, N., Reimer, K., Mengin-Lecreux, D., Davidson, A. R. & Maxwell, K. L. The phage tail tape measure protein, an inner membrane protein and a periplasmic chaperone play connected roles in the genome injection process of E.coli phage HK97. *Mol. Microbiol.* **96**, 437–447 (2015).
63. Xu, J. & Xiang, Y. crossm. **91**, 1–7 (2017).
64. Leiman, P. G., Chipman, P. R., Kostyuchenko, V. A., Mesyanzhinov, V. V. & Rossmann, M. G. Three-dimensional rearrangement of proteins in the tail of bacteriophage T4 on infection of its host. *Cell* **118**, 419–429 (2004).
65. Xu, J., Gui, M., Wang, D. & Xiang, Y. The bacteriophage ϕ 29 tail possesses a pore-forming loop for cell membrane penetration. *Nature* **534**, 544–547 (2016).
66. Hu, B., Margolin, W., Molineux, I. J. & Liu, J. The Bacteriophage T7 Virion Undergoes Extensive Structural Remodeling During Infection. *Bone* **339**, 576/579 (2013).
67. Sun, L. *et al.* Icosahedral bacteriophage Φ x174 forms a tail for DNA transport during infection. *Nature* **505**, 432–435 (2014).
68. Brüssow, H., Canchaya, C. & Hardt, W.-D. Phages and the Evolution of Bacterial Pathogens: from Genomic Rearrangements to Lysogenic Conversion. *Microbiol. Mol. Biol. Rev.* **68**, 560–602 (2004).
69. Azizian, R., Dawood, S., Nasab, M. & Ahmadi, N. A. Bacteriophage as a Novel Antibacterial Agent in Industry and Medicine. *J. Paramed. Sci.* **4**, 93–101 (2013).
70. Gill, J. & Hyman, P. Phage Choice, Isolation, and Preparation for Phage Therapy. *Curr. Pharm. Biotechnol.* **11**, 2–14 (2010).
71. Norkin, L. C. *Virology: molecular biology and pathogenesis. Choice Reviews Online* vol. 47 (2010).
72. Miller, E. S. *et al.* Bacteriophage T4 Genome. *Microbiol. Mol. Biol. Rev.* **67**, 86–156 (2003).
73. Rao, V. B. & Black, L. W. Structure and assembly of bacteriophage T4 head. *Virology* **7**, 356 (2010).
74. Chan, S., Shi, R., Tang, T. & Wang, M. T4 Bacteriophage Dominates T7 Bacteriophage During Co-infection of Escherichia coli C600. *J. Exp. Microbiol. Immunol.* **17**, 125–128 (2013).
75. Cuervo, A. *et al.* Direct measurement of the dielectric polarization properties of DNA. *Proc. Natl. Acad. Sci. U. S. A.* **111**, (2014).
76. Studier, F. W. The genetics and physiology of bacteriophage T7. *Virology* **39**, 562–574 (1969).
77. Teesalu, T., Sugahara, K. N. & Ruoslahti, E. *Mapping of vascular ZIP codes by phage display. Methods in Enzymology* vol. 503 (Elsevier Inc., 2012).
78. Kramberger, P., Urbas, L. & Štrancar, A. Downstream processing and chromatography based analytical methods for production of vaccines, gene therapy vectors, and bacteriophages. *Hum. Vaccines Immunother.* **11**, 1010–1021 (2015).
79. Ceglarek, I. *et al.* A novel approach for separating bacteriophages from other bacteriophages using affinity chromatography and phage display. *Sci. Rep.* **3**, 1–6 (2013).
80. Smrekar, F., Ciringer, M., Peterka, M., Podgornik, A. & Štrancar, A. Purification and concentration of bacteriophage T4 using monolithic chromatographic supports. *J. Chromatogr. B Anal. Technol. Biomed. Life Sci.* **861**, 177–180 (2008).
81. Trilisky, E. I. & Lenhoff, A. M. Sorption processes in ion-exchange chromatography of viruses. *J. Chromatogr. A* **1142**, 2–12 (2007).
82. Adriaenssens, E. M. *et al.* CIM® monolithic anion-exchange chromatography as a useful alternative to CsCl gradient purification of bacteriophage particles. *Virology* **434**, 265–

- 270 (2012).
83. Farkas, K. *et al.* Size exclusion-based purification and PCR-based quantitation of MS2 bacteriophage particles for environmental applications. *J. Virol. Methods* **213**, 135–138 (2015).
 84. Óslizło, A. *et al.* Purification of phage display-modified bacteriophage T4 by affinity chromatography. *BMC Biotechnol.* **11**, (2011).
 85. Aizpurua-Olaizola, O. *et al.* Affinity capillary electrophoresis for the assessment of binding affinity of carbohydrate-based cholera toxin inhibitors. *Electrophoresis* **39**, 344–347 (2018).
 86. Clark, J. R. & March, J. B. Bacteriophages and biotechnology: vaccines, gene therapy and antibacterials. *Trends Biotechnol.* **24**, 212–218 (2006).
 87. Sharp, R. Bacteriophages: Biology and history. *J. Chem. Technol. Biotechnol.* **76**, 667–672 (2001).
 88. D’Herelle, F. *The Bacteriophage and its Behavior*. (Baltimore, Md: Williams and Wilkins Company, 1926).
 89. Alanis, A. J. Resistance to antibiotics: Are we in the post-antibiotic era? *Arch. Med. Res.* **36**, 697–705 (2005).
 90. Jakobsson, H. E. *et al.* Short-term antibiotic treatment has differing long-term impacts on the human throat and gut microbiome. *PLoS One* **5**, 1–12 (2010).
 91. Loc-Carrillo, C. & Abedon, S. T. Pros and cons of phage therapy. *Bacteriophage* **1**, 111–114 (2011).
 92. Pires, D. P., Cleto, S., Sillankorva, S., Azeredo, J. & Lu, T. K. Genetically Engineered Phages: a Review of Advances over the Last Decade. *Microbiol. Mol. Biol. Rev.* **80**, 523–543 (2016).
 93. Zourob, M. *Recognition receptors in biosensors. Recognition Receptors in Biosensors* (Springer Sciences, 2010).
 94. Blasco, R., Murphy, M. J., Sanders, M. F. & Squirrell, D. J. Specific assays for bacteria using phage mediated release of adenylate kinase. *J. Appl. Microbiol.* **84**, 661–666 (1998).
 95. Neufeld, T., Schwartz-Mittelmann, A., Biran, D., Ron, E. Z. & Rishpon, J. Combined phage typing and amperometric detection of released enzymatic activity for the specific identification and quantification of bacteria. *Anal. Chem.* **75**, 580–585 (2003).
 96. Chang, T. C., Ding, H. C. & Chen, S. A conductance method for the identification of *Escherichia coli* O157:H7 using bacteriophage AR1. *J. Food Prot.* **65**, 12–17 (2002).
 97. Thouand, G., Vachon, P., Liu, S., Dayre, M. & Griffiths, M. W. Optimization and validation of a simple method using P22::luxAB bacteriophage for rapid detection of *Salmonella enterica* serotypes A, B, and D in poultry samples. *J. Food Prot.* **71**, 380–385 (2008).
 98. Carrière, C. *et al.* Conditionally replicating luciferase reporter phages: Improved sensitivity for rapid detection and assessment of drug susceptibility of *Mycobacterium tuberculosis*. *J. Clin. Microbiol.* **35**, 3232–3239 (1997).
 99. Bardarov, S. *et al.* Detection and drug-susceptibility testing of *M. tuberculosis* from sputum samples using luciferase reporter phage: Comparison with the *Mycobacteria* Growth Indicator Tube (MGIT) system. *Diagn. Microbiol. Infect. Dis.* **45**, 53–61 (2003).
 100. Funatsu, T., Taniyama, T., Tajima, T., Tadakuma, H. & Namiki, H. Rapid and sensitive detection method of a bacterium by using a GFP reporter phage. *Microbiol. Immunol.* **46**, 365–369 (2002).
 101. Goodridge, L. & Griffiths, M. Reporter bacteriophage assays as a means to detect foodborne pathogenic bacteria. *Food Res. Int.* **35**, 863–870 (2002).
 102. Liu, C. M., Jin, Q., Sutton, A. & Chen, L. A novel fluorescent probe: Europium complex hybridized T7 phage. *Bioconjug. Chem.* **16**, 1054–1057 (2005).
 103. Herriott, R. M. & Barlow, J. L. The protein coats or ghosts of coliphage T2. *J. Gen. Physiol.* **40**, 809–825 (1957).
 104. Anderson, D. L. & Bradley, S. G. the Action of Ultrasonic Vibrations on Actinophages. *J. Gen. Microbiol.* **37**, 67–72 (1964).
 105. Pinto, F., Maillard, J. Y. & Denyer, S. P. Effect of surfactants, temperature, and sonication on the virucidal activity of polyhexamethylene biguanide against the bacteriophage MS2. *Am. J. Infect. Control* **38**, 393–398 (2010).
 106. Electron Microscopy Sciences. *UranylLess Protocols of Use: Classic Contrast*. 2–4 (2019).
 107. Kolter, R., Siegele, D. A., & Tormo, A. The Stationary Phase of The Bacterial Life Cycle. *Annu. Rev. Microbiol.* **57**, 855–874 (1993).
 108. Swinnen, I. A. M., Bernaerts, K., Dens, E. J. J., Geeraerd, A. H. & Van Impe, J. F. Predictive modelling of the microbial lag phase: A

- review. *Int. J. Food Microbiol.* **94**, 137–159 (2004).
109. Blount, Z. D. The unexhausted potential of *E. coli*. *Elife* **4**, 1–12 (2015).
 110. Guerlava, P., Izac, V. & Tholozan, J. L. Comparison of different methods of cell lysis and protein measurements in *Clostridium perfringens*: Application to the cell volume determination. *Curr. Microbiol.* **36**, 131–135 (1998).
 111. Spiden, E. M., Scales, P. J., Kentish, S. E. & Martin, G. J. O. Critical analysis of quantitative indicators of cell disruption applied to *Saccharomyces cerevisiae* processed with an industrial high pressure homogenizer. *Biochem. Eng. J.* **70**, 120–126 (2013).
 112. Clokie, M. R. J. *et al.* A proteomic approach to the identification of the major virion structural proteins of the marine cyanomyovirus S-PM2. *Microbiology* **154**, 1775–1782 (2008).
 113. Suslick, K. S. Sonochemistry. *Science (80-.)*. **247**, 1439–1445 (1990).
 114. De Mey, M. *et al.* Comparison of protein quantification and extraction methods suitable for *E. coli* cultures. *Biologicals* **36**, 198–202 (2008).
 115. Qixing, J. *et al.* Effect of temperature on protein compositional changes of big head carp (*Aristichthys nobilis*) muscle and exudates. *Food Sci. Technol. Res.* **20**, 655–661 (2014).

Annex

I – Materials and Methods

Revitalization of Bacteriophages

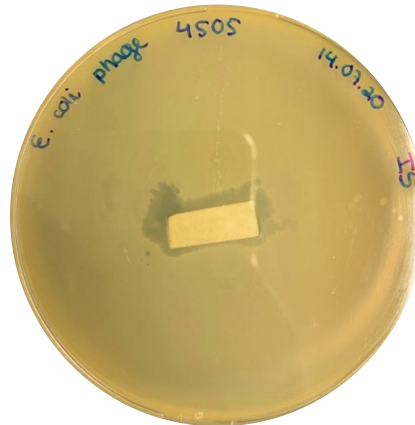


Figure A 1 – TSA medium plate where the host bacteria was plated using the double agar overlay assay supplemented with $MgCl_2$ 1 M. The filter paper containing the dried phage suspension is placed in the middle of the host plate with TSB medium on top. The clear zone around the filter paper is where the lysis of the host bacteria occurred.

II – Results and Discussion

Osmotic Shock Separation Method

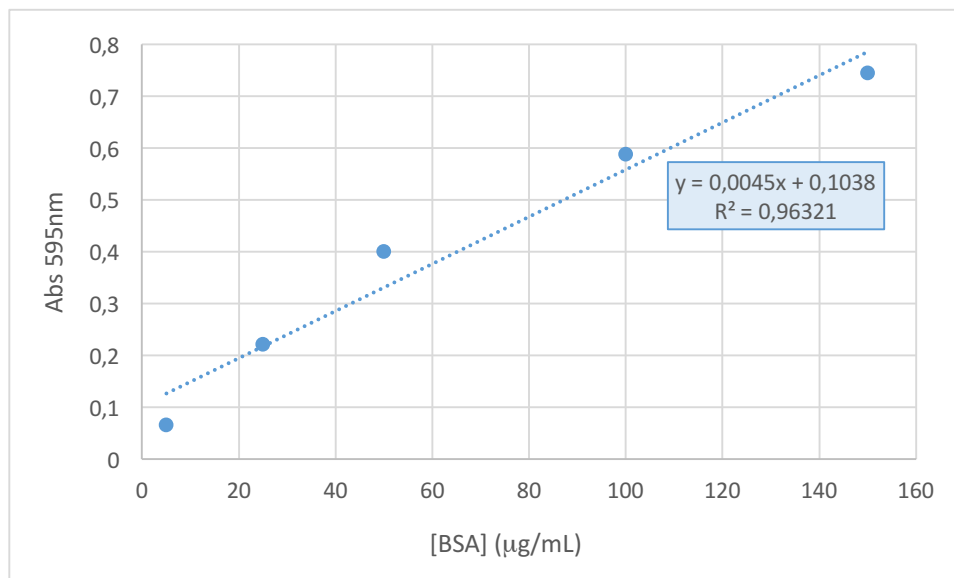


Figure A 2 – Linear calibration curve of BSA concentration in function of the absorbance at 595 nm for the osmotic shock test samples.

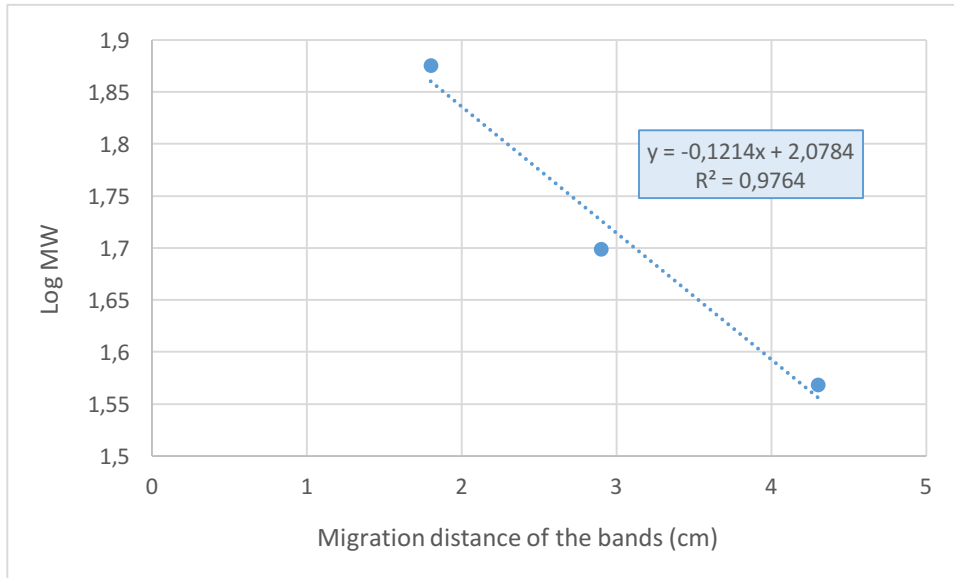


Figure A 3 – Standard curve of the log of the molecular weight (MW) of the ladder bands versus their migration distance. The tendency line allows the determination of the molecular weight (MW) of the osmotic shock gel with samples from 1 minute to 10 minutes of exposure with a band migration of 1.8 to 4.3 cm. This curve was obtained by the selection of these three values of interest for a more accurate calculation of the molecular weight.

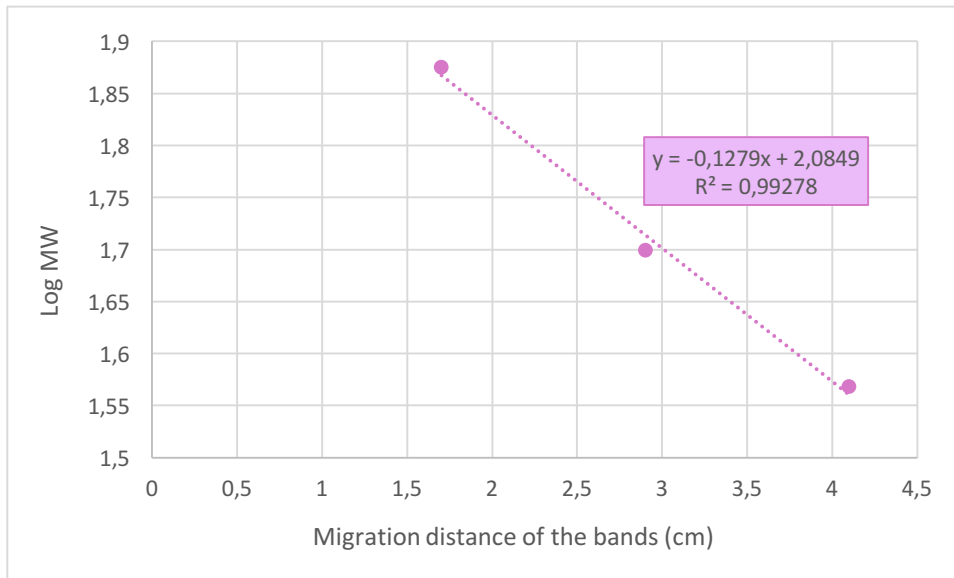


Figure A 4 – Standard curve of the log of the molecular weight (MW) of the ladder bands versus their migration distance. The tendency line allows the determination of the molecular weight (MW) of the osmotic shock gel with samples from 15 minute to 30 minutes of exposure with a band migration of 1.7 to 4.1 cm. This curve was obtained by the selection of these three values of interest for a more accurate calculation of the molecular weight.

Table A 1 – T4 bacteriophage gene products and their respective functions and molecular weights. Adapted from Clokie *et al.* and Miller *et al.*^{72,112}.

| | T4 gene product | Function | Molecular Mass (kDa) |
|-------------------|------------------------|--------------------------------------|-----------------------------|
| Head | gpalt | Phage head component | 75.817 |
| | gp23 | Major capsid protein | 56.021 |
| | gp24 | Head vertex protein | 46.993 |
| | gphoc | Head outer capsid protein | 40.387 |
| | IP III | Internal head protein | 21.687 |
| Tail | gp10 | Baseplate wedge subunit | 66.232 |
| | gp11 | Baseplate wedge subunit | 23.707 |
| | gp18 | Contractile tail sheath protein | 71.331 |
| | gp19 | Tail tube protein | 18.450 |
| | gp48 | Baseplate, tail-tube-association | 39.708 |
| | gp5 | Baseplate hub subunit | 63.116 |
| | gp6 | Baseplate wedge subunit | 74.383 |
| | gp7 | Baseplate wedge subunit | 119.215 |
| | gp8 | Baseplate wedge subunit | 37.983 |
| | gp9 | Baseplate wedge tail-fibre connector | 30.977 |
| | gp15 | Proximal tail sheath stabilizer | 31.557 |
| Tail fibre | gp12 | Short tail fibre | 56.214 |
| | gp34 | Long tail fibre component | 140.403 |
| | gp36 | Long tail fibre component | 23.342 |
| | gp37 | Tail fibre component | 109.224 |

Water Bath Ultrasonication Separation Method

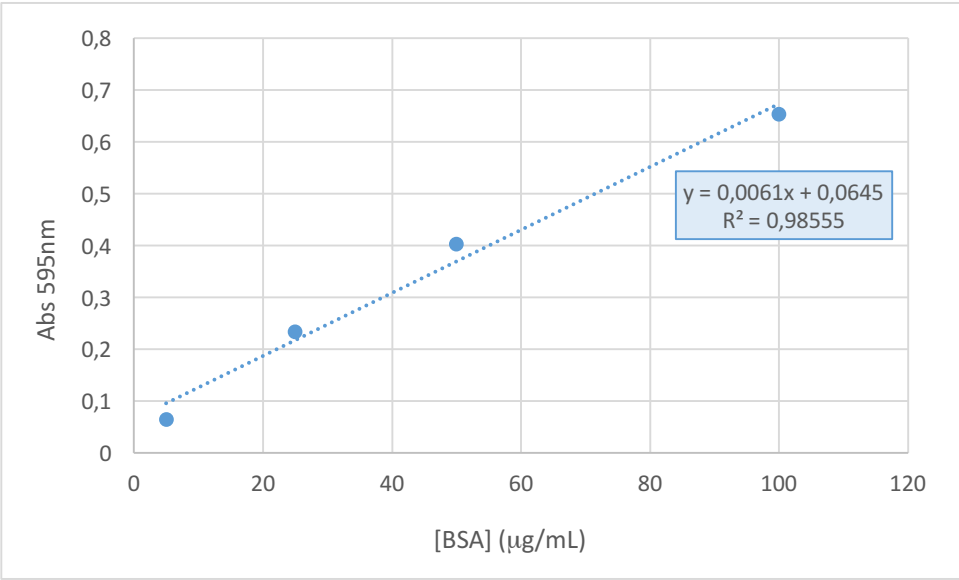


Figure A 5 – Linear calibration curve of BSA concentration in function of the absorbance at 595 nm for the water bath ultrasonication test samples.

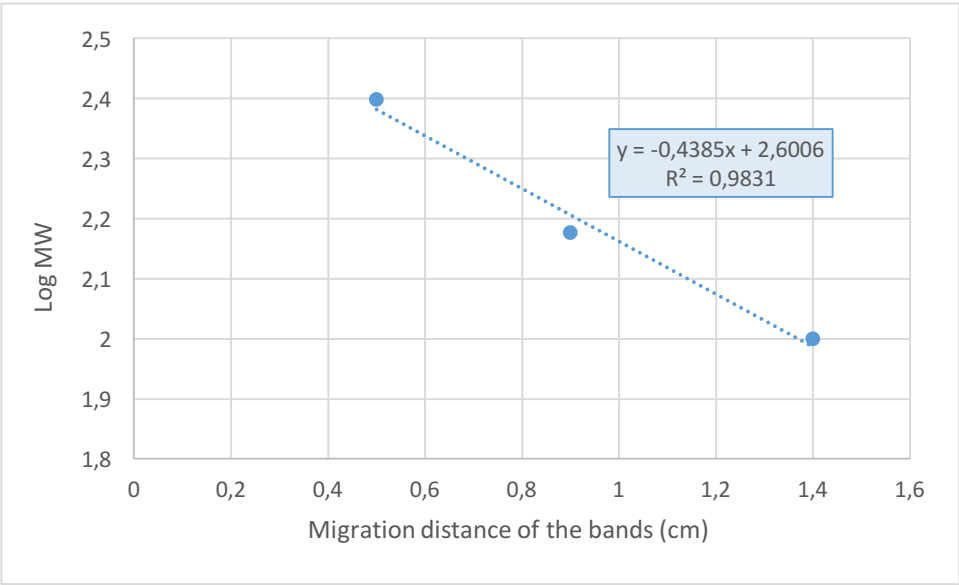


Figure A 6 – Standard curve of the log of the molecular weight (MW) of the ladder bands versus their migration distance. The tendency line allows the determination of the molecular weight (MW) of the water bath ultrasonication gel for a band migration of 0.5 to 1.4 cm. This curve was obtained by the selection of these three values of interest for a more accurate calculation of the molecular weight.

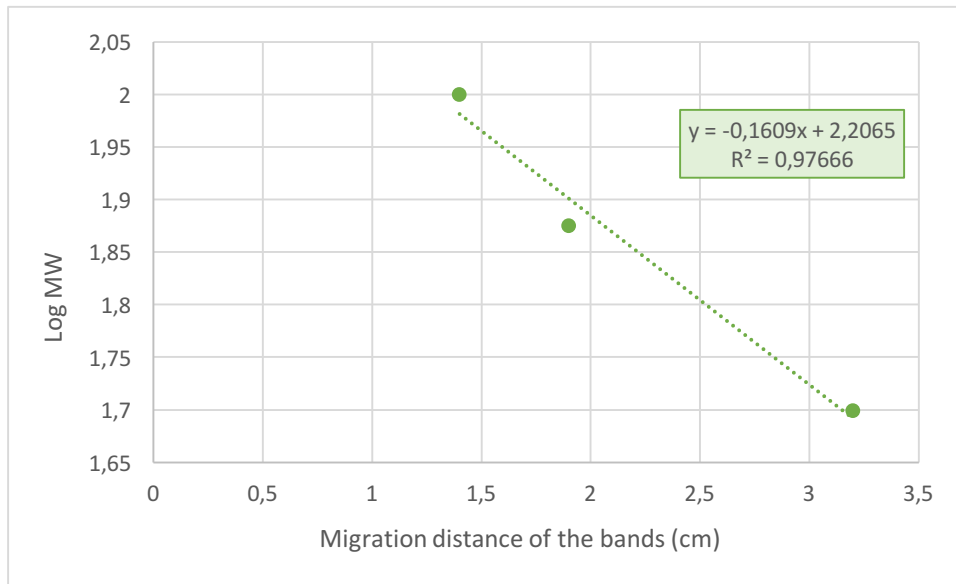


Figure A 7 – Standard curve of the log of the molecular weight (MW) of the ladder bands versus their migration distance. The tendency line allows the determination of the molecular weight (MW) of the water bath ultrasonication gel for a band migration of 1.4 to 3.2 cm. This curve was obtained by the selection of these three values of interest for a more accurate calculation of the molecular weight.

Probe Ultrasonication Separation Method

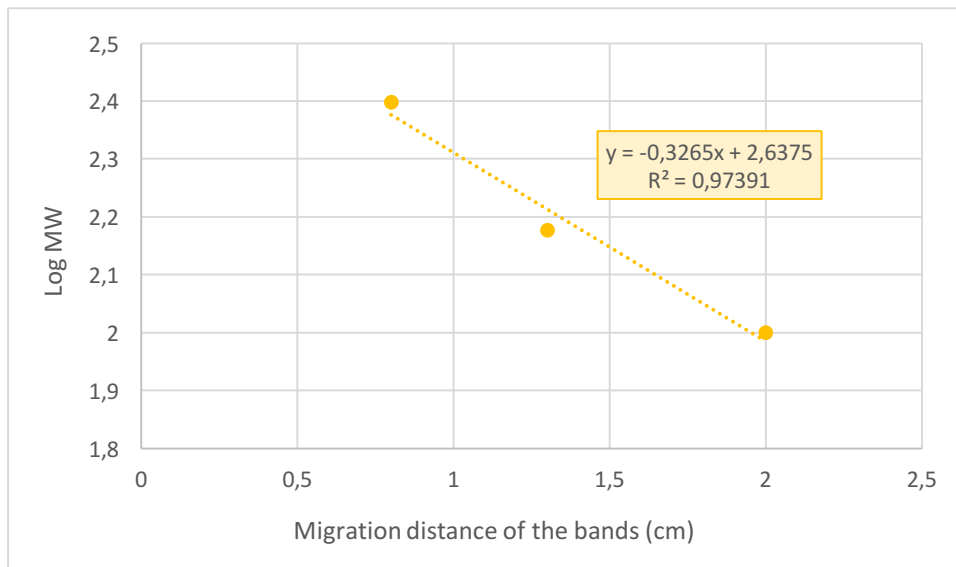


Figure A 8 – Standard curve of the log of the molecular weight (MW) of the ladder bands versus their migration distance. The tendency line allows the determination of the molecular weight (MW) of the 25 W probe ultrasonication gel for a band migration of 0.8 to 2.0 cm. This curve was obtained by the selection of these three values of interest for a more accurate calculation of the molecular weight.

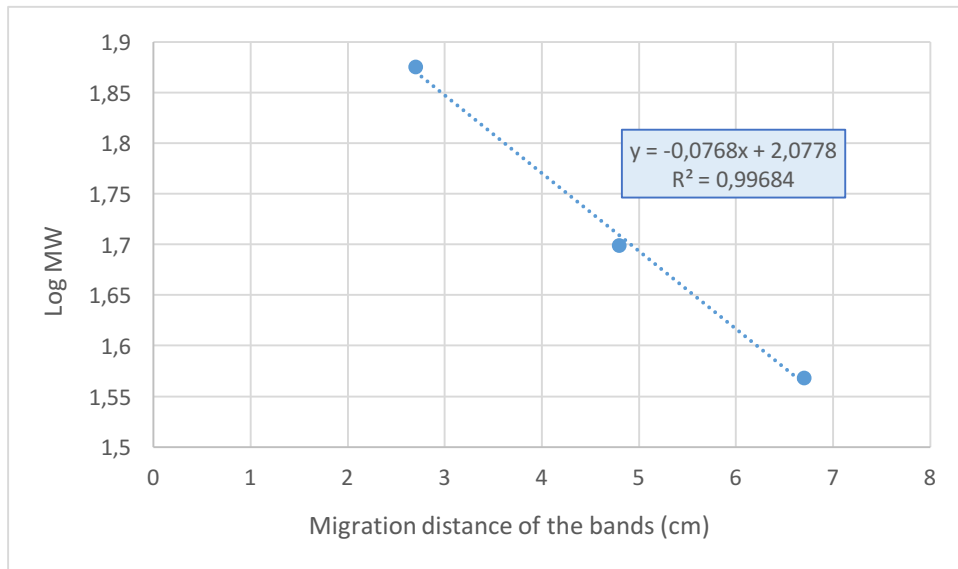


Figure A 9 – Standard curve of the log of the molecular weight (MW) of the ladder bands versus their migration distance. The tendency line allows the determination of the molecular weight (MW) of the 25 W probe ultrasonication gel for a band migration of 2.7 to 6.7 cm. This curve was obtained by the selection of these three values of interest for a more accurate calculation of the molecular weight.

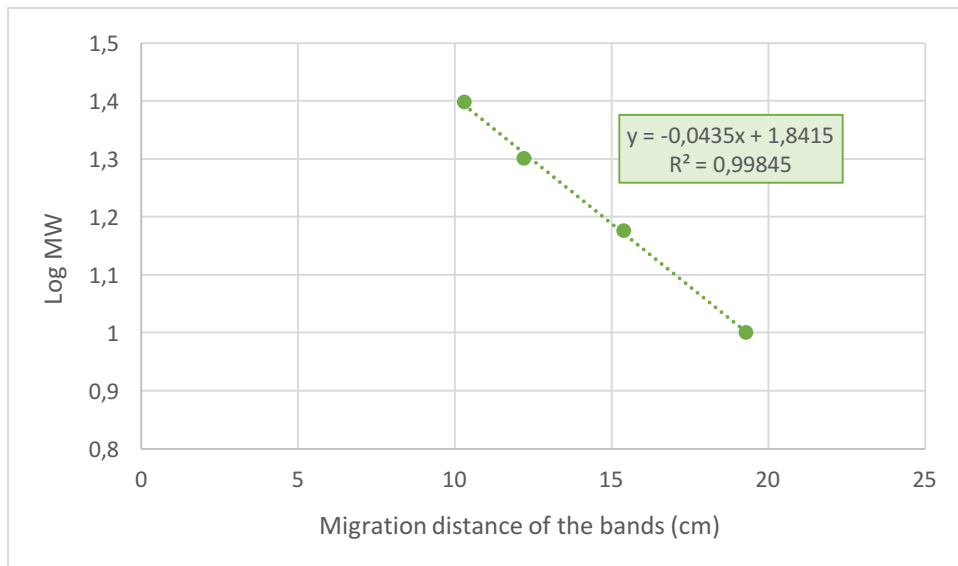


Figure A 10 – Standard curve of the log of the molecular weight (MW) of the ladder bands versus their migration distance. The tendency line allows the determination of the molecular weight (MW) of the 25 W probe ultrasonication gel for a band migration of 10.3 to 19.3 cm. This curve was obtained by the selection of these three values of interest for a more accurate calculation of the molecular weight.

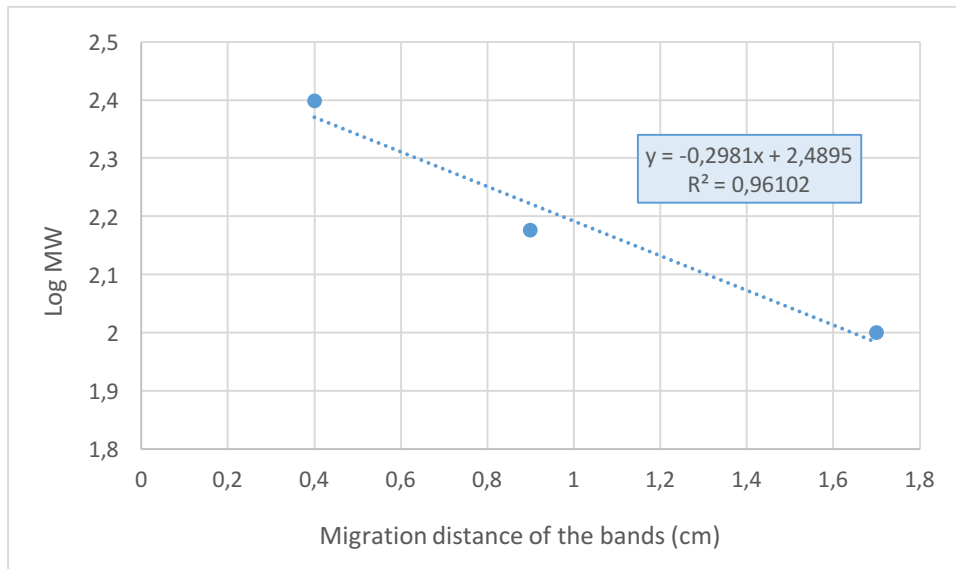


Figure A 11 – Standard curve of the log of the molecular weight (MW) of the ladder bands versus their migration distance. The tendency line allows the determination of the molecular weight (MW) of the 50 W probe ultrasonication gel for a band migration of 0,4 to 1,7 cm. This curve was obtained by the selection of these three values of interest for a more accurate calculation of the molecular weight.

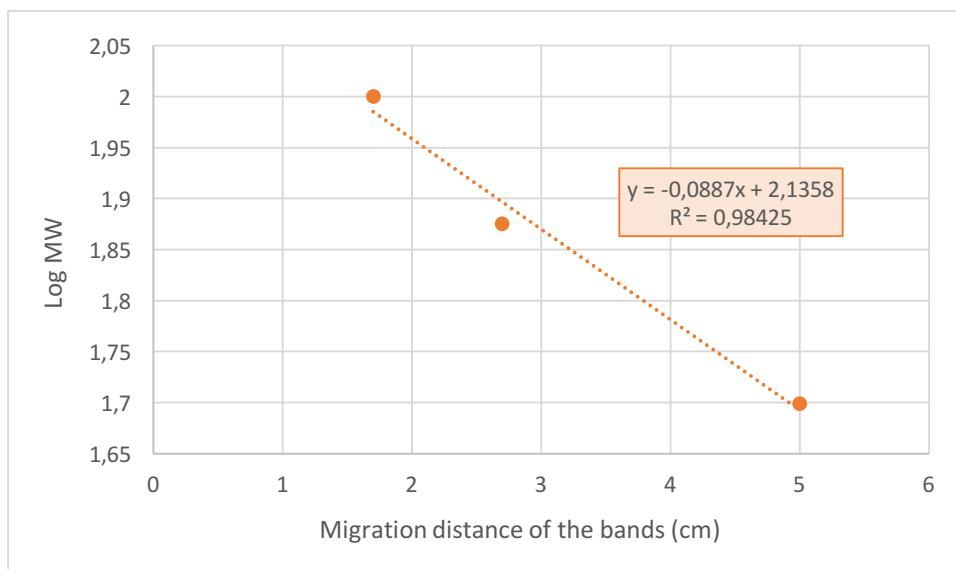


Figure A 12 – Standard curve of the log of the molecular weight (MW) of the ladder bands versus their migration distance. The tendency line allows the determination of the molecular weight (MW) of the 50 W probe ultrasonication gel for a band migration of 1,7 to 5,0 cm. This curve was obtained by the selection of these three values of interest for a more accurate calculation of the molecular weight.